UC San Diego
UC San Diego Electronic Theses and Dissertations

Title

Reactivity-guided isolation of marine and bacterial natural products in the genomic age

Permalink

https://escholarship.org/uc/item/13x1p8c3

Author

Castro Falcón, Gabriel Andrés

Publication Date

2019

Peer reviewed|Thesis/dissertation

UNIVERSITY OF CALIFORNIA SAN DIEGO

Reactivity-guided isolation of marine and bacterial natural products in the genomic age

A dissertation submitted in partial satisfaction of the requirements for the degree of
Doctor of Philosophy

in

Marine Biology

by

Gabriel A. Castro Falcón

Committee in charge:

    Professor Chambers C. Hughes, Chair
    Professor Lihini Aluwihare
    Professor William H. Gerwick
    Professor Bradley S. Moore
    Professor Dionicio Siegle

2019

The Dissertation of Gabriel A. Castro Falcón is approved, and it is acceptable in quality and form for publication on microfilm and electronically:

_____

_____

_____

_____

_____
Chair

University of California San Diego

2019

DEDICATION

to my Parents and Grandparents

EPIGRAPH

"The Devil's wisdom comes not from being the Devil, but from being old"

TABLE OF CONTENTS

LIST OF FIGURES AND TABLES

ACKNOWLEDGMENTS

Chapter 3 contains reprinted material, with permission, as it appears in *ACS Chemical Biology*, 2018, Gabriel Castro-Falcón, Natalie Millán-Aguiñaga, Catherine Roullier, Paul R. Jensen and Chambers C. Hughes. And it contains reproduced material as it appears in the manuscript in preparation for publication: Gabriel Castro-Falcon, Mohammad Alanjary, Nadine Ziemert and Chambers C. Hughes. The dissertation author was a co-investigator and author of these papers.

Chapter 4 is a reprint with permission of the manuscript in preparation of publication: Gabriel Castro-Falcón, Grant S. Seiler and Chambers C. Hughes. The dissertation author was a co-investigator and author of this paper.

VITA

EDUCATION

AUGUST 2009 – MAY 2014   University of Puerto Rico, Río Piedras
BACHELOR OF SCIENCE   Chemistry

JULY 2014 – AUGUST 2019   University of California, San Diego
DOCTOR OF PHILOSOPHY   Marine Biology

PUBLICATIONS

Ding, Y., Murphy, K., Poretsky, E., Mafu, S., et al. Multiple genes recruited from hormone pathways partition maize diterpenoid defenses. Nature Plants (accepted)

Moss, N. A., Seiler G. S., Leão T., Castro-Falcón, G., et al. Nature's combinatorial biosynthesis produces vatiamides A-F. Angew. Chem. Int. Ed. Engl. DOI: 10.1002/anie.201902571

Castro-Falcón, G., Millán-Aguiñaga. N., Roullier, C., and Hughes, C. C. Nitrosopyridine Probe to Detect Polyketide Natural Products with Conjugated Alkenes: Discovery of Novodaryamide and Nocarditriene. ACS Chem. Biol. 2018. doi: 10.1021/acschembio.8b00598

Castro-Falcón, G., Seiler, G., Demir, O., Rathinaswamy, M., et al. Neolymphostin A is an Irreversible PI3-kinase/mTOR Dual Inhibitor that Employs an Unusual Electrophilic Vinylogous Ester. J. Med. Chem. 2018. doi: 10.1021/acs.jmedchem.8b00975.

Mafu, S., Ding, Y., Murphy, K. M., Yaacoobi, O., et al. Discovery, biosynthesis and stress-related accumulation of dolabradiene-derived defenses in maize. Plant Physiol., 2018, 126, 2677

Petras, D., Nothias, L.F., Quinn, R. A., Alexandrov, T., et al. Mass spectrometry-based visualization of molecules associated with human habitats. Anal. Chem., 2016, 88, 10775

Castro-Falcón, G., Hahn, D., Reimer D. and Hughes, C. C. Thiol probes to detect electrophilic natural products based on their mechanism of action. ACS Chem. Biol., 2016, 11 (8), 2328

ABSTRACT OF THE DISSERTATION

Reactivity-guided isolation of marine and bacterial natural products in the genomic age

by

Gabriel A. Castro Falcón

Doctor of Philosophy in Marine Biology

University of California San Diego, 2019

Professor Chambers C. Hughes

By the turn of the 21th century, it became evident that even microorganisms intensely studied as sources of natural products contained the DNA instructions to produce many more compounds than those that were being extracted. Thus, in order to tap into this source of novel natural products, which could serve as structural leads for

the development of new drugs against emerging diseases like cancer and multi-resistant bacterial infections, new methods are urgently needed. In this work, a method dubbed "reactivity-guided isolation" is investigated as a drug discovery approach for different classes of natural products: 1) electrophilic natural products, a therapeutically-relevant class of natural products that covalently modifies their cellular targets, 2) conjugated alkene-containing natural products, a characteristic moiety found in natural products of polyketide origin, and 3) isocyanide-containing natural products, a functional group associated with the biological activity observed in various sponge metabolites. Using carefully designed chemoselective reagents, the method forms derivatives of these different classes of natural products that are UV-active and highly conspicuous via mass spectrometry (MS) by virtue of an isotopically-unique bromine or chlorine tag. Throughout development and application of this method we have expanded the toolbox for derivatizing natural products (and the reagents) and in the process we have synthesized high-value derivatives from high yielding coupling reactions; we have gain insight into the use of UV and MS tags and crystallization units for X-ray analysis that provide opportunities to simplify detection and structural elucidation of natural products; and we have discovered new natural products entities from microorganisms grown in the laboratory, and in some cases predict how they might interact with cellular components. The work presented here has the potential to streamline natural product discovery platforms and lead to new compounds useful in the treatment of diseases.

Chapter 1

Proceedings on natural products research

1.1 INTRODUCTION

Many organisms have the capacity to produce diffusible small molecules that allow them to interact with other individuals and with their environment. Although, we have yet to determine the structure or ecological importance for the vast majority, it is clear that these molecules have a differentiated purpose than the metabolites used for the basic functioning of the cell (like carbohydrates, proteins, nucleic acids, lipids). In fact, organisms have commandeered the biosynthetic machinery involved in the metabolism of basic metabolites, and remodeled it to expand the repertoire of small molecules, and over time created arguably some of the most interesting chemicals found in Nature. They have been responsible for defenses and symbioses between organisms, and maybe not surprisingly, humans have tapped into these natural products for their own indications, most significant being their therapeutic benefits.

1.2 NATURAL PRODUCTS IN HISTORY

Natural remedies have been used throughout history and could have been present in almost all civilizations. Plants and their components are the highly common constituents of remedies in the many ethnographical accounts. There are discoveries of plants being used as medicines 66 thousand years ago.[1] It was in the 18th century that the chemical components of plants were being isolated and assessed for their medicinal benefits.[2] For example, pharmacologically-active morphine was isolated from the opium

plant *Papaver somniferum* L. in the early 1800's by German pharmacist Friedich

Serturner. The glycoside digitoxin, an active constituent from foxglove plant *Digitalis*

purpureas L., was also isolated and used to enhance cardiac contractibility and treat

heart failures. Most famous is probably the case of salicin, obtained from the bark of

willow tree *Salix alba* L for the treatment of pain and inflammation., and later chemically

derivatized to make Aspirin, the worlds most used drug. Other compounds of paramount

importance isolated early on were the anti-malarial drug quinine from *Cinchona*

succirubra and pilocarpine from the plant *Pilocarpus jaborandi*.

1.3 GOLDEN AGE OF NATURAL PRODUCTS

The study of beneficial natural products obtained from microorganisms came

afterwards, notwithstanding, it quickly gained traction and eventually led to what is now

known as the golden age of natural products, tacking place from 1940's-2000's.[3-5] This

was a period where bacteria, mainly from the family Actinomycetes, were being isolated

from terrestrial sediments, monocultured in the laboratory and tested for the production

of substances that inhibit the growth or kill infectious diseases. Through the process of

bioactivity-guided isolation, where the components in a mixture are separated and

tested for their bioactivity, it was possible to purify the active constituents from

microorganisms. It has been estimated that between the 1950's-2000's around 10-20

million microorganism isolates were screened.[3] The most important antibiotics

discovered and further developed during this time include the β-lactams (penicillins and

cephalosporins), tetracyclines, aminoglycosides, chloramphenicol, macrolides and

glycopeptides.[4] The most important strictly synthetic compounds include the quinolones

and the sulfa drugs, azoles and oxazolidinones. Together, these cover the lion's share of all antibiotics that are currently used.

In realm of cancer chemotherapy, over 60% of the 140 compounds approved for treatment can be traced to a natural product, again with microorganisms playing an important role.[5] The most important compounds include actinomycin D, the anthracyclines, the glycopeptides, mitomycin C and the anthracenones. Nonetheless, other very important cancer drugs have been obtained from other sources. For example, the drugs etoposide, taxol, camptothecin, vinblastine and vincristine were discovered from plants, while the epothilones were discovered from fungi. Organisms from the marine environment, as well, have yielded halichondrin B, plitidepsin, ecteinascidin 743, dolastatin 10. Interestingly, these were originally discovered from sponges, tunicates or sea hares and subsequently shown or suspected to be produced by microorganisms.[6]

By the 1990's the pharmaceutical industries were collectively moving away from natural product screening campaigns, and instead investing in drug discovery platforms based on synthetic chemistry that allowed access to high number compounds that could be screened on different biological assays in high-throughput manner. The shift was also accompanied by the increased development of biological drugs, like monoclonal antibodies acting against vascular endothelial growth factors (VEGF) involved in angiogenesis.[5] With the shift, however, has come a reduction in the number of drugs delivered to the market. Currently, there is a critical need for new antibacterial drugs that can be used to fend off pathogens with increased resistance to the existing drugs.

1.4 GENOMIC ERA OF NATURAL PRODUCTS

The abandonment of industrial natural product drug development has come in a time when the study of biosynthesis of different types of natural products (polyketides, non-ribosomal peptides, ribosomal peptides, terpenes, alkaloids and others) is flourishing.[7] It has also come in a time when the development of new sequencing technologies, next-generation or massively-parallel sequencing, have allowed an exponential rise in the number of genomic information available for the different natural product producing organisms. Through genetic studies we now know that genes coding for natural product assembly lines are clustered together in the DNA (named "biosynthetic gene clusters" (BGC)) and that classical natural product discovery programs have failed to identify all the natural products that can be potentially produced by even the most heavily studied microorganisms, like, those producing antibiotic drugs.

Understanding how the biosynthetic machinery works is leading to rational manipulation and modification of pathways that lead to specifically designed, new "unnatural" natural products. Furthermore, the study of biosynthetic gene clusters is leading to discoveries and innovative methods on how to improve the classical natural products field seeking the find new, chemically complex, and bioactive compounds from Nature.

1) It has been useful find organisms to with the capacity to produce a new natural product of interest. In this regard, sub-regions in biosynthetic gene clusters that code for the construction of a moiety or a portion of interest in a natural product could be conserved across species and thus, could be queried to find other organisms that make different molecules but with the same moiety in the natural product. For example, Ben

Shen's research group has developed a high throughput polymerase chain reaction (PCR) approach to query 3,400 actinomycetes genomes for the presence of a well conserved enediyne PKS gene cassette responsible for incorporating the enediyne chromophore and pharmacophore moiety in the most toxic natural products known to date. 81 strains with the gene cassette lead to a new member of the 10-membered enediyne family of natural products, tiancimycin, closely related to dynemicin and uncialamycin.[8] On a similar study, the same laboratory group queried public databases of microbial genomes for the presence of genes responsible for sulfur incorporation in the case of leinamycin, an promising anticancer drug lead that features a unique 1,3-dioxo-1,2-dithiolane moiety spirofused to an 18-membered macrolactam. 49 bacteria harboring the gene signature, yet with different neighboring genes, were subsequently cultured. This led to the discovery distinct families related to leinamycins, the guangnanmycins and wishanmycin, produced by *Streptomyces* sp.[9]

2) It has been useful to find "super producers", organisms with the capacity to produce many natural products. For example, in a study led by Lena Gerwick's research group, the biosynthetic gene clusters of various cyanobacterial strains of the *Moorea* genus was compared to other cyanobacterial genomes available in public databases. They observed that, in fact, the genomes of *Moorea* spp. contain a greater proportion of gene clusters than any other genus, from 30-45 gene clusters, while others vary from 2-45 gene clusters.[10]

3) It has been instrumental in helping define who are the producers of many natural products found from macro-organisms like sponges, ascidians, plants, many of which cannot be cultured in the laboratory. In a study by the research group of David H.

Sherman, metagenomic DNA from colonies of the tunicate *Ecteinascidia turbinata*, a source of the clinically approved chemotherapeutic natural product ecteinascidin 743 (ET-743), was sequenced. By "binning" or computationally separating the sequences based on tetranucleotide frequency, they obtained the whole genome of Gammaproteobacterium *Candidatus* Endoecteinascida frumentensis, the main microorganism consistently associated with tunicates in the Mediterranean and Caribbean seas. There, the researchers found an extremely reduced genome and only one biosynthetic gene cluster, coding for ET-743, thus indicating the importance of the natural products in the symbiotic relationship between the bacterium and tunicate.[12]

4) It has been very useful in the process of structural elucidation of natural products, historical done by a combination of spectroscopic techniques. For example, in a pioneering study lead by the research groups of Bradley S. Moore, Paul R. Jensen and William Fenical, the first whole genome of a marine bacterium, salinosporamide A producer *Salinispora tropica* CNB-440, revealed many novel biosynthetic loci and one of these, along with spectroscopic information, was used to assign the structure of a pair of unstable polyene macrolactams, the salinilactams.[13] Based on the co-linearity rule of modular type I PKS systems, the genome data was used to corroborate the gross structure of the macrolactam and the absolute stereochemistry of three hydroxyl groups based on the classification of their respective ketoreductase (KR) domains a "A-type".

5) It has allowed for predictions on the mechanism of action of some natural products, since in some cases the biosynthetic gene clusters incorporate extra copies of housekeeping genes coding for the protein target of these compounds, as was shown by researchers in Bradley S. Moore's group.[14] In a recent case, the research group of

6

Rolf Müller searched for topoisomerase inhibitors by first querying an in-house myxobacterial genetic database with a sequence known to code for a pentapeptide repeat protein (PRP) responsible for self-resistance in against the gyrase inhibitor cystobactamid from Cystobacter ferrugineus. After identifying bacteria with similar genes, they developed mutant strains by deleting repressor regulators and inserting of heterologous promoters that yielded the antimicrobial and cytotoxic pyxidicyclines confirmed to inhibit *E. coli* topoisomerase IV and human topoisomerase I.[15]

6) Lastly, it has been useful to get a global picture of what types or classes of natural products are still to be discovered. In a study lead by William W. Metcalf and Neil L. Kelleher, more than 11 thousand biosynthetic gene clusters from 803 Actinobacteria were compared to each other using a cluster analysis in order to understand the space occupied by the different BGCs.[11] They calculated that around 15 thousand Actinomyces strains have to be sequenced in order to access all natural product gene clusters at which point the number of BGCs for the two most abundant groups, PKSI and NRPS, will be around 6-8 thousand. The study pointed towards specific taxonomic family (such as Streptomycetales and Pseudonocardiales) that harbor the greatest number and diversity of gene clusters.

1.6 CURRENT STATE AND MODERN NATURAL PRODUCT CHEMISTRY

The field of natural product has been invigorated through advances in analytical chemistry. Initially, the process of structural elucidation of natural products was difficult and extensive, since it relied on numerous synthetic and chemical degradation steps. With the advent of user friendly ultraviolet (UV), infrared (IR), X-ray and mass

spectrometry (MS) instruments in the 1960's that analysts were able make significant improvements in their structural predictions.[16] Furthermore, also during this time the first nuclear magnetic resonance (NMR) instrument became commercially available that allow the analyst to acquire ^1H and ^{13}C spectrum of compounds, albeit with low sensitivity. Advancements made with this technique, include the development of the pulsed Fourier transform NMR, the introduction of higher field NMR with superconducting magnets and the development of pulse sequences that allowed performing ^{13}C spectral editing and 2D NMR experiments like COSY, HETCOR, NOESY and later the HMBC in the early 1980's. Since then, further improvements in magnets and electronic components have allowed reaching levels of sensitivity 10,000 better than the first commercial NMR.

High pressure (or performance) liquid chromatography (HPLC) is today one of the most widely applicable separation techniques that can be combined with a variety of detectors for the analysis of organic molecules.[17] In natural products chemistry, was is typically extracted from organism using organic solvents consists of a mixture of many molecules of varying degrees of polarity and of different chemical composition. HPLC profiling analyses consume very little amount of sample and can deliver significant data on sample composition depending of what types of detectors are hyphenated. The most common are the UV and the MS coupled detectors, appearing in analytical laboratories after the 1990's and which together can give very useful properties about compounds such as the presence of specific chromophores and the molecular weight, respectively. With some mass spectrometers, tandem MS (or MS/MS), it's possible to measure the weight of fragments produced from the molecule, and thus get information about the

molecule and its components. Both, the UV and MS/MS spectrum can be thought as a "fingerprint" for a compound

A recent publication by William H. Gerwick's and Roger F. Linington's laboratories described the current state of the natural products field in terms of the structural novelty of each new natural product that is described.[18] They first created a database of known natural products by surveying the literature for reports of microbial and marine natural products and to each structure they assigned a novelty score (Tanimoto index), by comparing it to all other natural products described before. With these, they were able to address points such as that from the 40-90's represented a time of steadily increasing discovery and since the 90's the number of structures described per year has been more or less stable (at ~1,500). Also, the discovery of novel structures considerably dropped from the 40-90's and since then has also stabilized. At the current rate, 10% of the new natural products described have a low similarity to everything else discovered (with a Tanimoto score of < 0.4). Studies like this one, highlight the vast number of natural products isolated so far, it points towards a foreseeable boundary to what remains to be discovered and it underscores the importance and power of natural product databases.

The modern computer age is allowing the storage and rapid access to information. In the current state of the field, it is increasingly important to quickly discern between known and unknown natural products, a process termed dereplication. The high rate of re-discovery of known natural products has been attributed as a major reason why industries have pursued other avenues in drug discovery. Nonetheless, there has been significant progress in the streamlining the discovery of new molecules.

Analytical high-throughput instrument like the HPLC-UV-MS/MS is capable of measuring specific properties of maybe hundreds of compounds in a 30-minute run, just requiring very small amounts of material. Then computer programs are used to quickly detect and compare the interesting features (UV, MS and MS/MS properties) of all the analytes in the sample with the properties of known natural products contained in a database, and discern between new and unknown molecules in the sample. In this regard, the research group of Pieter C. Dorrestein has developed the software and methodology to compare MS/MS spectra from HPLC runs with itself, in order to identify structural similarities between molecules in the sample, and with a library or database of MS/MS data gathered from known compounds.[19]

As a way to expand on the analytical tools that can aid in the discovery of new natural products, our laboratory has developed chemoselective reactions that signal the presence of natural products with particular functional groups or moieties using an HPLC-UV-MS/MS.

1.7 REACTIVITY-GUIDED ISOLATION

One promising approach that complements traditional bioactivity-guided isolation utilizes the inherent reactivity of a metabolite to inform the detection and isolation process. Using soluble reagents, it is possible to label natural product functional groups or structural features in an extract. And, although the original metabolites are irreversibly modified, the resulting adducts often have enhanced visibility by UV and MS.

The Marfey's reaction is an early application of this method, in which enantiomeric amino acids are modified with1-fluoro-2,4-dinitrophenyl-5-L-alanine amide (FDAA) to give diastereomeric adducts with strongly absorbing chromophores that can be resolved and easily detected using HPLC-UV instrumentation.[20] More than thirty years after its invention, this reaction is still widely used to experimentally determine the stereochemistry of amino acids in natural products but it is also useful for increasing the detection limit of many pharmaceutical containing a reactive amine. Derivatization reactions performed prior to the analysis is very common for example for gas chromatography separations, where polar functional groups containing activated hydrogen like carboxylic acids (COOH), alcohols (OH), amines (NH2), and thiols (SH) are protected to prevent intermolecular hydrogen bonding and increase the analytes volatility.[21] Another early example of this method is the use of bromo-benzoyl chloride to derivatized primary or secondary alcohols in natural products and yield compounds with enhanced crystallinity and heavy atoms necessary for absolute structural elucidation using x-ray diffraction analysis. Many examples can of this type of reaction can be seen in the literature and was the inspiration for us in the development of the reagents described in Chapter 2 of this thesis.[22,23]

The fields of click-chemistry, protein conjugation and bioorthogonal chemistry have also been instrumental for the development of reactivity-guided isolation. In classical protein conjugation, functional groups found in proteins, such as the side-chain functionalities of lysine, cysteine, tyrosine and tryptophan amino acids, are derivatized with reagents, containing a reactive portion and a tag portion, to allow direct visualization or enrichment of the target molecules.[24] Many reagents have emerged

11

from these efforts and include, for example, the thiol, acetamide and maleimide

reagents. Importantly, these reactions need to be chemoselective and applicable in

cellular pH and temperature conditions. With the goal of studying biomolecules in their

native environments, beginning in the early 2000's, Carlyn R. Bertozzi's group and

many others have developed the area of bioorthogonal chemistry. Herein, an un-native

reporter group is metabolically incorporated into a biomolecule of interest and

subsequently reacted using chemoselective reagents.[25] From the numerous reactions

that have been developed for these goals, the azide-terminal alkyne click-reaction and

the tetrazine-*trans*-cyclooctene reaction have shown great application. In this thesis, the

tetrazine and isonitrile bioorthogonal reaction, which has been used for visualizing

proteins and carbohydrates in cells, has been adapted for use in natural product

detection, as you will see in Chapter 4.[26,27]

   In the field of natural products, the use of reactions that aid the analysis and

isolation of natural products of specific functional groups is becoming more common.

Recently, researchers have utilized reactive resins to immobilize and selectively elute

natural products based on chemical functionality.[28-30] For example, the group of Erin C.

Carlson has created different siloxyl-functionalized resins, with varying alkyl and leaving

groups, that allow the chemoselective capture of natural products containing hydroxyls,

phenols and/or carboxylic acids, and their subsequent release using fluoride or acidic

conditions. Importantly, this strategy has been validated to enrich known natural

products found in complex crude extracts.

   By far, simple functional groups found in primary and secondary metabolites

have been targeted, including ketones and aldehydes, carboxylic acids, amines, thiols,

and alcohols. Methods that, instead, target structural units common to secondary metabolism are inherently more valuable for the discovery of new secondary metabolites, and these have been the focus of this thesis.[31-36] For example, the group of Douglas A. Mitchell, has implemented the use of soluble dithiothreitol to find natural products with "dehydrated amino-acids" (i.e. the α, β-unsaturated amides functional group).[33] Genome mining was used to predict the organisms that could produce this type of moiety and subsequent culturing and probing of crude extracts with the reaction led to the discovery of an analogue in the family of cyclothiazomycin, which are ribosomally synthesized and post-translationally modified peptide natural products.

In this thesis, we explore three different type of reactions that we believe could help in identifying new natural products. These reactions have passed through a series of validation steps where they are tested first with a variety of substrates and extracts before using them to screen for unknown natural products with targeted functional groups. Chapter 2 describes the design and use of thiol reagents (or probes) to target a pharmacologically-active class of natural products called electrophilic natural products. We show applications to find antibacterial and cytotoxic natural products from *Salinispora* spp., like tirandalydigin and the neolymphostins, the latter or which was later confirmed by us to covalently inhibit phosphoinositide 3-kinase (PI3K) in a similar manner as the thiol reagent, and we suggest potential avenues for cyanobacterial natural products that also Chapter 3 describes the design and use of nitroso reagents (or probes) to target conjugated double bonds (dienes, trienes, polyenes), a characteristic moiety of polyketide natural products, many of which are of clinical significance. This led to the detection of the new metabolites, novodaryamide and

nocarditriene, from *Streptomyces* and *Nocardiopsis* strains. Furthermore, since there is

a polyketide synthase signature for the biosynthesis of the conjugated double bond

moiety, we developed a script to find potential producers from a public DNA database of

genome-sequenced bacteria. Using the nitroso reagent on a handful of these bacteria

led to the discovery of thrixazol and epostatin B from *Saccharothrix espanaensis*.

Finally, Chapter 4 describes the design and use of tetrazine reagents (or probes) to

target isonitrile (a.k.a. isocyanide)-containing natural products, a functional group which

has been associated to the inhibition activity against the parasite *Plasmodium*

falciparum of many sponge natural products. In this undertaking we developed reagents

that exhibited pronounce ionization by HPLC-MS/MS in order to facilitate the process of

detection of minor metabolites. This is currently being used to uncover isocyanides

produced by sponges and nudibranchs, which are known sources of this type of

compound.

1.7 REFERENCES

(1) Fabricant, D. S., Farnsworth, N. R. (2001) The value of plants used in traditional medicine for drug discovery. *Environ. Health Perspect. 109, 69-75.*

(2) Yuan, H., Ma, Q., Ye, L., Piao, G. (2016) The traditional medicine and modern medicine from natural products. *Molecules, 21, 559*

(3) Katz, L., Baltz, R. H. (2016) Natural product discovery: past, present, and future. *J. Ind. Microbiol. Biotechnol. 43, 155-176.*

(4) Demain, A. L. (2014) Importance of microbial natural products and the need to revitalize their discovery. *J. Ind. Microbiol. Biotechnol. 41, 185-201.*

(5) Giddings, L. A., Newman, D. J. (2013) Microbial natural products: molecular blueprints for antitumor drugs. *J. Ind. Microbiol. Bioitechnol. 40, 1181-1210.*

(6) Gerwick H. W., Fenner, A. M. (2013) Drug discovery from marine microbes. *Microb. Ecol. 65, 800-806.*

(7) Wright, G. D. (2019) Unlocking the potential of natural products in drug discovery. *Microb. Biotechnol. 12, 55-57.*

(8) Yan, X., Ge, H., Huang, T., Hindra, Yang, D., Teng, Q., Crnovčić, I., Li, X., Rudof, J. D., Lohman, J. R., Gansemans, Y., Zhu, X., Huang, Y., Zhao, L. X., Jiang, Y., Van Nieuwerburgh, F., Rader, C., Duan, Y., Shen. B. (2016) *MBio, 7, e02104-16.*

(9) Pan, G., Xu, Z., Guo, Z., Hindra, Ma, M., Yang, D., Zhou, H., Gansemans, Y., Zhu, X., Huang, Y., Zhao, L. X., Jiang, Y., Cheng, J., Van Nieuwerburgh, F., Suh, J. W., Duan, Y., Shen, B. (2017) Discovery of the leinamycin family of natural products by mining actinobacterial genomes. *Proc. Natl. Acad. Sci. USA, 114, E11131-E11140.*

(10) Leao, T., Castelão, G., Krorobeynikov, A., Monroe, E. A., Podell, S., Gluckhov, E., Allen, E. E., Gerwick, W. H., Gerwick, L. (2017) Comparative genomics uncovers the prolific and distinctive metabolic potential of the cyanobacterial genus Moorea. *Proc. Natl. Acad. Sci. USA, 114, 3198-3203.*

(11) Doroghazi, J. R., Albright, J. C., Goering, A. W., Ju, K. S., Haines, R. R., Tchalukov, K. A., Labeda, D. P., Kelleher, N. L., Metcalf, W. W. A roadmap for natural product discovery based on large-scale genomics and metabolomics. *Nat Chem. Biol. 10, 963-970.*

(12) Schofield, M. M., Jain, S., Porat, D., Dick, G. J., Sherman, D. H. (2015) Identification and analysis of the bacterial endosymbiont specialized for production of the chemotherapeutic natural product ET-743. *Environ. Microbiol. 17, 3964-3975.*

(13) Udwary, D. W., Zeigler, L., Asolkar, R. N., Singan, V., Lapidus, A., Fenical, W., Jensen, P. R., Moore, B. S. (2007) Genome sequencing reveals complex secondary metabolome in the marine actinomycete Salinispora tropica. *Proc. Natl. Acad. Sci. USA, 104, 10376-10381.*

(14) Tang, X., Li, J., Millán-Aguiñaga, N., Zhang, J. J., O'Neill, E. C., Ugalde, J. A., Jensen, P. R., Mantovani, S. M., Moore, B. S. (2015) Identification of thiotetronic acid antibiotic biosynthetic pathways by target-directed genome mining. *ACS Chem. Biol. 10, 2841-2849.*

(15) Panter, F., Krug, D., Baumann, S., Müller, R. (2018) Self-resistance guided genome mining uncovers new topoisomerase inhibitors from myxobacteria. *Chem. Sci. 9, 4898-4908.*

(16) Breton, R. C., Reynolds, W. F. (2013) Using NMR to identify and characterize natural products. *Nat. Prod. Rep., 30, 501.*

(17) Seger, C., Sturm, S., Stuppner, H. (2013) Mass spectrometry and NMR spectroscopy: modern high-end detectors for high resolution separation techniques-state of the art in natural product HPLC-MS, HPLC-NMR, and CE-MS hypenations. *Nat. Prod. Rep. 30, 970.*

(18) Pye, C. R., Bertin, M. J., Lokey, R. S., Gerwick, W. H., Linington, R. G. (2017) Retrospective analysis of natural products provides insights for future discovery trends. *Proc. Natl. Acad. Sci. USA, 114, 5601-5606.*

(19) Yang, J. Y., Sanchez, L. M., Rath, C. M., Liu, X., Boudreau, P. D., Bruns, N., Gluckhov, E., Wodtke, A., de Felicio, R., Fenner, A, Wond, W. R., Linington, R. G. Zhang, L., Debonsi, H. M., Gerwick, W. H., Dorrestein, P. C. (2013) Molecular networking as a dereplication strategy. *J. Nat. Prod. 76, 1686-1699.*

(20) Marfey, P. (1984) Determination of D-amino acids. II. Use of a bifunctional reagent, 1,5-difluoro-2,4-dinitrobenzene. Carlsberg Res. Commun. 49, 591–596.

(21) Danielson, N. D., Gallagher, P. A. (2000) Chemical reagents and derivatization procedures in drug analysis. *Encylopedi of Analytical Chemistry, 7042–7076.*

(22) Kiyota, N., Shingu, K., Yamaguchi, K., Yoshitake, Y., Harano, K., Yoshimitsu, H., Ikeda, T., Nohara, T. (2007) New C28 steroidal glycosides from Tubocapsicum anomalum. *Chem. Parm. Bull. 55, 34–36.*

(23) Kuroda, Y., Hasegawa, K., Noguchi, K., Chiba, K., Hasumi, K., Kitano, Y. (2018) Confirmation of the absolute configuration of Stachybotrin C using single-crystal X-ray diffraction analysis of its 4-bromobenzyl ether derivative. *J. Antibiot. (Tokyo) 71, 584–591.*

(24) Sletten, E. M., Bertozzi, C. R. (2009) Bioorthogonal chemistry: fishing for selectivity in a sea of functionality. *Angew. Chemie - Int. Ed. 48, 6974–6998.*

(25) Devaraj, N. K. (2018) The future of bioorthogonal chemistry. *J. Am. Chem. Soc. 4, 952–959.*

(26) Henning, S., Neves, A. A., Stairs, S., Brindle, K. M., and Leeper, F. J. (2011) Exploring isonitrile-based click chemistry for ligation with biomolecules. Org. Biomol. Chem. 9, 7303–7305.

(27) Stairs, S., Neves, A. A., Stçckmann, H., and Wainman, Y. A. (2013) Metabolic glycan imaging by isonitrile–tetrazine click chemistry. ChemBioChem 14, 1063–1067.

(28) Carlson, E. E., and Cravatt, B. F. (2007) Enrichment tags for enhanced-resolution profiling of the polar metabolome. J. Am. Chem. Soc. 129, 15780–15782.

(29) Carlson, E. E., and Cravatt, B. F. (2007) Chemoselective probes for metabolite enrichment and profiling. Nat. Methods 4, 429–435.

(30) Odendaal, A. Y., Trader, D. J., and Carlson, E. E. (2011) Chemoselective enrichment for natural products discovery. Chem. Sci. 2, 760–764.

(31) Jeon, H., Lim, C., Lee, J. M., and Kim, S. (2015) Chemical assay-guided natural product isolation via solid-supported chemodosimetric fluorescent probe. Chem. Sci. 6, 2806–2811.

(32) Miles, C. O., Sandvik, M., Nonga, H. E., Rundberget, T., Wilkins, A. L., Rise, F., and Ballot, A. (2012) Thiol derivatization for LC-MS identification of microcystins in complex matrices. Environmetal Sci. Technonlogy 46, 8937–8944.

(33) Cox, C. L., Tietz, J. I., Sokolowski, K., Melby, J. O., Doroghazi, J. R., and Mitchell, D. A. (2014) Nucleophilic 1,4-additions for natural product discovery. ACS Chem. Biol. 4, 2014–2022.

(34) Rudolf, G. C., Koch, M. F., Mandl, F. A. M., and Sieber, S. A. (2015) Subclass-specific labeling of protein-reactive natural products with customized nucleophilic probes. *Chem. - A Eur. J. 21, 3701–3707.*

(35) Tørring, T., Shames, S. R., Cho, W., Roy, C. R., Crawford, J. M. (2017) Acyl histidines: new N-acyl amides from Legionella pneumophila. *ChemBioChem, 18, 638-646.*

(36) Gless, B. H., Bojer, M. S., Peng, P., Baldry, M., Ingmer, H., Olsen, C. A. (2019) Identification of autoinducing thiodepsipeptides from staphylococci enabled by native chemical ligation. *Nat. Chem. 11, 463-469.*

Chapter 2

Thiol probes to detect electrophilic natural products based on their mechanism of action: method validation, discovery of tirandalydigin, discovery and mechanism of action of neolymphostins, and labelling of non-cytotoxic jamaicamides and phycocyanobilins.

2.1 ABSTRACT

New methods are urgently needed to find novel natural products as structural leads for the development of new drugs against emerging diseases like cancer and multi-resistant bacterial infections. Here, we introduce a reactivity-guided drug discovery approach for electrophilic natural products, a therapeutically-relevant class of natural products that covalently modifies their cellular targets, in crude extracts. Using carefully designed halogenated aromatic reagents, the process furnishes derivatives that are UV-active and highly conspicuous via mass spectrometry by virtue of an isotopically-unique bromine or chlorine tag. In addition to the identification of high-value metabolites, the process facilitates the difficult task of structure elucidation by providing derivatives that are primed for X-ray crystallographic analysis. We show that a cysteine probe efficiently and chemoselectively labels enone-, β-lactam-, and β-lactone-based electrophilic natural products (parthenolide, andrographolide, wortmannin, penicillin G, salinosporamide), whilst a thiophenol probe preferentially labels epoxide-based electrophilic natural products (triptolide, epoxomicin, eponemycin, cyclomarin, salinamide). Using the optimized method, we were able to detect and isolate the epoxide-bearing natural product tirandalydigin from *Salinispora* and thereby link an orphan gene cluster to its gene product.

2.2 INTRODUCTION

Until recently,[1] reactivity-guided isolation has not been employed for the identification of natural product pharmacophores that would lead directly to biologically-active metabolites with a high potential for therapeutic development.

An important class of natural products owe their potent biological activity to an electrophilic moiety that engages the cellular target of the molecule in a covalent linkage.[2,3] Due to the misconceived notion that they would be too toxic, the drug industry has historically avoided the development of covalent drugs, despite the unparalleled success of aspirin and penicillin. Recently, however, there has been a resurgence of interest in covalent drugs.[4] In addition to the newly-approved covalent proteasome inhibitor carfilzomib, whose structure is based on the natural product epoxomicin, several covalent kinase inhibitors with striking selectivity and potency are in clinical trials or have been approved by the FDA.[5] Interestingly, the electrophilic mechanism of action of all 39 FDA-approved covalent drugs was discovered serendipitously, only after they were selected and developed for their biological activity.[4]

2.3 RESULTS AND DISCUSSION

2.3.1 Development and validation of thiol probes with pure natural products

We set out to apply a reactivity-guided approach for the deliberate discovery of electrophilic natural products. Given the reactivity of thiolates with naturally-occurring electrophilic moieties,[6-15] which has previously been exploited to classify certain electrophilic natural products,[6] we wished to design and synthesize a thiol-based probe that would tag these compounds in a crude extract. These "pharmacophore probes"

consist of three parts: 1) a highly chemoselective reagent that reacts covalently with a specified pharmacophore, 2) an easily identifiable UV/Vis or mass spectrometric tag, and 3) a linker that joins the reagent and tag. We tested several different probe designs. Two probes proved superior to the others in terms of reactivity, chemoselectivity, and stability (Figure 2.1). Cysteine probe **1** was synthesized in three steps from *L*-cystine, whilst thiophenol probe **2** was obtained commercially. These probes possess each of the characteristics of an ideal pharmacophore probe. In addition to the thiol functionality, both have a chromophore owing to the aromatic ring and a conspicuous MS isotopic pattern (^{81}Br:^{79}Br 1:1 and ^{35}Cl:^{37}Cl 3:1). Though UV-active halogenated metabolites are not entirely uncommon, prior analysis of an extract can rapidly identify these endogenous molecules and thereby discount them as labeled electrophilic natural products. The rationale for different halogen atoms on probes **1** and **2** will be discussed later

Both probes incorporate a halogenated aromatic ring. The introduction of this moiety, especially bromobenzoyl substituents, is a long-established method for obtaining crystalline derivatives of natural products that are amenable to X-ray crystallographic analysis.[17-21] Thus, the probes not only react with the desired pharmacophore but produce an adduct that is inherently more crystalline. The cysteine probe, furthermore, contains a defined *R*-stereocenter that facilitates determinations of absolute stereochemistry.
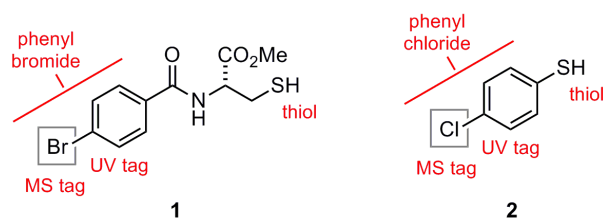
Figure 2.1 Pharmacophore probes **1** and **2**.

We relied initially on four substrates to assess the coupling efficiency of our thiol probes and optimize reaction conditions. Parthenolide (**3**) from feverfew (*Tanacetum parthenium*) contains a reactive butenolide moiety that is known to interact covalently with Cys171 of Iκβ kinase and inhibit this enzyme (**12**) (Figure 2.2).[22] Treatment of **3** with probe **1** in triethylamine and *N,N*-dimethylformamide (DMF) afforded **4** as a single isomer in 36% yield after HPLC purification. The addition of triethylamine was essential for the reaction to proceed at an appreciable rate, presumably via formation of the corresponding thiolate. Andrographolide (**5**) from the plant *Andrographis paniculata* contains a substituted butenolide that reacts with Cys62 of p50 and so inhibits NF-κB activation (**13**).[23] The probe efficiently reacted with **5** as well to give **6** as a mixture of diastereomers. The formation of diastereomeric products is not desired since it complicates the analysis, but we were able to purify the major diastereomer using reversed-phase HPLC. Via reaction with Lys802, wortmannin (**7**) from the fungus *Talaromyces wortmanii* is a covalent inhibitor of phosphoinositide 3-kinase (**14**).[24-27] Metabolite **7** reacted with thiol **1** in a manner completely analogous to the natural product's mechanism of action, producing a ring-opened structure. Importantly, this particular reaction was conducted in dichloromethane (DCM) since undesired elimination reactions occurred in DMF. The most famous electrophilic natural product,

penicillin G (**9**), contains a β-lactam ring that is essential for its antibacterial activity. The mechanism of action of **9** involves acylation of a key serine residue of the bacterial transpeptidase enzyme (**15**).[28] Thiol **1** engaged in an efficient coupling reaction with **9** to cleanly produce a pair of diastereomers. Purification and NMR analysis of the amino acid **10** proved difficult so the labeling reaction was immediately followed by acetylation to give **11**.
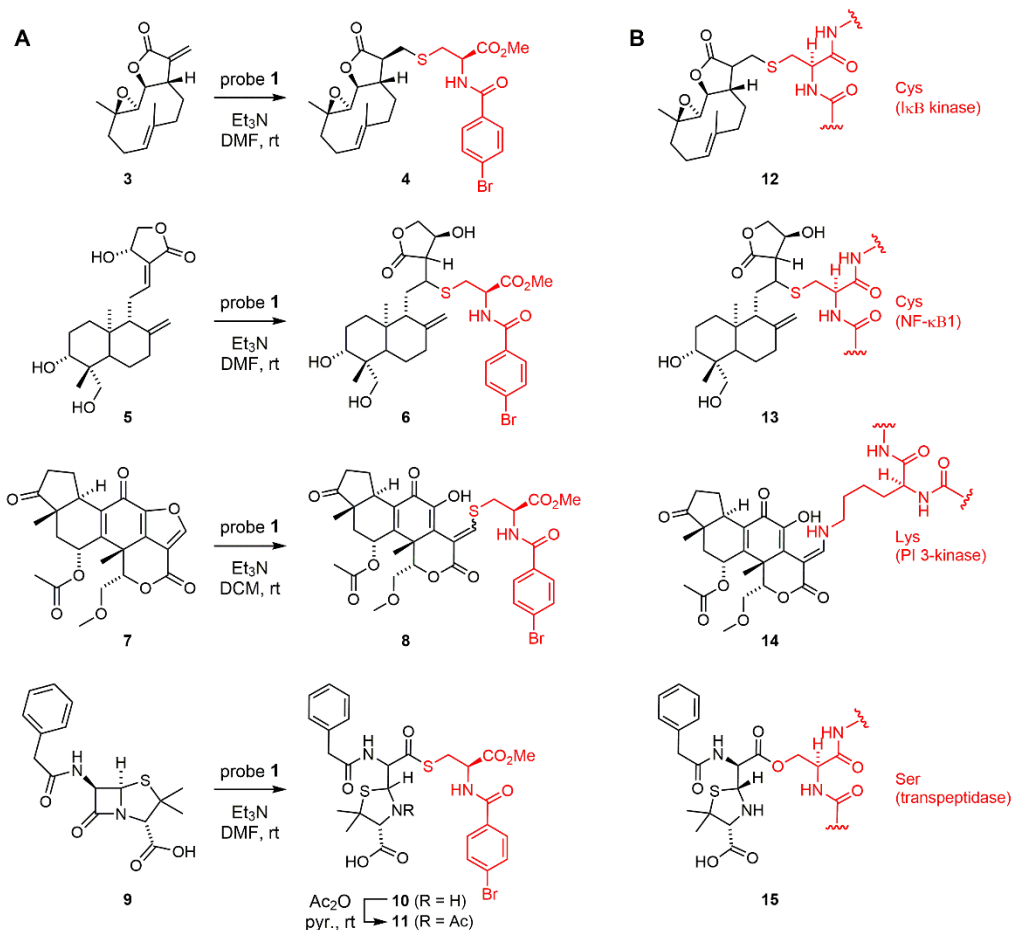
Figure 2.2 (A) Reaction of probe **1** with enone- and β-lactam-based electrophilic natural products parthenolide (**3**), andrographolide (**5**), wortmannin (**7**), penicillin G (**9**). Et₃N = triethylamine, DMF = *N*,*N*-dimethylformamide, DCM = dichloromethane, Ac₂O = acetic anhydride, pyr. = pyridine, rt = room temperature. (B) Natural products bound to the key nucleophilic amino acid residue of their respective cellular targets.

2.3.2 Development and validation of thiol probes with crude natural products

22

We then screened a number of strains from the tropical marine bacterial genus *Salinispora* in order to demonstrate the method in crude extracts. Upon reaction of **1** with the extract of *S. tropica* strain CNB-392, we observed the formation of two new compounds with UV absorption at 254 nm and brominated isotope patterns (Figure 2.3). Surprisingly, of the scores of other metabolites in the crude extract, none appeared to react with the probe. The first adduct, thioester **16**, was purified and analyzed by NMR and then retrosynthetically disconnected to salinosporamide A (**18**), a well-known covalent proteasome inhibitor from *Salinispora*.[44] The second adduct, thioester **17**, is highly reminiscent of the threonine adduct in the crystal structure of the enzyme-inhibitor complex (**19**).[30] Thus, whether the electrophilic moiety is an α,β-unsaturated enone, an α,β,γ,δ-unsaturated enone, a β-lactam or β-lactone, the thiol probe simultaneously tags the compound and elucidates its mode of action by mimicking the key nucleophilic residue on the cellular target responsible for covalent binding. This occurs whether the key amino acid residue on the target is cysteine, lysine, serine or threonine (see Figure 2.2, **12**–**15**).

Notably, a saturated solution of thioester **17** in benzene produced crystals amenable to X-ray analysis within 12 h (see Figure 2.3). A common characteristic of molecules containing a "heavy" bromine atom and a key feature of the method, a near-zero Flack parameter of 0.068 was readily obtained and allowed for the unambiguous assignment of the absolute configuration of **17** and, hence, the natural product (**18**).[31]
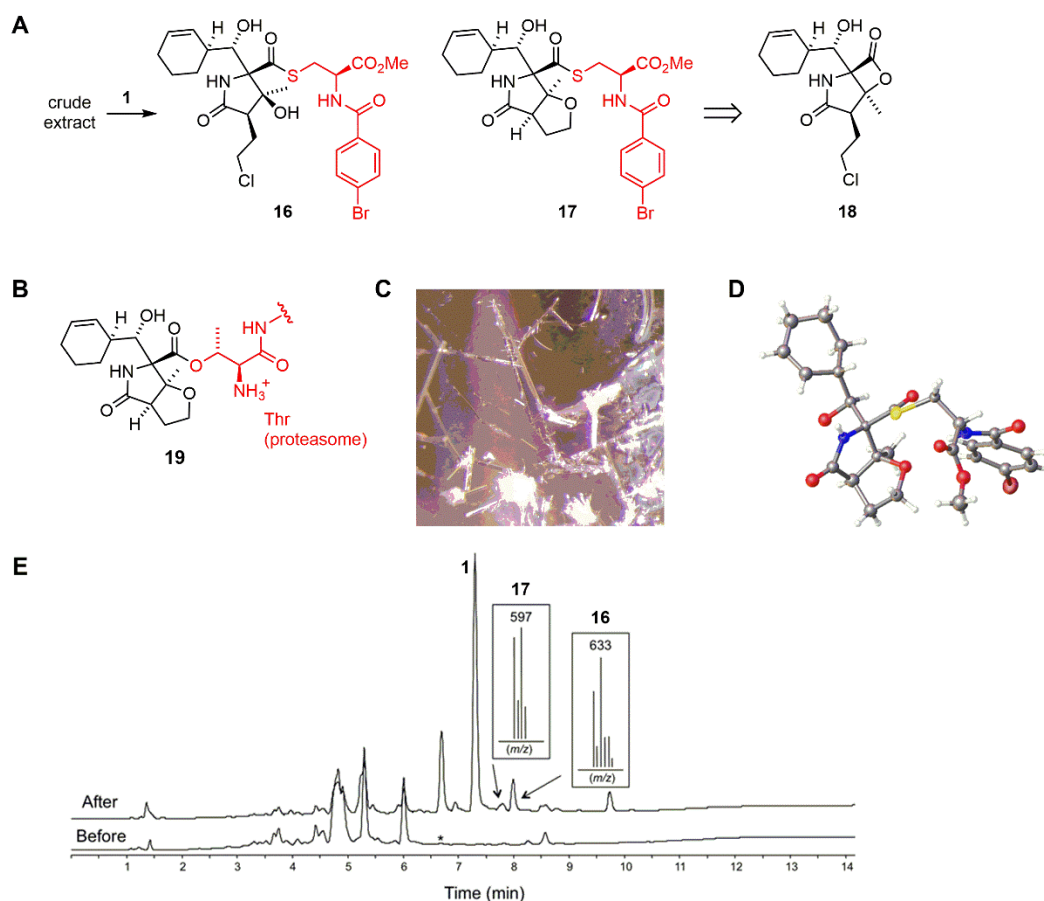
Figure 2.3 Reactivity-guided isolation of salinosporamide A (**18**). A) Reaction of probe **1** with the crude extract of strain CNB-392 produces brominated products **16** and **17**, which can be retrosynthetically traced back to salinosporamide A (**18**). (B) Salinosporamide A bound to the proteasome. (C) Crystals of **17** formed via slow evaporation from benzene. (D) X-ray crystal structure of **17**. (E) LC/MS chromatogram (254 nm) of the crude extract before and after treatment with **1**, including the conspicuous MS isotope clusters of **16** and **17**. The retention time of **18** is indicated with an asterisk.

Although probe **1** is capable of engaging enone-, β-lactam-, and β-lactone-based electrophilic metabolites, its reactivity with epoxide-based electrophilic natural products was poor. Using triptolide (**20**), originally discovered from thunder god vine (*Tripterygium wilfordii*), and the bacterial metabolite epoxomicin (**22**) as model substrates, we determined that thiophenol probe **2** displayed remarkable reactivity

24

toward epoxides (Figure 2.4). It has been shown that triptolide (**20**) exerts its biological effects via inhibition and covalent modification of Cys342 of the transcription factor TFIIA (**24**).[32-34] In a manner that predicted the particular epoxide that is modified by the enzyme, the probe reacted with the 12,13-epoxide of **20** to yield **21**.[34] Likewise, epoxomicin (**22**), a covalent proteasome inhibitor with an epoxy ketone functionality, gave **23** under the same conditions.[35] Unlike adducts formed from **1** and enone-, β-lactam-, and β-lactone-based electrophilic natural products, the structure of **23** does not mimic the morpholino adduct observed in the co-crystal structure of **22** and the proteasome, which like other covalent proteasome inhibitors involves reaction with the N-terminal threonine residue (**25**).[36]
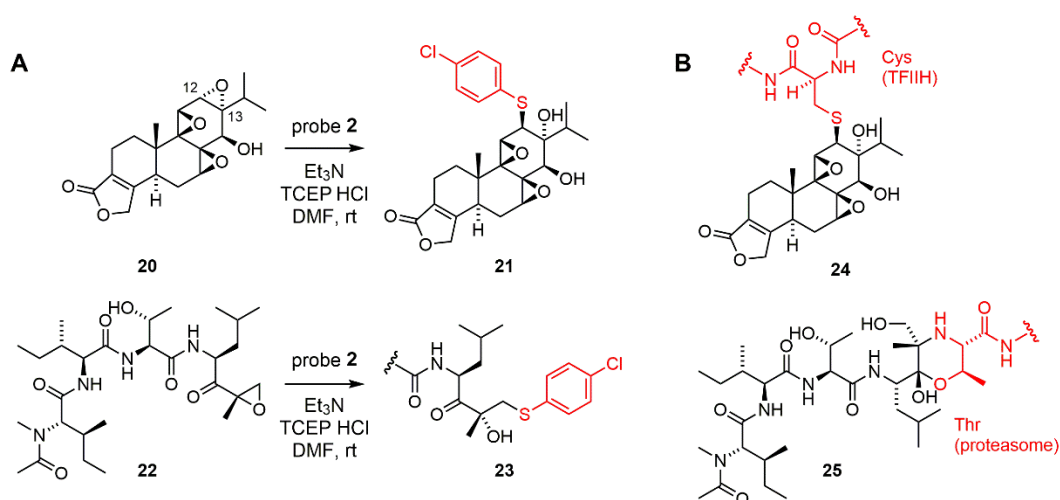
Figure 2.4 (A) Reaction of probe **2** with epoxide-based electrophilic natural products triptolide (**20**) and epoxomicin (**22**). Et₃N = triethylamine, TCEP HCl = tris(2-carboxyethyl)phosphine hydrochloride, DMF = N,N-dimethylformamide, rt = room temperature. (B) Natural products bound to the key nucleophilic amino acid residue of their respective cellular targets.

In order to demonstrate the effectiveness of probe **2** in crude extracts, we first treated extract from *Streptomyces hygroscopicus* strain ATCC 53709 with probe **2**. This gave a major chlorinated adduct (**26**), which was retrosynthetically disconnected to the

proteasome inhibitor eponemycin (**27**), in addition to several minor chlorinated

compounds from eponemycin analogues (Figure 2.5).[37,38] Like epoxomicin (**22**) the

epoxide moiety in **27** is essential for the molecule's potent irreversible inhibition of the

proteasome. When probe **2** was treated with extract from *Streptomyces* sp. strain CNB-

382, a suite of chlorinated compounds was produced. The major adduct (**28**) can be

traced back to cyclomarin A (**29**).[39] The other chlorinated compounds were derived from

new cyclomarin analogues. In terms of its purported activity against *Mycobacterium*

tuberculosis, which involves inhibition of the ClpC1 subunit of the caseinolytic

protease,[40,41] and its activity against malaria,[42] the epoxide is dispensable. Treatment of

extract from *Streptomyces* sp. strain CNB-091 with probe **2** yielded a single chlorinated

product (**30**), which is derived from salinamide A (**31**), in addition to the chloride-

containing analogue salinamide B.[43,44] Again, the epoxide ring is not required for

inhibition of bacterial RNA polymerase.[45,46] Thus, reactivity-guided isolation of epoxide-

containing natural products with probe **2** leads to the discovery of epoxide-based

electrophilic natural products, like eponemycin, as well as natural products that contain

epoxides that do not appear involved in the mechanism of action, like cyclomarin and

salinamide.

Probe **1** reacts much more readily with β-lactam- and β-lactone-based

electrophilic natural products and probe **2** reacts much faster with epoxide-containing

natural products. This orthogonal reactivity allows them to be employed in extracts

simultaneously. Since probe **1** is brominated and probe **2** is chlorinated, the isotopic

patterns of labelled natural products point toward their structural origin. Competition

experiments using probes **1** and **2** indicated that brominated probe **1** reacted exclusively

with the β-lactam in penicillin G (**9**) and the β-lactone in salinosporamide A (**18**) whilst

chlorinated probe **2** alone reacted with the epoxide in salinamide A (**31**). Interestingly,

some chlorinated products formed from reaction of salinosporamide A (**18**) and probe **2**

via a substitution reaction with the alkyl chloride functionality in **18**. This result was

validated using salinosporamide B, which lacks an alkyl chloride and shows no reactivity

with probe **2**. Probe reactivity was not exclusive with parthenolide (**3**), which bears a

highly-reactive exocyclic enone, as a ~1:1 mixture of brominated and chlorinated

parthenolide adducts was produced.

Figure 2.5 Reactivity-guided isolation of eponemycin (**27**), cyclomarin (**29**), and salinamide (**31**). Reaction of probe **2** with the crude extract of (A) strain ATCC 53709 produces chlorinated product **26**, (C) strain CNB-382 gives chlorinated product **28**, and (E) strain CNB-091 gives chlorinated product **30**. (B,D,F) LC/MS chromatograms (254 nm) of the crude extracts before and after treatment with **2**, including the conspicuous MS isotope clusters of **26**, **28**, and **30**. The retention times of **27**, **29**, and **31** are indicated with an asterisk.

A crude extract → **2** → **26** ⟹ eponemycin (**27**)

B

C crude extract → **2** → **28** ⟹ cyclomarin A (**29**)

D

E crude extract → **2** → **30** ⟹ salinamide A (**31**)

F

29

2.3.3 First discovery of antibacterial tirandalydigin in *Salinispora* spp.

Though genome mining techniques that can predict natural product structures have progressed considerably, detecting and isolating gene products produced in minute quantities still remains a challenge. As reactivity-guided isolation directly probes molecular structure, it is an ideal method for enabling genome mining efforts. For instance, the genome of *Salinospora pacifica* strain CNT-003 contained an orphan gene cluster that was predicted to encode a member of the tirandamycin family of natural products (Figure 1.6).[47] While screening *Salinispora* extracts with the probes, we noticed the formation of a distinct chlorinated adduct (**32**) upon reaction of **2** with the extract of strain CNT-003. We suspected that we had labelled the gene product of the tirandamycin cluster, as many of these metabolites contain epoxides. In this case, the probe-natural product adduct was not isolated. Instead, the molecular formula of the original metabolite was calculated to be $C_{22}H_{27}NO_6$, and the compound was then directly isolated from the crude extract using its calculated mass and predicted UV properties. The ^{1}H NMR spectrum clearly matched tirandalydigin (**33**), a compound closely related biosynthetically and structurally to the tirandamycins.[48,49] Like cyclomarin A (**28**) and salinamide A (**31**), the epoxide in **33** does not appear essential to its activity as a bacterial RNA polymerase inhibitor.
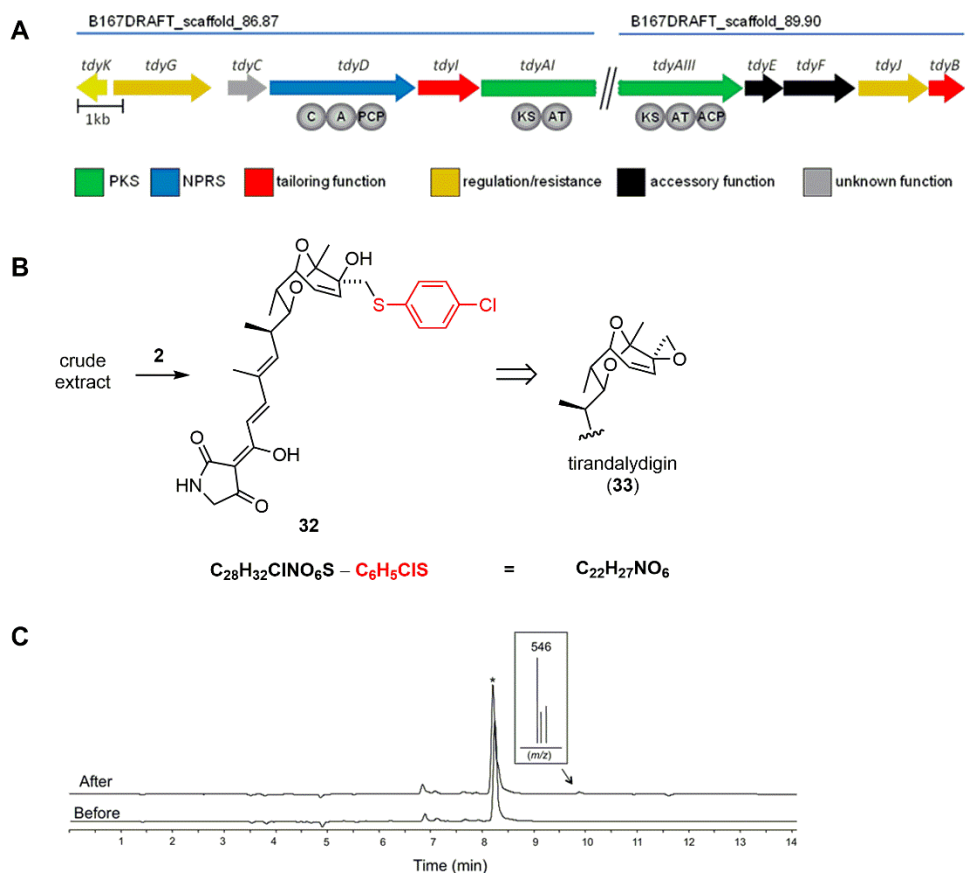
Figure 2.6 Using reactivity-guided isolation to validate genome mining efforts: A) A partial NRPS-PKS hybrid gene cluster found in *Salinispora pacifica* strain CNT-003 and analyzed bioinformatically to code for a natural product in the tirandamycin family (Tdy). The gene cluster is located on two contigs and is missing 6 PKS modules; B) Reaction of probe **2** with crude CNT-003 extract gave a single labelled compound (**32**). The molecular formula calculated for the original natural product was $C_{22}H_{27}NO_6$, which matched tirandalydigin (**33**). Epoxide **33** was then detected and isolated from the extract using its calculated mass. NRPS (nonribosomal peptide synthetase), PKS (polyketide synthase), KS (ketosynthase domain), AT (acyltransferase domain), ACP (acyl carrier protein), C (condensation domain), A (adenylation domain), PCP (peptidyl carrier protein)

2.3.4 Assessment of biological activity of electrophilic natural products and adducts

Given the central role that the electrophilic moieties play in the natural products' biological activity, we examined the relative cytotoxicity of the natural products and their corresponding thiol adducts (Table 2.1). Against the HCT-116 colon cancer cell line,

31

enones **3**, **5**, and **7**, as well as their corresponding thiol adducts **4**, **6**, and **8**, showed

only moderate cytotoxicity (11−32 µM). Salinosporamide (**18**) (IC_{50} = 41 nM) was

converted into thioester **16**, which maintained remarkable activity (IC_{50} = 14 nM), and

thioester **17**, which showed little cytotoxicity (IC_{50} = 14 µM). Like lactacystin and other

salinosporamide-based thioesters,[50,51] **16** is capable of reforming the β-lactone ring that

is crucial to proteasome inhibition, while **17** cannot undergo this transformation.[52,53] The

cytotoxicity of the epoxide-based electrophilic natural products **20**, **22**, and **27** is greatly

diminished 100−1000 fold upon ring-opening thioether formation, highlighting the

importance of this reactive pharmacophore. Metabolites **9**, **29**, and **31**, which have

demonstrated antibacterial activity and prokaryotic targets, and their derivatives were

not tested in the HCT-116 bioassay.

Table 2.1 Cytotoxicity of selected compounds against the human colon cancer line HCT-116

natural product	cytotoxicity (IC_{50}, µM)	thiol adduct	cytotoxicity (IC_{50}, µM)
18	0.041	**16**	0.014
		17	14
20	0.0080	**21**	62
22	0.0054	**23**	85
27	0.17	**26**	24

2.3.5 Labelling neolymphostins from *Salinispora arenicola* crude extract and further clarifying their mechanism of action

Treatment of crude extract from *Salinispora arenicola* strain CNY-486 with **1** in

triethylamine and *N*,*N*-dimethylformamide produced two pairs of diastereomeric adducts

with a mass isotope pattern that indicated the presence of a single bromine atom

(Figure 2.7). The formation of diastereomeric products is indicative of an electrophilic natural product containing a Michael acceptor, since the reaction involves the formation of new stereocenters with little to no diastereoselectivity. A pair of diastereomers (**34a**, **34b**) were purified by reversed phase C18 HPLC, and their structures were determined using a combination of NMR and MS techniques. Retrosynthetic analysis led to the identification of neolymphostin A (**36**), which revealed that reaction occurred at the vinylogous ester substituent (C-11) of the natural product.[54-57] The other diasteromeric pair of adducts (**35a, 35b**) stemming from neolymphostin B (**37**) were also isolated and characterized (Figure 2.7).

As the lymphostins have been reported to inhibit lymphocyte-specific tyrosine kinase (Lck), phosphoinositide 3-kinase (PI3K), and the mammalian target of rapamycin (mTOR),[54,56,57] we first set out to determine if our isolated natural product showed similar activity using an active-site dependent competition binding assay.[58] Indeed, neolymphostin (**36**) showed strong affinity for all four isoforms of PI3K [K_d = 0.88 (α), 5.7 (β), 3.5 (γ), and 4.9 (δ) nM] and mTOR (K_d = 10 nM). Binding to Lck, however, was less pronounced (K_d = 4.6 μM). For comparison, wortmannin, a fungal natural product and well-established covalent PI3K inhibitor, was also measured in the binding assay. This metabolite showed strong affinity for PI3K [K_d = 5.4 (α), 7.6 (β), 15 (γ), and 5.5 (δ) nM] but little affinity for mTOR (K_d = 9.2 μM).[59-61]
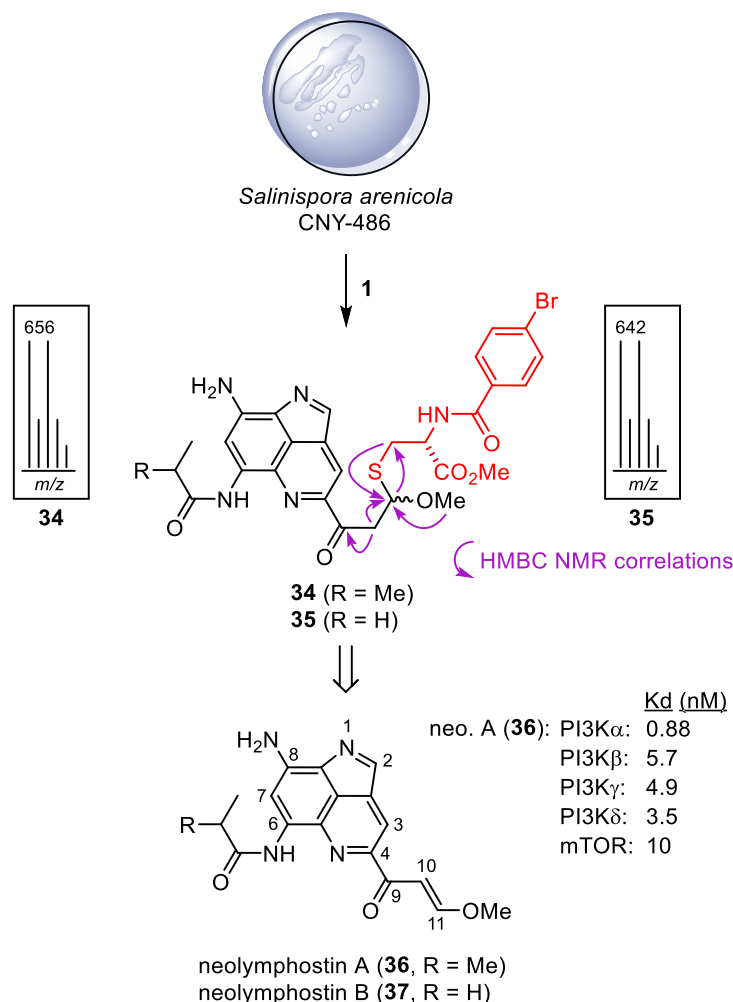
Figure 2.7 Identification of neolymphostin as an electrophilic natural product. Treatment of extract from *Salinispora* strain CNY-486 with **1** produced brominated adducts **34** and **35**, both as a mixture of diastereomers, which are derived from neolymphostin A (**36**) and B (37).

To rapidly assess whether the interaction of neolymphostin with the PI3Ks was reversible or irreversible, we then measured the K_d for neolymphostin-treated PI3Kα and PI3Kγ with and without an intermediate dilution step according to the scanKINETIC platform (Figure 2.8A). In study arm A and C, the inhibitor and kinase were combined and equilibrated for 6 h and 1 h, respectively, before measuring the K_d. The fact that these dissociation constants are comparable suggests rapid association kinetics. In

study arm B the inhibitor and kinase were combined and equilibrated for 1 h, diluted 30-fold, and re-equilibrated before measuring the K_d, while in study arm D the pair were immediately diluted and equilibrated before measuring the K_d. Importantly, dilution after inhibitor and kinase were first combined gave dissociation constants similar to study arm C, which is expected of a covalent inhibitor. Known covalent kinase inhibitors like wortmannin show the same pattern.

To verify that the inhibition identified was due to covalent attachment and to identify the site of modification, we carried out mass spectrometry tandem MS/MS experiments on the full-length complex of PI3Kα (composed of the proteins p110α and p85α). The tandem MS/MS data of pepsin-generated peptides was queried for modification of lysine side chains, since docking experiments suggested an appropriately positioned lysine residue was present in the binding pocket. Searches were carried out for lysine modifications of either 306.11 or 338.14 amu, which correspond to the mass of neolymphostin with or without subsequent elimination of methanol. Covalent modification was detected for only a single amino acid in PI3Kα, corresponding to a +306.11 amu modification on Lys802 (Figure 2.8B), and a timecourse experiment showed that modification of the kinase was complete within 2 min. This is the same catalytic residue that is covalently modified upon addition of wortmannin, revealing that bacteria and fungi produce metabolites able to target this conserved residue in the PI3K family of enzymes.[59]
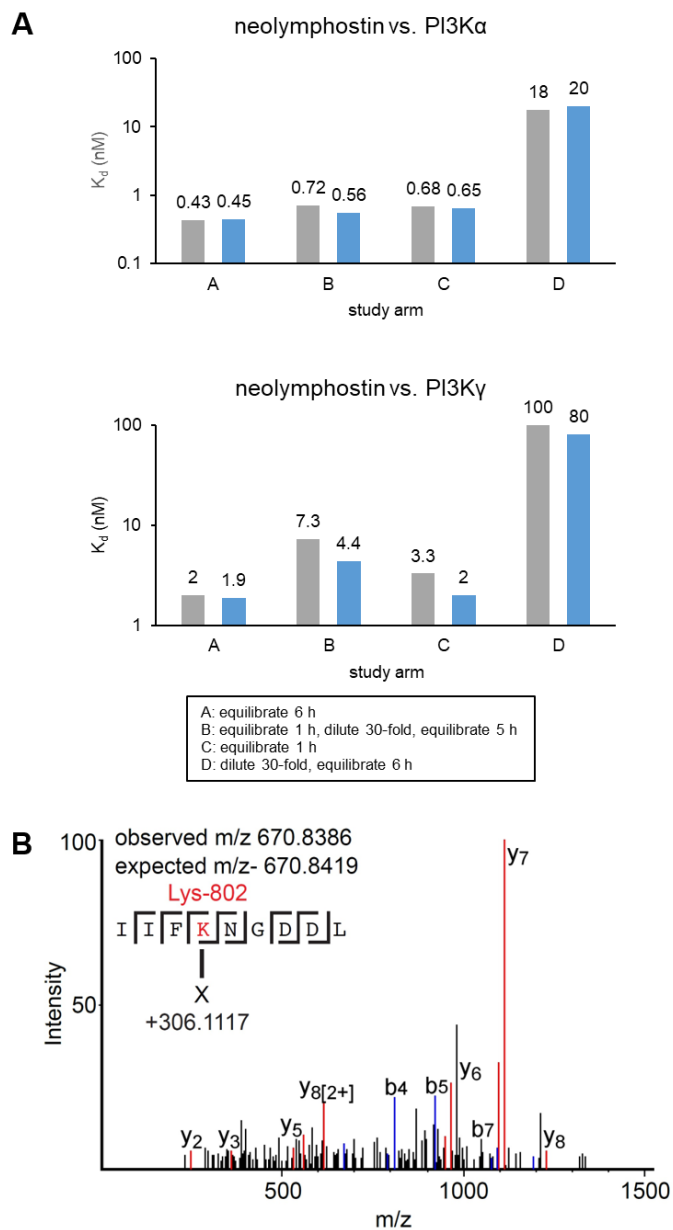
Figure 2.8 The interaction of neolymphostin with the PI3Ks is covalent. A) Incubation studies with PI3Kα and PI3Kγ performed in duplicate (first: grey; second: blue) B) Tandem MS/MS spectrum of a neolymphostin-modified PI3Kα peptide containing Lys802. Different b and y fragments and their location are indicated, with both the observed and expected masses of the precursor annotated.

2.3.6 Labelling non-cytotoxic natural products, jamaicamides and phycocyabillins

In our continued efforts to discover new ENPs using the thiol labelling method,

we identified a "hit" in an extract from cyanobacterial strain *Moorea producens* JHB with

UV absorbance at 254 nm and a distinct dibromo-chloro isotope pattern (see Figure 2.9). The pseudomolecular ion m/z $(M+H)^+$ 884.1335 was consistent with the molecular formula $C_{38}H_{48}Br_2ClN_3O_7S$ (calcd for $C_{38}H_{49}Br_2ClN_3O_7S$ 884.1341). Subsequent structure elucidation by ^1H and 2D NMR revealed **38**, which was retrosynthetically disconnected to give jamaicamide A (**40**).[62] Thiol **1** appeared to have added to the *N*-acyl-5-methyl-3-pyrrolin-2-one moiety in a highly diastereoselective manner to give a *trans*-substituted pyrrolidinone. Another adduct (**39**) with a bromo-chloro isotope pattern was derived from jamaicamide B (**41**).

Additionally, we utilized thiol probes **1**-**2** to explore the reactivity of cyanobacterial bile pigment phycocyanobilin (PCB). PCB was obtained from refluxing of commercial colorant Linablue G1 in ethanol using an optimized protocol.[63] This colorant contains phycocyanin, a photosynthetic protein from the cyanobacterium *Arthrospira platensis* that is covalently bonded to PCB via thioether linkage. The reaction mixture was purified by flash chromatography to yield a fraction concentrated in PCB and containing PCB derivatives in minor quantities. A portion of this material was esterified with EtOH and H_2SO_4 (50:1) to yield PCB di-ethyl ester as the main product. Thiophenol **2**, and not **1**, efficiently reacted with PCB, both before and after esterification, to give a more hydrophobic adduct with pseudo-molecular ions at m/z 775.2132 $[M+H]^+$, calcd for $C_{39}H_{44}BrN_4O_6S$, 775.2165 and at m/z 831.2800 $[M+H]^+$, calcd for $C_{43}H_{52}BrN_4O_6S$, 831.2791, respectively. Notably, no base was employed in these reactions. Isolation and NMR structural elucidation of adducts **42** and **43** confirmed the site of covalent bond formation to be the expected 3' position of PCB ($\delta_{C(42)}$ = 48.2 and $\delta_{C(43)}$ = 47.8

ppm) (Figure 2.10). This is exactly the same position modified by a cysteine residue in phycocyanin to form the holoprotein.
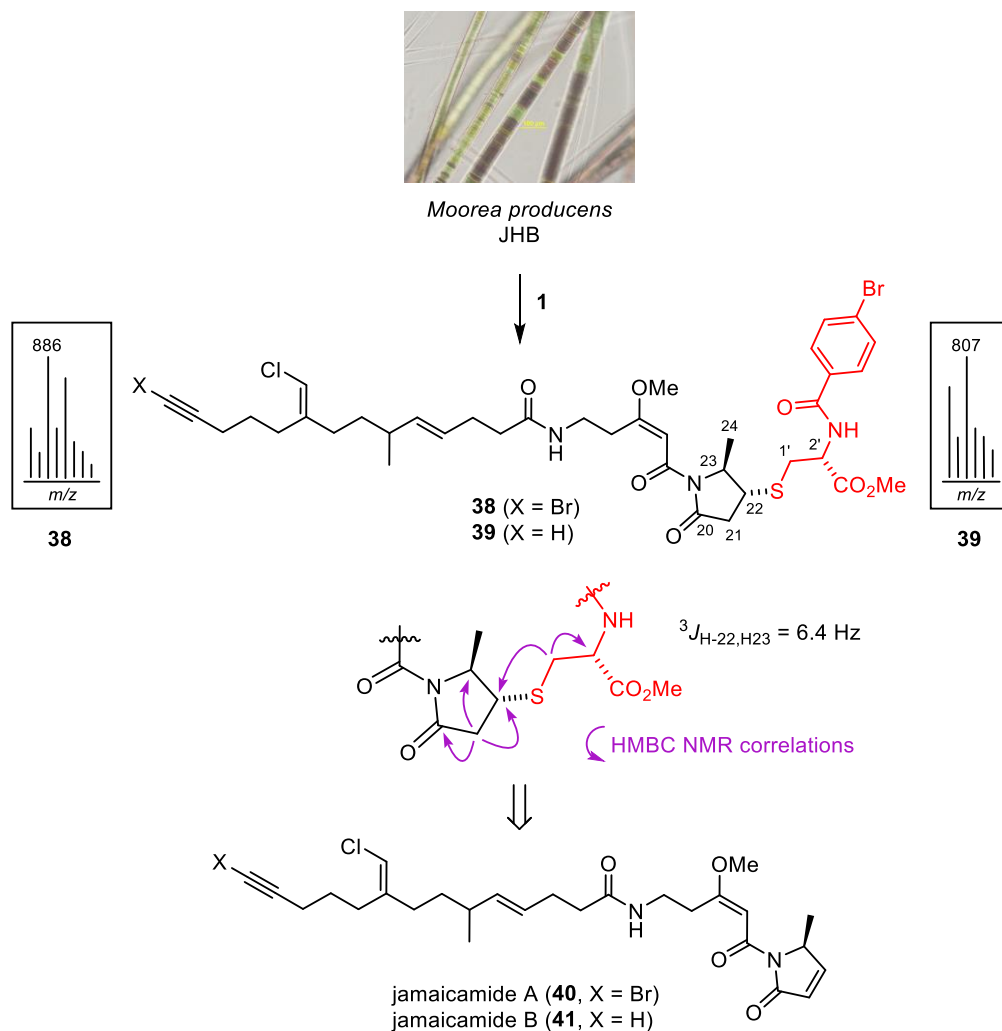
Figure 2.9 Reactivity-guided isolation of jamaicamides A (**4**) and B (**5**) from *Moorea producens* strain JHB extract. Treatment of extract with **1** produced dibromo-chloro adduct **2** and bromo-chloro adduct **3**, which are derived from **4** and **5**, respectively.
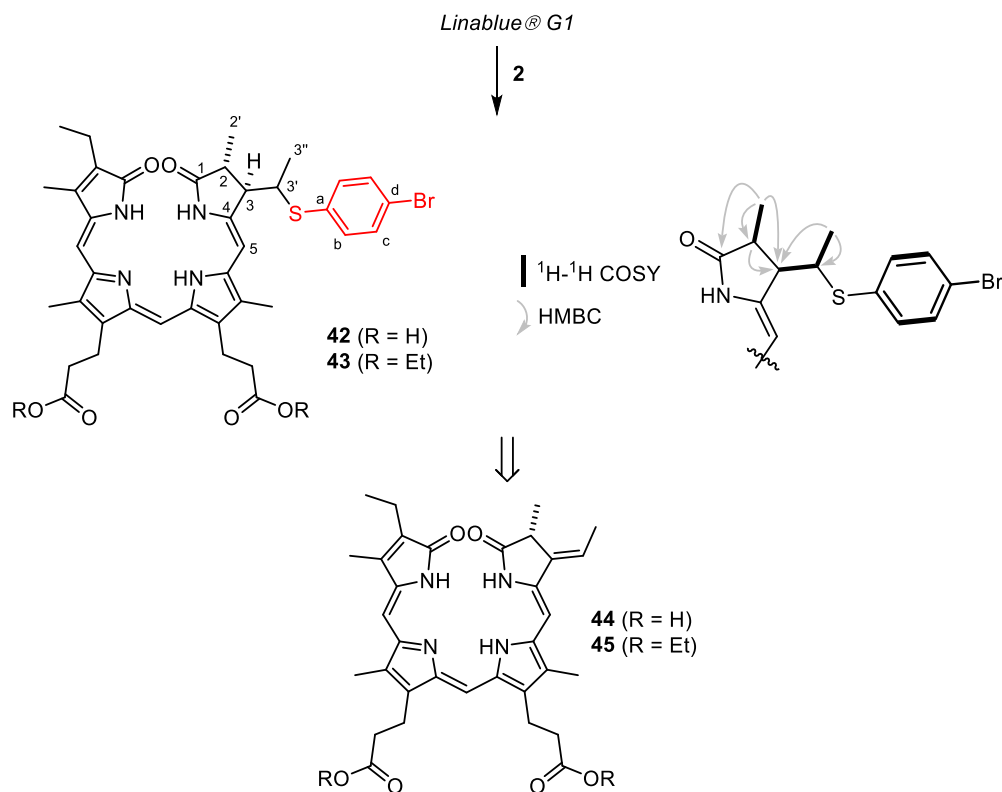
Figure 2.10 Reactivity of phycocaynobilin (**44**) and phycocyanobilin di-ethyl ester (**45**) from commercial colorant Linablue G1. Treatment of extract of ethanolyzed Linablue G1 with **1** produced **42** and **43**.

In contrast to our previous findings with electrophilic natural products, jamaicamide A (**40**) and phycocyanobilin (**44**) do not have cytotoxic properties and so do not appear to irreversibly inhibit any enzyme crucial for cellular viability. Against H-460 human lung and Neuro-2a mouse neuroblastoma cell lines, **40** was only moderately cytotoxic with an LC_{50} of 15 µM.[62] Similarly, ammosamide C, another compound recently identified using thiol **1**, has little *in vitro* cytotoxicity toward an HCT-116 colon

cancer cell line.[64] These compounds, therefore, do not have a straightforward biomedical application as chemotherapeutic agents.

However, an intriguing application of these molecules may be as activators of the Keap1-Nrf2 pathway, where their thiol reactivity and lack of apparent cytotoxicity become an asset. The Keap1-Nrf2 pathway plays an important role in cells by detecting and detoxifying harmful electrophilic compounds.[65-67] Keap1 is a repressor protein that resides in the cell cytoplasm and associates with the transcription factor Nrf2, funneling it into the ubiquitin proteasome pathway. Keap1 "senses" toxic electrophilic and reactive oxygen species in a cell when several of its exposed cysteine residues are covalently modified via nucleophilic substitution and conjugate addition reactions. This results in a conformational change that causes Keap1 to dissociate from Nrf2. Nrf2 is then free to enter the nucleus and induce the expression of detoxifying enzymes by binding to the antioxidant response element (ARE) in the regulatory regions of certain genes. Importantly, the Keap1-Nrf2 pathway can be activated by exogenous small molecules that disrupt the protein-protein interaction (PPI) between Keap1 and Nrf2. This produces a resilient cell population that is resistant to oxidative and electrophilic insults and mitigates a number of pathological disorders.[67]

One method of activating this pathway is to disrupt the Keap1-Nrf2 PPI by taking advantage of the cysteine-rich nature of Keap1 and introducing electrophilic, thiol-reactive compounds into the cell. Each molecule has a readily-identifiable electrophilic warhead that presumably reacts with key Keap1 cysteine residues. Importantly, these electrophilic Keap1 inhibitors must tread a fine line between behaving like highly-reactive promiscuous electrophiles that are likely to produce off-target toxicity and weak

40

electrophiles that lack reactivity with Keap1. Due to the concern of possible off-target

reactions and a general malaise for electrophilic compounds, most recent efforts in the

drug industry have sought to disrupt the Keap1-Nrf2 interaction using compounds that

interact non-covalently with the target.[66,68,69] Nonetheless, dimethylfumarate is an FDA

approved drug and several clinical trials involving electrophilic Keap1 inhibitors are

ongoing.[70]

2.4 CONCLUSIONS

The tremendous potential for the discovery of natural products that inspire new

drugs has not been realized because there is a shortage in the number of new methods.

Reactivity-guided isolation, a hybrid of traditional natural products chemistry and

synthetic organic chemistry, was invented to help access the high value chemical space

of natural product extracts. This approach, which can be applied to bacterial, fungal,

and plant extracts alike, could transform the field of natural products.

Here, we show that neolymphostin, a closely-related derivative of lymphostin, is a

covalent kinase inhibitor that competitively binds to the ATP-binding pocket of the PI3-

kinases and mTOR. Given that the lymphostins possess a relatively simple ATP-like

structure devoid of any chirality, the level of selectivity that neolymphostin demonstrated

in the kinase panel toward the PI3Ks and mTOR is somewhat surprising. Further

studies are needed to understand the structural basis for the kinase selectivity of the

inhibitors.

There are many natural products with electrophilic functional groups that seem to

be non-cytotoxic, for example jamaicamide and PCB, and nonetheless, are reactive

towards the thiol probes used in this study. An application for such compounds could be

to serve as inhibitors of the Keap1-Nrft PPI and therefore, activate the Keap1-Nrf2-ARE pathway that lead to expression of proteins, genes, and metabolites that protect the cell.

2.5 METHODS

Preparation of cysteine thiol probe (1). To cooled methanol (150 mL) at 0 °C was slowly added thionyl chloride (7.60 mL, 105 mmol) followed by L-cystine (10.0 g, 41.6 mmol), and the reaction mixture was heated at reflux for 12 h. The solution was concentrated until the volume was reduced to 15 mL. Diethyl ether (30 mL) was added, and 12.4 g of cystine dimethyl ester precipitated out of solution. To a white heterogeneous solution of the dimethyl ester (3.64 g, 13.6 mmol) in acetonitrile (150 mL), 4-bromobenzoyl chloride (6.22 g, 28.7 mmol) and triethylamine (7.50 mL, 54.3 mmol) were added. The reaction mixture left stirring for 2 h. A saturated ammonium chloride solution (300 mL) was added, and the resulting solution was extracted with ethyl acetate (2 x 200 mL). The combined organic extracts were washed with a saturated sodium bicarbonate solution (400 mL), brine (200 mL), dried over Na_2SO_4, and concentrated. A saturated solution of the product in dichloromethane (50 mL) was prepared. Then, hexanes (30 mL) was added to the solution, and 6.96 g (81%) of dibromobenzoyl disulfide precipitated out of solution. To a solution of the disulfide (6.0 g, 9.4 mmol) in a 2:1 dichloromethane-methanol mixture, tris(2-chloroethyl)phosphine hydrochloride salt (4.0 g, 14 mmol) and triethylamine (5.0 mL, 38 mmol) were added. The reaction was left for 3 h. Flash chromatography of the crude material on silica gel (hexanes-ethyl acetate, 4:6) yielded 5.4 g (90%) of cysteine thiol probe (**1**) as a white solid. UV/Vis: λ_{max} = 241 nm; $[\alpha]_D$ = +3.3 (*c* 0.020, CHCl$_3$); IR (KBr) $\tilde{v}$ =3323, 1742, 1635, 1524, 1219 cm^{-1}; ^{1}H NMR 7.71 (d, 8.6 Hz, 2H), 7.61 (d, 8.6 Hz, 2H), 7.01 (br d,

1H), 5.07 (ddd, 7.1, 4.0, 4.0 Hz, 1H), 3.84 (s, 3H), 3.14 (dd, 9.1, 4.0 Hz, 2H), 1.38 (t, 9.1 Hz, 1H); ^{13}C NMR 170.3, 165.8, 132.1, 131.7, 128.5, 126.6, 53.7, 52.8, 26.7; HRESI-Q-TOF-MS: m/z (M+H)$^+$ 317.9800 calcd for $C_{11}H_{13}{}^{79}BrNO_3S$, found 317.9784.

Generation of crude extracts. *Streptomyces hygroscopicus* ATCC-53709 was grown in ISP1 medium (5 g L^{-1} of tryptone and 3 g L^{-1} of yeast extract in deionized water) while *Streptomyces* spp. CNB-091 and CNB-382 and *Salinispora* spp. CNB-392, CNT-003 and CNY-484 were grown in A1 seawater medium (10 g L^{-1} of starch, 4 g L^{-1} of yeast extract and 2 g L^{-1} of peptone in 75% seawater and 25% deionized water). From cryovials, these strains were first grown in starter cultures (25 mL) and after 7 days the whole volume was used to inoculate pre-cultures (1 L). After 3−4 days, 25 mL aliquots of the pre-cultures were used to inoculate producing cultures (1 L). The cultures were incubated at 27 °C with rotatory shaking at 150 rpm for 3−7 days, after which Amberlite XAD-16N resin (~20 g L^{-1}) was added and left shaking for 2 h. The resin was filtered through cheesecloth, washed with deionized water, and extracted with acetone. The acetone was removed under reduced pressure, and the resulting aqueous layer was extracted with ethyl acetate. The combined organic extracts were concentrated. *Moorea producens* JHB samples were prepared from material cultured in separate technical replicates in artificial seawater media using a 16–8 h standard light-dark cycle at 28°C. The cultures were collected by rapid vacuum filtration from the media at room temperature, combined, and extracted iteratively with 2:1 dichloromethane/methanol to afford the crude extract. The phycocyanin-based colorant Linablue G1 was purchased from DIC Europe GmBH (Düsseldorf, Germany). All other reagents and solvents were purchased commercially and were used without further purification. A suspension of

43

Linablue G1 (20 g) in 96% ethanol (250 mL) in a 500 mL round-bottomed flask was heated under reflux overnight in an oil bath at 95°C. The solution was allowed to cool and then directly filtered through a fritted Büchner funnel to remove precipitated protein. The deep blue filtrate was concentrated with a rotary evaporator to yield 1.4 g of crude material. This material was then fractionated on a Teledyne flash chromatography system (4 g C18 cartridge, 360 nm) with a 15 min solvent gradient from 10–100% solvent B followed by 100% solvent B (solvent A: water with 5 mM ammonium formate, pH 3.2; solvent B: 9:1 methanol/water with 5 mM ammonium formate, pH 3.2) and a 30 mL min–1 flow rate. Fractions containing PCB and derivatives were combined in separate flasks and concentrated to dryness with a rotary evaporator. In order to obtain esterified PCB, to a solution of the PCB mixture (20 mg) at room temperature was added a 50:1 EtOH:H2SO4 solution (2 mL). After 12 h at room temperature, the mixture was diluted with EtOAc (25 mL), washed successively with water (25 mL) and brine (25 mL), dried over sodium sulfate, and concentrated.

Labeling reaction. To pure natural product or crude extract, probe **1** or **2** (1.2−1.5 equiv), and triethylamine (2.0−4.2 equiv) was added dry *N,N*-dimethylformamide which had been previously sparged with gaseous nitrogen for 10 min. The reaction vessel was kept under inert atmosphere using a nitrogen gas source and bubbler. The reaction was conducted with or without added tris(2-chloroethyl)phosphine hydrochloride salt (1.2−1.4 equiv) to prevent unwanted dimerization of the probes. The progress of the reaction was monitored on an analytical Agilent 1100 Series HP system (1.0 mL min^{-1}) with UV (210 and 254 nm) and ELS detection, and also on an analytical Agilent 1260 Infinity Series LC system coupled to a

6530 Series Q-TOF mass spectrometer, both using a C18(2) Phenomenex Luna column (5 µm, 100 x 4.6 mm) with a 10 minute solvent gradient from 10 % to 100 % acetonitrile + 0.1% formic acid in water. When HPLC analysis indicated complete conversion (1.5−24 h), the mixture was concentrated. The adducts were then purified by isocratic reversed-phase HPLC (acetonitrile and water + 0.1% trifluoroacetic acid) using a C8(2) Phenomenex Luna column (5 µm, 250 x 10 mm) with UV detection (254 nm). Preparative reversed-phase HPLC purifications were performed with a C18(2) Phenomenex Luna column (10 µm, 250 x 21.2 mm) with UV detection (254 nm).

MS identification of covalent Lys802 modification. PI3Kα preincubated with 4 µM neolymphostin was brought to a final concentration of 0.8 µM in a total of 50 µL non-deuterated buffer (10 mM HEPES pH 7.5, 100 mM NaCl in water). After adding 20 µL of ice-cold quench buffer (2 M guanidine-HCl, 3% formic acid), the samples were immediately frozen in liquid nitrogen and stored at −80°C. Peptides were digested and separated in a similar manner to the HDX-MS method described below. Peptide identification was carried out in PEAKS 7. The search was performed with a mass error threshold of 5 ppm for precursors and 0.1 Da for fragments. Variable modification of Lys with a mass of 306.1117 was included. The false discovery rate for peptides was set at 0.1%.

Cytotoxicity assays. The human colorectal cancer cell line HCT-116 (ATCC CCL-247) was cultured in McCoy's 5A medium (Life Technologies) supplemented with 10% fetal bovine serum (FBS, Invitrogen), 30 mM HEPES (Fisher Scientific) and 100 µg mL^{-1} penicillin/streptomycin (Invitrogen) and incubated in tissue culture flasks with a surface of 75 cm² at 37 °C in a 5% CO_2 atmosphere. Routine passaging of cells was

conducted every 3 to 4 days. The cell layer was briefly rinsed in 10 mL Dulbecco's phosphate-buffered saline (DPBS) with Ca^{2+} and Mg^{2+} (Life Technologies) and detached from the culture flask using 2 mL of 0.25% (w/v) trypsin-EDTA (Life Technologies) at 37 °C. For the subcultivation 8 mL of complete McCoy's 5A medium was added to the detached cells, cells were aspirated by gently pipetting and then transferred into a new culture flask (1 mL into 20 mL fresh medium). Cytotoxicity in half maximal inhibitory concentrations (IC_{50}) of the natural products (**3**, **5**, **7**, **18**, **20**, **22**, **27**) and their adducts (**4**, **6**, **8**, **16**, **17**, **21**, **23**, **26**) were tested using the colorimetric 3-(4,5-dimethylthiazol-2-yl)-5-(3-carboxymethoxyphenyl)-2-(4-sulfophenyl)-2H-tetrazolium (MTS) bioassay. HCT-116 cells (2.5×10^4 cells mL^{-1}) were incubated for 24 h at 37 °C in a 5% CO_2 atmosphere in flat-bottom 96-well plates. Compounds in DMSO were added in a concentration of 10 mg mL^{-1}, 1 mg mL^{-1} or 0.1 mg mL^{-1} based on their activity, serially diluted, and incubated for additional 72 h. As reference, the standard anticancer drug etoposide VP-16 (Sigma Aldrich) with an IC_{50} of 0.49–4.9 µM in a concentration of 4 mg mL^{-1} in DMSO and DMSO (ATCC) were tested as positive and negative controls, respectively. IC_{50} values were determined after a 3 h incubation of the colorimetric indicator using MTS (1.9 mg mL^{-1} in DPBS, Promega) in the presence of phenazine methosulfate (PMS, 0.044 mg mL^{-1} in DPBS, Sigma Aldrich). MTS is reduced by living cells into a formazan product with an absorbance maximum at 490 nm in phosphate-buffered saline. Quantification of the formazan product at 490 nm representing the proportional cell survival rates and the calculation of the IC_{50} values were determined by an E^{Max} microplate reader (Molecular Devices) using the analysis software SoftMax Pro.

2.6 ACKNOWLEDGMENTS

2.7 REFERENCES

(1) Rudolf, G. C., Koch, M. F., Mandl, F. A. M., and Sieber, S. A. (2015) Subclass-specific labeling of protein-reactive natural products with customized nucleophilic probes. *Chem. - A Eur. J. 21, 3701–3707.*

(2) Drahl, C., Cravatt, B. F., and Sorensen, E. J. (2005) Protein-reactive natural products. *Angew. Chemie - Int. Ed. 44, 5788–5809.*

(3) Gersch, M., Kreuzer, J., and Sieber, S. A. (2012) Electrophilic natural products and their biological targets. *Nat. Prod. Rep. 29, 659–682.*

(4) Singh, J., Petter, R. C., Baillie, T. A., and Whitty, A. (2011) The resurgence of covalent drugs. *Nat. Rev. Drug Discov. 10, 307–317.*

(5) Sanderson, K. (2013) Irreversible kinase inhibitors gain traction. *Nat. Rev. Drug Discov. 12, 649–51.*

(6) Corey, E. J., Clark, D. A., Goto, G., Marfat, A., Mioskowski, C., Samuelsson, B., and Hammarstroem, S. (1980) Stereospecific total synthesis of a" slow reacting substance" of anaphylaxis, leukotriene C-1. *J. Am. Chem. Soc. 102, 1436–1439.*

(7) Corey, E. J., Albright, J. O., Barton, A. E., and Hashimoto, S. (1980) Chemical and enzymic syntheses of 5-HPETE , a key biological precursor of slow-reacting substance of anaphylaxis (SRS), and 5-HETE. *J. Am. Chem. Soc. 102, 1435–1436.*

(8) Llinás, A., Donoso, J., Vilanova, B., Frau, J., Muñoz, F., and Page, M. I. (2000) Thiol-catalysed hydrolysis of benzylpenicillin. *J. Chem. Soc. Perkin Trans. 2 1521–1525.*

(9) Martinelli, M. J., Vaidyanathan, R., Khau, V. Van, and Staszak, M. A. (2002) Reaction of cryptophycin 52 with thiols. *Tetrahedron Lett. 43, 3365–3367.*

(10) Oda, K., and Yoshida, A. (2003) Side chain substitution reaction of 2-arylsulfinyl and 2-arylsulfonyl intermediates for 1β-methylcarbapenems. *Tetrahedron Lett. 38, 3–4.*

(11) Naidu, B. N., Sorenson, M. E., Connolly, T. P., and Ueda, Y. (2003) Michael addition of amines and thiols to dehydroalanine amides: A remarkable rate acceleration in water. *J. Org. Chem. 68, 10098–10102.*

(12) Matsuura, F., Peters, R., Anada, M., Harried, S. S., Hao, J., and Kishi, Y. (2006) Unified total synthesis of pteriatoxins and their diastereomers. *J. Am. Chem. Soc. 128, 7463–7465.*

(13) Taubinger, A. A., Fenske, D., and Podlech, J. (2008) Synthesis of β,β-diamino acids from α-amino acid derived β-lactams. *Synlett 539–542.*

(14) Schoof, S., Pradel, G., Aminake, M. N., Ellinger, B., Baumann, S., Potowski, M., Najajreh, Y., Kirschner, M., and Arndt, H. D. (2010) Antiplasmodial thiostrepton derivatives: Proteasome inhibitors with a dual mode of action. *Angew. Chemie - Int. Ed. 49, 3317–3321.*

(15) Heinold, A., Siewert, B., Schwarz, S., Barthel, A., and Kluge, R. (2012) Full paper synthesis and biological evaluation of antitumor-active arglabin derivatives. *Arch. Pharm. (Weinheim). 345, 215–222.*

(16) Avonto, C., Taglialatela-scafati, O., Pollastro, F., Minassi, A., Marzo, V. Di, Petrocellis, L. De, and Appendino, G. (2011) An NMR spectroscopic method to identify and classify thiol- trapping agents : Revival of Michael acceptors for drug discovery? *Angew. Chemie - Int. Ed. 467–471.*

(17) Gerwick, W. H., Fenical, W., Engen, D. Van, and Clardy, J. (1980) Isolation and structure of spatol, a potent inhibitor of cell replication from the brown seaweed Spatoglossum schmittii. *J. Am. Chem. Soc. 7441, 7991–7993.*

(18) Pettit, G. P., Herald, D. L., Feng, G., Sengupta, D., and Herald, C. L. (1991) Antineoplastic agents. 200. Absolute configuration of the bryostatins. *J. Org. Chem. 97, 1337–1340.*

(19) Ondeyka, J. G., Helms, G. L., Hensens, O. D., Goetz, M. A., Zink, D. L., Tsipouras, A., Shoop, W. L., Slayton, L., Dombrowski, A. W., Polishook, J. D., Ostlind, D. A., Tsou, N. N., Ball, R. G., and Singh, S. B. (1997) Nodulisporic acid A, a novel and potent insecticide from a Nodulisporium sp. Isolation, structure determination, and chemical transformations. *J. Am. Chem. Soc. 7863, 8809–8816.*

(20) Shigemori, H., Komaki, H., Yazawa, K., Mikami, Y., Nemoto, A., Tanaka, Y., Sasaki, T., In, Y., Ishida, T., and Kobayashi, J. (1998) Brasilicardin A. A novel tricyclic metabolite with potent immunosuppressive activity from actinomycete Nocardia brasiliensis. *J. Org. Chem. 63, 6900–6904.*

(21) Brady, S. F., Bondi, S. M., and Clardy, J. (2001) The guanacastepenes: A highly diverse family of secondary metabolites produced by an endophytic fungus. *J. Am. Chem. Soc. 123, 9900–9901.*

(22) Kwok, B. H. B., Koh, B., Ndubuisi, M. I., Elofsson, M., and Crews, C. M. (2001) The anti-inflammatory natural product parthenolide from the medicinal herb Feverfew directly binds to and inhibits I-kappa B kinase. *Chem. Biol. 8, 759–766.*

(23) Xia, Y.-F., Ye, B.-Q., Li, Y.-D., Wang, J.-G., He, X.-J., Lin, X., Yao, X., Ma, D., Slungaard, A., Hebbel, R. P., Key, N. S., and Geng, J.-G. (2004) Andrographolide attenuates inflammation by inhibition of NF-kappa B activation through covalent modification of reduced cysteine 62 of p50. *J. Immunol. 173, 4207–4217.*

(24) Arcaro, A., and Wymann, M. P. (1993) Wortmannin is a potent phosphatidylinositol 3-kinase inhibitor: the role of phosphatidylinositol 3,4,5-trisphosphate in neutrophil responses. *Biochem. J. 296, 297–301.*

(25) Norman, B. H., Shih, C., Toth, J. E., Ray, J. E., Dodge, J. A., Johnson, D. W., Rutherford, P. G., Schultz, R. M., Worzalla, J. F., and Vlahos, C. J. (1996) Studies on the mechanism of phosphatidylinositol 3-kinase inhibition by wortmannin and related analogs. *J. Med. Chem. 39, 1106–1111.*

(26) Wymann, M. P., Bulgarelli-Leva, G., Zvelebil, M. J., Pirola, L., Vanhaesebroeck, B., Waterfield, M. D., and Panayotou, G. (1996) Wortmannin inactivates phosphoinositide 3-kinase by covalent modification of Lys-802, a residue involved in the phosphate transfer reaction. *Mol. Cell. Biol. 16, 1722–1733.*

(27) Walker, E. H., Pacold, M. E., Perisic, O., Stephens, L., Hawkins, P. T., Wymann, M. P., and Williams, R. L. (2000) Structural determinants of phosphoinositide 3-kinase inhibition by wortmannin, LY294002, quercetin, myricetin, and staurosporine. *Mol. Cell 6, 909–919.*

(28) Yocum, R. R., Waxman, D. J., Rasmussen, J. R., and Strominger, J. L. (1979) Mechanism of penicillin action: penicillin and substrate bind covalently to the same active site serine in two bacterial D-alanine carboxypeptidases. *Proc. Natl. Acad. Sci. U. S. A. 76, 2730–2734.*

(29) Feling, R. H., Buchanan, G. O., Mincer, T. J., Kauffman, C. A., Jensen, P. R., and Fenical, W. (2003) Salinosporamide A: A highly cytotoxic proteasome inhibitor from a novel microbial source, a marine bacterium of the new genus Salinospora. *Angew. Chemie - Int. Ed. 42, 355–357.*

(30) Groll, M., Huber, R., and Potts, B. C. M. (2006) Crystal structures of salinosporamide A (NPI-0052) and B (NPI-0047) in complex with the 20S proteasome reveal important consequences of β-lactone ring opening and a mechanism for irreversible binding. *J. Am. Chem. Soc. 128, 5136–5141.*

(31) Flack, H. D. (1983) On enantiomorph-polarity estimation. *Acta Crystallogr. Sect. A 39, 876–881.*

(32) McCallum, C., Kwon, S., Leavitt, P., Shen, D. M., Liu, W., and Gurnett, A. (2007) Triptolide binds covalently to a 90 kDa nuclear protein. Role of epoxides in binding and activity. *Immunobiology 212, 549–556.*

(33) Titov, D. V., Gilman, B., He, Q.-L., Bhat, S., Low, W.-K., Dang, Y., Smeaton, M., Demain, A. L., Miller, P. S., Kugel, J. F., Goodrich, J. A., and Liu, J. O. (2011) XPB, a subunit of TFIIH, is a target of the natural product triptolide. *Nat. Chem. Biol. 7, 182–188.*

(34) He, Q.-L., Titov, D. V., Li, J., Tan, M., Ye, Z., Zhao, Y., Romo, D., and Liu, J. O. (2015) Covalent modification of a cysteine residue in the XPB subunit of the general transcription factor TFIIH through single epoxide cleavage of the transcription inhibitor triptolide. *Angew. Chemie - Int. Ed. 54, 1859–1863.*

(35) Kim, K. B., Myung, J., Sin, N., and Crews, C. M. (1999) Proteasome inhibition by the natural products epoxomicin and dihydroeponemycin: Insights into specificity and potency. *Bioorg. Med. Chem. Lett. 9, 3335–3340.*

(36) Groll, M., Kim, K. B., Kairies, N., Huber, R., and Crews, C. M. (2000) Crystal structure of epoxomicin: 20S proteasome reveals a molecular basis for selectivity of α,β-epoxyketone proteasome inhibitors. *J. Am. Chem. Soc. 122, 1237–1238.*

(37) Meng, L., Kwok, B. H. B., and Sin, N. (1999) Eponemycin exerts its antitumor effect through the inhibition of proteasome function. *Cancer Res. 59, 2798–2801.*

(38) Schorn, M., Zettler, J., Noel, J. P., Dorrestein, P. C., Moore, B. S., and Kaysser, L. (2014) Genetic basis for the biosynthesis of the pharmaceutically important class of epoxyketone proteasome inhibitors. *ACS Chem. Biol. 9, 301–309.*

(39) Renner, M., Shen, Y., Cheng, X., Jensen, P. R., Frankmoelle, W., Kauffman, C. A., Fenical, W., Lobkovsky, E., and Clardy, J. (1999) Cyclomarins A-C, new anti infl ammatory cyclic peptides produced by a marine bacterium (Streptomyces sp.). *J. Am. Chem. Soc. 121, 11273–11276.*

(40) Schmitt, E. K., Riwanto, M., Sambandamurthy, V., Roggo, S., Miault, C., Zwingelstein, C., Krastel, P., Noble, C., Beer, D., Rao, S. P. S., Au, M., Niyomrattanakit, P., Lim, V., Zheng, J., Jeffery, D., Pethe, K., and Camacho, L. R. (2011) The natural product cyclomarin kills mycobacterium tuberculosis by targeting the ClpC1 subunit of the caseinolytic protease. *Angew. Chemie - Int. Ed. 50, 5889–5891.*

(41) Vasudevan, D., Rao, S. P. S., and Noble, C. G. (2013) Structural basis of mycobacterial inhibition by cyclomarin A. *J. Biol. Chem. 288, 30883–30891.*

(42) Bürstner, N., Roggo, S., Ostermann, N., Blank, J., Delmas, C., Freuler, F., Gerhartz, B., Hinniger, A., Hoepfner, D., Liechty, B., Mihalic, M., Murphy, J., Pistorius, D., Rottmann, M., Thomas, J. R., Schirle, M., and Schmitt, E. K. (2015) Gift from nature: Cyclomarin A kills mycobacteria and malaria parasites by distinct modes of action. *ChemBioChem 16, 2433–2436.*

(43) Trischman, J. A., Tapiolas, D. M., Jensen, P. R., Dwight, R., Fenical, W., Mckee, T. C., Ireland, C. M., Stout, T. J., and Clardy, J. (1994) Salinamides A and B: anti-inflammatory depsipeptides from a marine Streptomyces. *J. Am. Chem. Soc. 157–158.*

(44) Moore, B. S., Trischman, J. A., Seng, D., Kho, D., Jensen, P. R., and Fenical, W. (1999) Salinamides, antiinflammatory depsipeptides from a marine streptomycete. *J. Org. Chem. 64, 1145–1150.*

(45) Degen, D., Feng, Y., Zhang, Y., Ebright, K. Y., Ebright, Y. W., Gigliotti, M., Vahedian-Movahed, H., Mandal, S., Talaue, M., Connell, N., Arnold, E., Fenical, W., and Ebright, R. H. (2014) Transcription inhibition by the depsipeptide antibiotic salinamide A. *Elife 1–29.*

(46) Hassan, H. M., Degen, D., Jang, K. H., Ebright, R. H., and Fenical, W. (2014) Salinamide F, new depsipeptide antibiotic and inhibitor of bacterial RNA polymerase from a marine-derived Streptomyces sp. *J. Antibiot. (Tokyo). 68, 206–209.*

(47) Ziemert, N., Lechner, A., Wietz, M., Millán-Aguiñaga, N., Chavarria, K. L., and Jensen, P. R. (2014) Diversity and evolution of secondary metabolism in the marine actinomycete genus Salinispora. *Proc. Natl. Acad. Sci. U. S. A. 111, E1130–E1139.*

(48) Brill, G. M., McAlpine, J. B., and Whittern, D. (1988) Tirandalydigin, a novel tetramic acid of the tirandamycin-streptolydigin type. II. Isolation and structural characterization. *J. Antibiot. (Tokyo). 41, 36–44.*

(49) Karwowski, J. P., Jackson, M., Theriault, R. J., Barlow, G. J., Coen, L., Hensey, D. M., and Humphrey, P. E. (1992) Tirandalydigin, a novel tetramic acid of the tirandamycin-streptolydigin type. I. Taxonomy of the producing organism, fermentation and biological activity. *J. Antibiot. (Tokyo). 45, 1125–1132.*

(50) Omura, S., Fujimoto, T., Otoguro, K., Matsuzaki, K., Moriguchi, R., Tanaka, H., and Sasaki, Y. (1991) Lactacystin, a novel microbial metabolite, induces neuritogenesis of neuroblastoma cells. *J. Antibiot. (Tokyo). 44, 113–116.*

(51) Reed, K. A., Manam, R. R., Mitchell, S. S., Xu, J., Teisan, S., Chao, T. H., Deyanat-Yazdi, G., Neuteboom, S. T. C., Lam, K. S., and Potts, B. C. M. (2007) Salinosporamides D-J from the marine actinomycete Salinispora tropica, bromosalinosporamide, and thioester derivatives are potent inhibitors of the 20S proteasome. *J. Nat. Prod. 70, 269–276.*

(52) Dick, L. R., Cruikshank, A. A., Grenier, L., Melandri, F. D., Nunes, S. L., and Stein, R. L. (1996) Mechanistic studies on the inactivation of the proteasome by lactacystin. *J. Biol. Chem. 271, 7273–7276.*

(53) Dick, L. R., Cruikshank, A. A., Destree, A. A., Grenier, L., McCormack, T. A., Melandri, F. D., Nunes, S. L., Palombella, V. J., Parent, L. A., Plamondon, L., and Stein, R. L. (1997) Mechanistic studies on the inactivation of the proteasome by lactacystin in cultured cells. *J. Biol. Chem. 272, 182–188.*

(54)   Aotani, Y.; Nagata, H.; Yoshida, M. Lymphostin (LK6-A), a novel immunosuppressant from Streptomyces sp. KY11783: Structural elucidation. J. Antibiot. (Tokyo). 1997, 50, 543–545.

(55)   Nagata, H.; Ochiai, K.; Aotani, Y.; Ando, K.; Yoshida, M.; Takahashi, I. Taxonomy of the producing organism, fermentation, isolation. J. Antibiot. (Tokyo). 1997, 50, 537–542.

(56)   Nagata, H.; Yano, H.; Sasaki, K.; Sato, S.; Nakanishi, S.; Takahashi, I.; Tamaoki, T. Inhibition of lymphocyte kinase Lck and phosphatidylinositol 3-kinase by a novel immunosuppressant, lymphostin. Biosci. Biotechnol. Biochem. 2002, 66, 501–507.

(57)   Miyanaga, A.; Janso, J. E.; McDonald, L.; He, M.; Liu, H.; Barbieri, L.; Eustáquio, A. S.; Fielding, E. N.; Carter, G. T.; Jensen, P. R.; Feng, X.; Leighton, M.; Koehn, F.

E.; Moore, B. S. Discovery and assembly-line biosynthesis of the lymphostin pyrroloquinoline alkaloid family of mTOR inhibitors in Salinispora bacteria. J. Am. Chem. Soc. 2011, 133, 13311–13313.

(58)   Fabian, M. A.; Biggs, W. H.; Treiber, D. K.; Atteridge, C. E.; Azimioara, M. D.; Benedetti, M. G.; Carter, T. A.; Ciceri, P.; Edeen, P. T.; Floyd, M.; Ford, J. M.; Galvin, M.; Gerlach, J. L.; Grotzfeld, R. M.; Herrgard, S.; Insko, D. E.; Insko, M. A.; Lai, A. G.; Lélias, J.-M.; Mehta, S. A.; Milanov, Z. V; Velasco, A. M.; Wodicka, L. M.; Patel, H. K.; Zarrinkar, P. P.; Lockhart, D. J. A small molecule-kinase interaction map for clinical kinase inhibitors. Nat. Biotechnol. 2005, 23, 329–336.

(59)   Wymann, M. P.; Bulgarelli-Leva, G.; Zvelebil, M. J.; Pirola, L.; Vanhaesebroeck, B.; Waterfield, M. D.; Panayotou, G. Wortmannin inactivates phosphoinositide 3-kinase by covalent modification of Lys-802, a residue involved in the phosphate transfer reaction. Mol. Cell. Biol. 1996, 16, 1722–1733.

(60)   Brunn, G. J.; Williams, J.; Sabers, C.; Wiederrecht, G.; Lawrence, J. C.; Abraham, R. T. Direct inhibition of the signaling functions of the mammalian target of rapamycin by the phosphoinositide 3-kinase inhibitors, wortmannin and LY294002. EMBO J. 1996, 15, 5256–5267.

(61)   Arcaro, A.; Wymann, M. P. Wortmannin is a potent phosphatidylinositol 3-kinase inhibitor: the role of phosphatidylinositol 3,4,5-trisphosphate in neutrophil responses. Biochem. J. 1993, 296, 297–301.

(62) Edwards, D. J.; Marquez, B. L.; Nogel, L. M.; McPhail, K.; Goeger, D.; Roberts, M. A.; Gerwick, W. H. (2004) Structure and biosynthesis of the jamaicamides, new mixed polyketide-peptide neurotoxins from the marine cyanobacterium Lyngbya majuscula. *Chem. Biol. 11, 817–833.*

(63) Roda-Serrat, M. C., Christensen, K. V., El-Houri, R. B., Fretté, X., Christensen, L. P. (2018). Fast cleavage of phycocyanobilin from phycocyanin for use in food colouring. *Food Chemistry, 240, 655–661.*

(64) Reimer, D.; Hughes, C. C. (2017) Thio-based probe for eleectrophilic natural products reveals that most of the ammosamides are artifacts. *J. Nat. Prod. 80, 126–133.*

(65) Jaramillo, M. C.; Zhang, D. D. (2013) The emerging role of the Nrf2-Keap1 signailing pathway in cancer. *Genes Dev. 27, 2179–2191.*

(66) Sun, H.; Zhu, J.; Lin, H.; Gu, K.; Feng, F. (2017) Recent progress in the development of small molecule Nrf2 modulators: a patent review (2012-2016). *Expert Opin. Ther. Pat. 27 (7), 763–785.*

(67) Yamamoto, X. M.; Kensler, T. W.; Motohashi, H. (2018) The Keap1-Nrft2 system: a thiol-based sensor-effector apparatus for maintaining redox homeostasis. *Physiol. Rev. 98, 1169–1203.*

(68) Pallesen, J. S.; Tran, K. T.; Bach, A. (2018) Non-covalent small-molecule kelch-like ech-associated protein 1-nuclear factor erythroid 2-related factor 2 (Keap1-Nrf2) inhibitors and their potential for targeting central nervous system diseases. *J. Med. Chem. 61, 8088–8103.*

(69) Jiang, Z.Y.; Lu, M. C.; You, Q. D. (2016) Discovery and development of kelch-like ech-associated protein 1: nuclear factor erythroid 2-related factor 2 (KEAP1:NRF2) protein-protein interaction inhibitors: achivments, challenges and future directions. *J. Med. Chem. 59, 10837–10858.*

(70) Cuadrado, A.; Rojo, A. I.; Wells, G.; Hayes, J. D.; Cousin, S. P.; Rumsey, W. L.; Attucks, O. C.; Franklin, S.; Levonen, A. L.; Kensler, T. W.; Dinkova-Kostova, A. T. (2019) Therapeutic targeting of the NRF2 and KEAP1 partnership in chronic diseases. *Nat. Rev. Drug Discov. 18, 295–317.*

Chapter 3

Nitrosopyridine probe to detect polyketide natural products with conjugated alkenes: Discovery of novodaryamide, nocarditriene, thrixazol and epostatin B

3.1 ABSTRACT

An optimized nitroso-based probe that facilitates the discovery of conjugated alkene-containing natural products in unprocessed extracts was developed. It chemoselectively reacts with conjugated olefins via a nitroso-Diels Alder cyclization to yield derivatives with a distinct chromophore and an isotopically-unique bromine atom. Comparing the reactivity and spectral properties of five brominated arylnitroso reagents with model compounds spiramycin, bufalin, rapamycin, and rifampicin led to the identification of 5-bromo-2-nitrosopyridine as the most suitable probe structure. The utility of the dienophile probe was then demonstrated in bacterial extracts. Tylactone, novodaryamide and daryamide A, piperazimycin A, and the saccharamonopyrones A and B were cleanly labeled in extracts from their respective bacterial producers, in high regioselectivity but with varying degrees of diastereoselectivity. Application of the method led to the discovery of a new natural product called nocarditriene, containing an unprecedented epoxy-2,3,4,5-tetrahydropyridine structure, from marine-derived *Nocardiopsis* sp. strain CNY-503. Furthermore, we developed a genome mining tool to find strains containing polyketide gene clusters with two or more repeating KS-AT-DH-KR-ACP domain sequences, which are required for the biosynthesis of conjugated alkenes, and the metabolomes of some of these were screened with the probe to find

new diene-containing natural products. This led to the discovery of thrixazol and epostatin B from *Saccharothrix espanaensis* DSM-44229.

3.2 INTRODUCTION

Polyketides are formed from a series of Claisen condensation reactions between thioester-bound subunits that are catalyzed by acyl transferase (AT), ketosynthase (KS) and acyl carrier protein (ACP) domains. Ketoreductase (KR), dehydratase (DH), and enoylreductase (ER) domains partially or completely reduce the polyketide. Successive modules with a KS-AT-DH-KR-ACP domain architecture produce conjugated dienes (n = 2), trienes (n = 3), tetraenes (n = 4), etc., where n is the number of modules. Thus, a conjugated alkene correlates well with polyketide metabolism. Although this functionality does not represent a pharmacophore *per se*, many natural products with a conjugated alkene nonetheless possess remarkable biological properties. For example, spiramycin (**1**) is a diene-containing antibiotic and antiparasitic drug, and bufalin (**2**) is a pyrone-containing cardiotonic steroid isolated from toad venom (Figure 3.1). Rapamycin (**3**) is an immunosuppressant drug used to prevent organ rejection.[1,2] A semisynthetic derivative of rifamycin, rifampicin (**4**) is an antibiotic used for the treatment of several types of bacterial infection, including tuberculosis,[3] and avermectin B_{1a} (**5**) is an insecticide whose significance was underscored by Omura's 2015 Nobel Prize in Medicine.[4] As expected, the biosynthetic gene clusters of the microbial metabolites **1** and **3**-**5** have been demonstrated to contain the KS-AT-DH-KR-ACP motif, within the *srmG* gene (modules 2-3) for spiramycin,[5] the *rapB* gene (modules 8-10) for rapamycin,[6] the *rifE* gene (modules 9-10) for rifamycin,[7] and the *aveA3* gene (modules 9-10) for avermectin.[8]
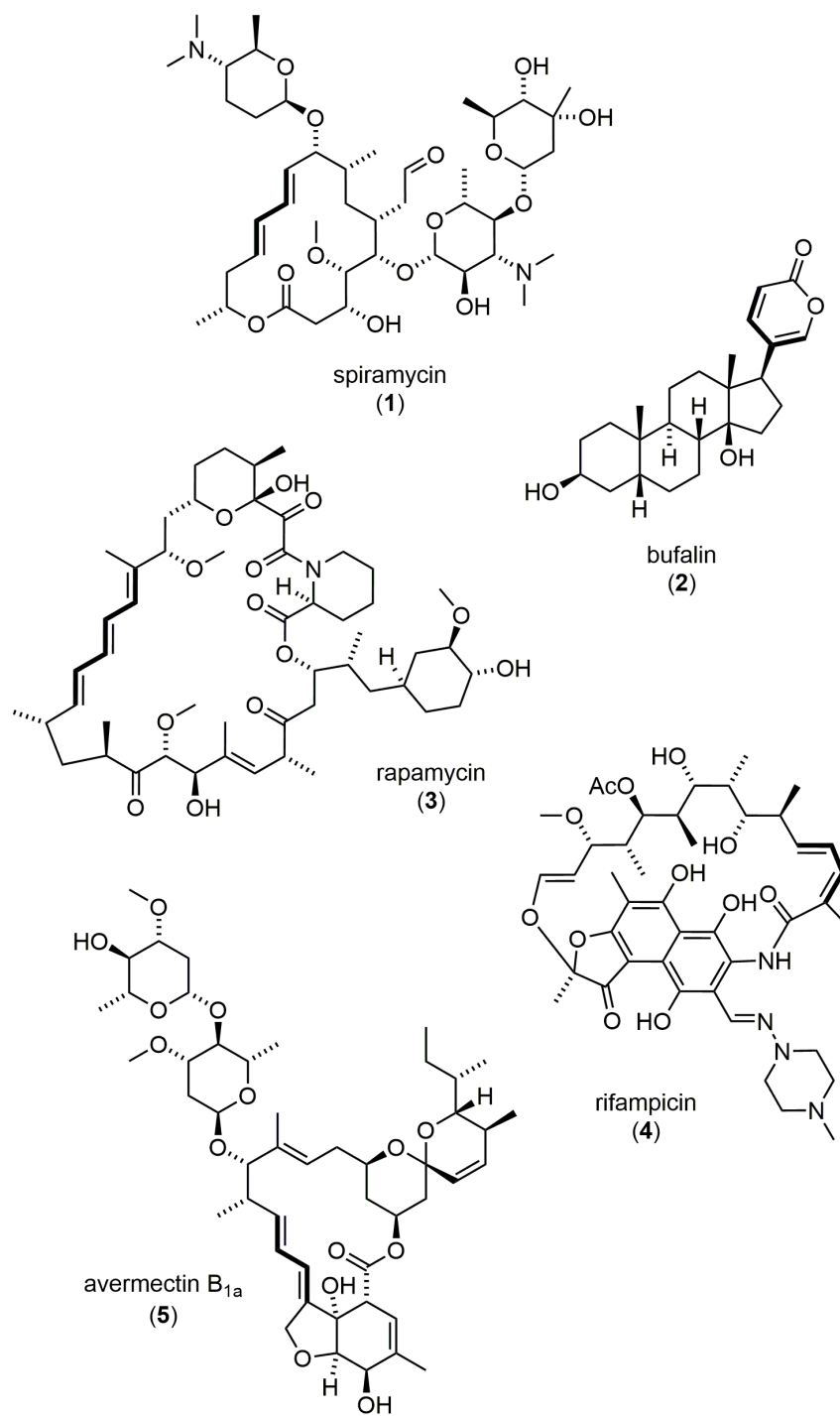
Figure 3.1 Conjugated alkene-containing compounds spiramycin (**1**), bufalin (**2**), rapamycin (**3**), rifampicin (**4**), avermectin B_{1a} (**5**).

The nitroso Diels-Alder (NDA) reaction is a well-established, concerted, chemo- and regioselective cycloaddition that may well be exploited as a general method for the discovery of conjugate alkene-containing polyketides like rapamycin and avermectin.[9,10] NDA reactions with nitrosobenzenes have been known for a century.[11] In 2007, Miller and co-workers described the synthesis and reactivity of nitrosopyridines in NDA reactions.[12-14] Furthermore, the application of these reagents for the derivatization of complex diene-containing natural products such as leucomycin A7, ergosterol, and colchicine was also detailed.

3.3 RESULTS AND DISCUSSION

3.3.1 Evaluation of nitroso aryl probes with pure natural products

We thought to exploit the NDA reaction, particularly using bench-stable nitrosoarenes, for the discovery of conjugated alkene-containing natural products in unprocessed extracts. We installed a bromine atom onto each of our candidate nitrosoarene "probes" since this atom gives a unique signature in a mass spectrometer due to the 1:1 abundance of two bromine isotopes (^{79}Br:^{81}Br). 4-Bromonitrosobenzene (**6**) was prepared in one step from 4-bromoaniline using oxone (Figure 3.2).[15] 5-Bromo-2-nitrosopyridine (**7**) and isomers **8**-**10** were prepared in a two-step oxidation from the corresponding aminobromopyridines.[12,16]
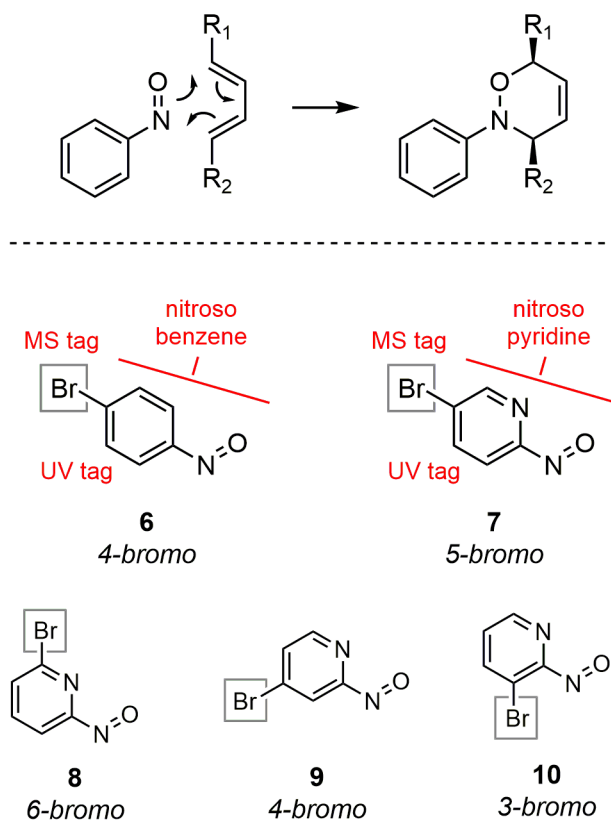
Figure 3.2 The nitroso Diels-Alder reaction, bromonitrosobenzene **6** and bromonitrosopyridines **7-10.**

We first evaluated the five candidate probes using spiramycin (**1**) as substrate (Figure 3.3). Diene **1** exhibits a nondistinct UV/vis absorption profile with a single λ_{max} = 232 nm under typical LC-MS conditions (acetonitrile, water, 0.1% formic acid). Reaction of spiramycin with nitrosobenzene probe **6** required prolonged heating at 60 ºC in tetrahydrofuran (THF) to yield products **11a**/**11b** as a mixture of diastereomers in 64% yield. In contrast, reaction of spiramycin with nitrosopyridine probe **7** was complete within 3 h at room temperature, again yielding a mixture of diastereomers **12a**/**12b** in 59% yield. The superior reactivity of nitrosopyridines in NDA reactions is well-documented.[14] The major diastereomers **11a** and **12a** were purified and characterized by comprehensive 2D NMR analysis. The C-10/C-13 carbon chemical shift [**12a**: *O-*

substituted: δ_C = 75.9; *N*-substituted: δ_C = 51.0] defined the regioselectivity of the reaction. Although cycloaddition of spiramycin with **8** and **9** also proceeded at room temperature, reaction did not occur between spiramycin and probe **10**. The lack of reactivity in **10** is likely due to the proximity of the large bromine substituent to the reactive site. At this point, we decided to proceed with 5-bromonitrosopyridine probe **7** for the remainder of the study since 1) it exhibited favorable reactivity at room temperature compared to **6** and 2) it yielded adducts with prominent UV/vis absorption characteristics compared to those from **8** and **9**, including long-wavelength λ_{max} at 260 and 310 nm. We also included 4-bromonitrosobenzene **6** in subsequent reactions, whenever possible, as a benchmark. Lastly, *N,N'*-bis(5-bromophenyl)diazene *N*-oxide and *N,N'*-bis(5-bromopyridin-2-yl)diazene *N*-oxide, known azoxy by-products of the reaction, were observed in the spiramycin reaction and in subsequent reaction mixtures.[16]

Both probes labeled bufalin (**2**) (see Figure 3.3). Bufalin was converted to 1,5-dihydro-2H-pyrrol-2-ones **13** and **14** using probes **6** and **7**, respectively, both at room temperature and in a completely diastereoselective manner. In both cases, the first cycloaddition was followed by decarboxylation and reaction with a second equivalent of probe. Elevated temperatures were not required for the reaction of bufalin and **6** since the natural product is locked in the s-*cis* conformation. However, the reaction did not proceed to completion at room temperature, and the yield of **13** was therefore low (29%). Heating led to the formation of several by-products. The mechanism and structure elucidation of **13** and **14** are discussed in greater detail below.

Both probes **6** (24 h at 60 °C) and **7** (3 h at room temperature) likewise labeled

rapamycin (**3**) (see Figure 3.3). ^{1}H NMR spectra of the reaction mixtures both showed

an apparent 1.3:1 mixture of diastereomeric adducts **15a/15b** and **16a/16b**. The C-1/C-

4 carbon chemical shift (**16a**: *N*-substituted: δ_C = 57.9; *O*-substituted: δ_C = 70.7) defined

the regioselectivity of the reaction. The diastereomers could not be separated by

reversed-phase HPLC using a variety of stationary phases. This result was unexpected

since rapamycin is reported, in a study to make nonimmunosuppresive rapamycin

analogues, to react with nitrosobenzene with high diastereoselectivity.[17,18] Indeed,

repeating the published reaction with nitrosobenzene under the reported conditions also

gave a diastereomeric mixture.

We next examined the reactivity of the probes with more challenging diene-

containing substrates rifampicin (**4**) and avermectin B$_{1a}$ (**5**) (see Figure 3.3). Here, the

dienes are 1,1-disubstituted, and so nitroso Diels-Alder reaction demands the formation

of a crowded quaternary carbon stereocenter. Although conversion to brominated

adducts using probe **6** was not observed, treatment of rifampicin (**4**) with probe **7** at

room temperature afforded **17** as a single diastereomer, which was purified in 25% yield

and characterized by 2D NMR analysis. The C-16/C-19 carbon chemical shift (*N*-

substituted: δ_C = 67.0; *O*-substituted: δ_C = 77.4) defined the regioselectivity of the

reaction. Unexpectedly, the first equivalent of probe **7** was consumed in an oxidation-

reduction reaction to give rifampicin quinone. To the best of our knowledge, rifampicin

derivatives resembling **17** have not been reported. Avermectin B$_{1a}$ (**5**) was not labeled

to a significant extent with either probe. Thus, there are certain steric or conformational

factors that can prevent efficient labeling of a diene-containing natural product, despite

the presence of the KS-AT-DH-KR-ACP sequence tag in the sequenced *Streptomyces avermitilis* genome.[8]
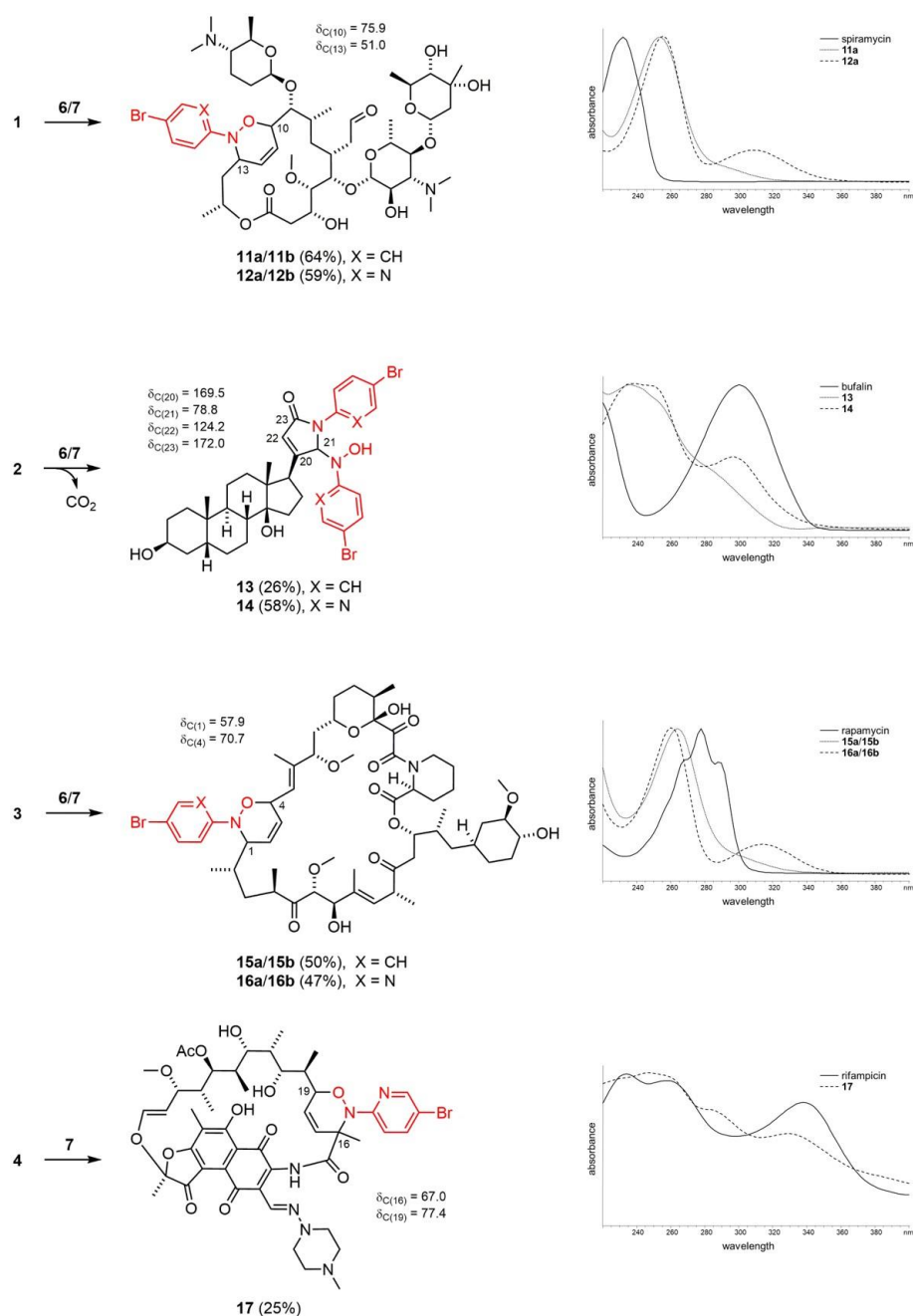
Figure 3.3 Reaction of nitrosobenzene **6** (THF, 60 ºC, 12 h) and nitrosopyridine **7** (THF, rt, 3 h) with conjugated alkene-containing compounds **1-4**. Reaction with bufalin (**2**) and **6** was conducted at room temperature. Key carbon chemical shifts for products from reaction with **7** are shown. UV/vis profiles of the substrates (**1-4**), the nitrosobenzene adducts (**11a**, **13**, **15a**), and the nitrosopyridine adducts (**12a**, **14**, **16a**, **17**) are depicted for comparison.

We then attempted to understand the reactivity of the nitrosoarenes with bufalin (**2**). The fact that **2** reacted with two equivalents of probe was clear from LC-MS analysis of the reaction mixture, which showed a dibrominated 1:2:1 isotopic cluster for the product. However, the structure of the adducts **13** and **14** could not be determined with certainty. Thus, given that the adducts generally exhibit superior crystallinity compared to the parent compounds, we set out to determine the structures by X-ray crystallography. A concentrated solution of 1,5-dihydro-2*H*-pyrrol-2-one **13** in DMSO yielded X-ray quality crystals in short order using the vapor diffusion method. Analysis of the crystal derived in this way revealed 5-imino-dihydro-2*H*-pyrrol-2-one **18** (Figure 3.4A) (CCDC 1546784). Apparently, a water molecule was lost during the recrystallization attempts, as indicated by an increase in retention time, an 18 amu decrease in molecular mass, and a change in UV/vis profile involving a new long wavelength-absorbing chromophore.

Ultimately, we synthesized a model 5-hydroxyamino-1,5-dihydro-2H-pyrrol-2-one by reacting probe **6** with α-pyrone (**19**) to give **20** in good yield, and this compound gave X-ray quality crystals via slow evaporation from CDCl$_3$ (Figure 3.4B) (CCDC 1841575). Some conversion of **20** to the corresponding 5-imino-1,5-dihydro-2*H*-pyrrol-2-one was observed during silica gel chromatography, which decreased the yield of **20**. Finally, good agreement between **13**/**14** and **20** in ^{1}H and 2D NMR data allowed unambiguous assignment of the structure of **13** and **14** (Figure 3.4C). Eventually, we realized that the reaction between α-pyrone and nitrosobenzene to give the corresponding 1,5-dihydro-2*H*-pyrrol-2-one was first reported in 1976.[19] Also described was the tendency of 5-

hydroxyamino-1,5-dihydro-2*H*-pyrrol-2-ones to dehydrate to the analogous imino compounds, under conditions that include silica gel chromatography.

The proposed mechanism for conversion of bufalin to **13**/**14** is outlined in Figure 3.4D. Bicyclic intermediate **21** decarboxylates to 1,2-oxazine **22** following the first cycloaddition reaction. Claisen-type rearrangement gives **23**. The aldehyde and imine react intramolecularly to give **24**, which re-aromatizes to **25**. A 1,5-dihydro-2*H*-pyrrol-2-one tautomer, hydroxypyrrole **25** reacts with electrophiles at the 2-position. As nitroso compounds are electrophilic at the nitrogen center, **25** undergoes a rapid addition reaction to give **13**/**14**.
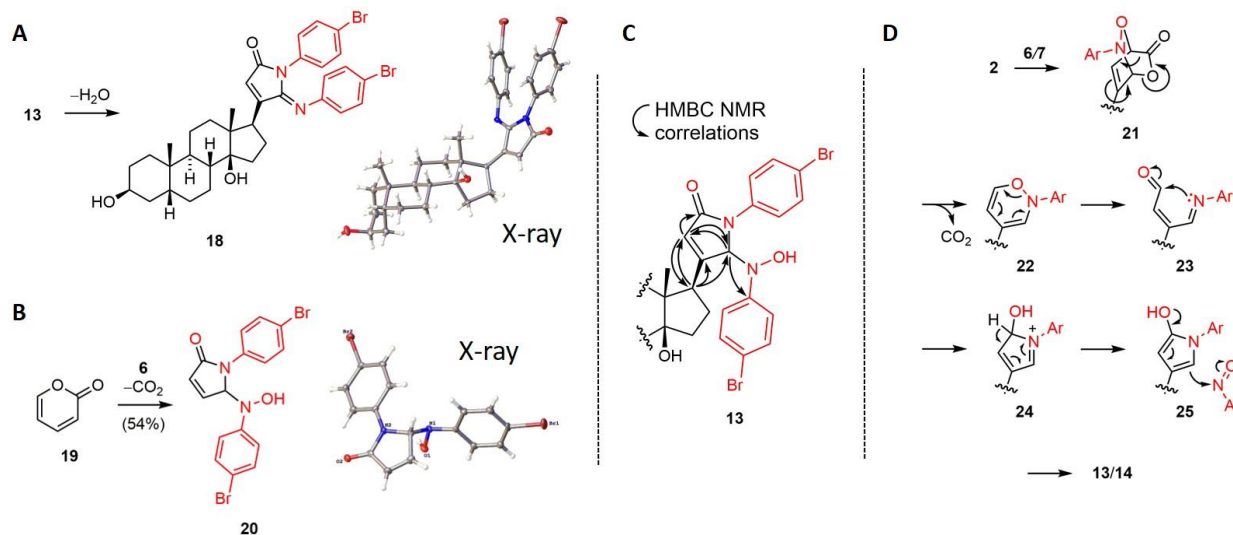
Figure 3.4 The bufalin reaction. A) 5-Hydroxyamino-1,5-dihydro-2H-pyrrol-2-one **13** dehydrated to 5-imino-1,5-dihydro-2*H*-pyrrol-2-one **18**, whose structure was verified by X-ray crystallographic analysis. B) Using model pyrone **19**, the 5-hydroxyamino-1,5-dihydro-2*H*-pyrrol-2-one **20** was isolated from the reaction mixture, and this compound was also subjected to crystallographic analysis. C) HMBC NMR correlations for **13**. D) Proposed mechanism for the formation of **13**/**14** from bufalin.

3.3.2 Evaluation of nitroso aryl probe 7 with natural products in crude extract

Using 30 mL cultures we then screened ten marine-derived bacterial extracts including species from *Streptomyces*, *Salinispora*, *Nocardia*, *Micromonospora*, *Kocuria*,

Saccharomonospora, *Frankia*, and *Nocardiopsis* using probe **7** at room temperature.

The presence of one or more UV-active (254 nm) peaks with a brominated isotope

pattern in the LC-MS chromatogram of the reaction mixture indicated a "hit." Inspection

of the LC-MS chromatogram of the original extract was used to exclude endogenous

brominated compounds. Although the small number of samples allowed for manual

inspection of LC-MS data, we applied the recently-developed bioinformatics tool

MeHaloCoA to detect brominated cycloadducts in an automated fashion.[20] The UV/vis

profiles for the peaks of interest were also examined in order to determine if they

conformed to the profiles of "typical" adducts like **11a** and **16a**. Strains with "hits" were

grown in 1 – 3 L cultures in order to obtain enough material for NMR studies on

metabolites of interest.

Treatment of extract from *Salinispora pacifica* strain CNT-084 with probe **7** gave

a single brominated compound **26**, of unknown structure, with the molecular formula

$C_{28}H_{41}BrN_2O_6$ [*m/z* (M+H)$^+$ 581.2384, calcd for $C_{28}H_{42}BrN_2O_6$ 581.2226] (Figure 3.5).

Although this adduct did not survive isolation and characterization, its formula was used

to calculate the molecular formula of the parent natural product ($C_{23}H_{38}O_5$). In addition,

analysis of the genome of strain CNT-084 showed that it contained a PKS gene cluster

with high sequence homology to the rosamicin gene cluster.[21] Taken together, we

surmised that we had labeled tylactone (**27**), a diene-containing biosynthetic precursor

to rosamicin, which we subsequently purified and characterized.[22,23]

When extract from marine *Streptomyces* sp. CNQ-085 was treated with probe **7**,

two labeled compounds were produced (see Figure 3.5). The molecular formula of

bromide **28** was determined as $C_{23}H_{29}BrN_4O_6$ [*m/z* (M+Na)$^+$ 559.1160, calcd for

C$_{23}$H$_{29}$BrN$_4$O$_6$Na 559.1168]. The formula of the parent natural product was then calculated to be C$_{18}$H$_{26}$N$_2$O$_5$, corresponding to daryamide A (**30**), a known weakly cytotoxic natural product from this strain.[24] The molecular formula of bromide **29** was determined as C$_{23}$H$_{27}$BrN$_4$O$_6$ [*m/z* (M+H)$^+$ 535.1176, calcd for C$_{23}$H$_{28}$BrN$_4$O$_6$ 535.1192]. As before, the formula of the parent natural product was then calculated to be C$_{18}$H$_{24}$N$_2$O$_5$ [*m/z* (M+Na)$^+$ 371.1576, calcd for C$_{18}$H$_{24}$N$_2$O$_5$Na 371.1583], suggesting that the metabolite is an oxidized analogue of daryamide A. The planar structure of **29** was elucidated following extensive 1D and 2D NMR (COSY, HSQC, HMBC) experiments. Retrosynthetic logic and subsequent characterization of the parent natural product revealed a new daryamide, named novodaryamide (**31**). COSY and HMBC correlations analogous to **30** defined the propanamide-substituted epoxy-cyclohexenone ring; COSY correlations also defined the reactive (2E,4E)-7-methylocta-2,4-dienamide. Novodaryamide contains the intact epoxyquinone pharmacophore found in manumycin and related metabolites.[25] Recently, Fu, *et al.*, synthesized **31** via oxidation of daryamide D.[26] Notably, the absolute stereochemistry of the daryamides in the original publication was misassigned because the Mosher's analysis was interpreted incorrectly.[24]

Figure 3.5 RGI of conjugated alkene-containing natural products in extracts. LC chromatograms at 254 nm are shown both before (black) and after (red) the labeling reaction. A) Treatment of extract from *Salinispora* strain CNT-084 with **7** yielded brominated cycloadduct **26**, which is derived from tylactone (**27**). B) Extract from *Streptomyces* strain CNQ-085 gave **28** and **29** after reaction, which are derived from daryamide A (**30**) and novodaryamide (**31**). ^{1}H-^{1}H COSY and HMBC correlations are shown for the novodaryamide cycloadduct (**29**) and novodaryamide (**31**). "Oxide" refers to *N,N'*-bis(5-bromopyridin-2-yl)diazene *N*-oxide.

A

Salinispora sp.
CNT-084

7

581

m/z

26

C₂₈H₄₁BrN₂O₆

tylactone
(**27**)

B

Streptomyces sp.
CNQ-085

7

537

m/z

$\delta_{C(2')}$ = 74.1
$\delta_{C(5')}$ = 51.8

28

daryamide A
(**30**)

535

m/z

$\delta_{C(2')}$ = 74.0
$\delta_{C(5')}$ = 51.6

29

[NEW NATURAL PRODUCT]

novodaryamide A
(**31**)

| ¹H-¹H COSY
⟩ HMBC

29

31

68

Four chloro-brominated products in approximately equal amounts were observed when extract from *Streptomyces* sp. strain CNQ-593 was treated with probe **7** (Figure 3.6). The molecular formula of $C_{36}H_{50}BrClN_{10}O_{11}$ was determined from the dominant HRMS ions [*m/z* (M+Na)+ 935.2418, calcd 935.2430], and the calculated formula ($C_{31}H_{47}ClN_8O_{10}$) matched the chlorinated natural product piperazimycin A (**34**).[27] HPLC purification and subsequent NMR analysis of all adducts confirmed the formation of dihydro-1,2-oxazine products via a Diels-Alder reaction between nitroso probe **7** and the conjugated diene in piperazimycin A. It was apparent that the four products are regio- and stereoisomers, suggesting that the diene side chain of **34** is highly flexible and electronically symmetrical.
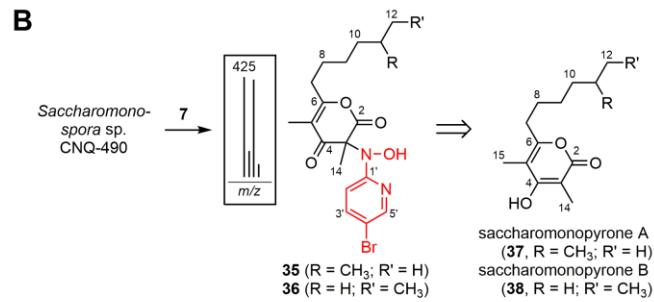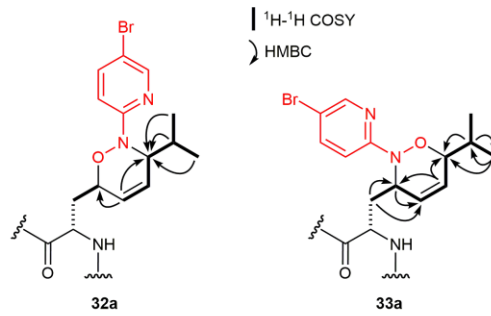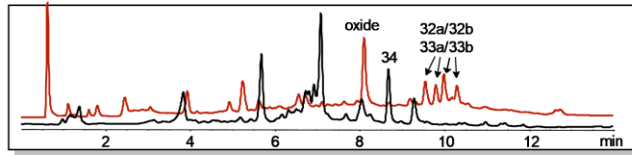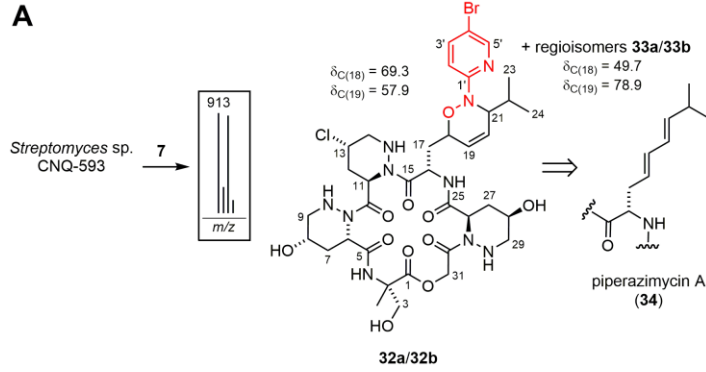
Pyrones **37** [*m/z* (M+H)+ 239.1639, calcd for $C_{14}H_{23}O_3$ 239.1640] and **38** [*m/z* (M+H)+ 239.1640, calcd for $C_{14}H_{23}O_3$ 239.1640] with the molecular formula $C_{14}H_{22}O_3$ were discovered in extracts from *Saccharomonospora* sp. strain CNQ-490 following a telling reaction of the extract with **7**, which produced two brominated compounds, **35** [*m/z* (M+H)+ 425.0831, calcd for $C_{16}H_{26}BrN_2O_4$ 425.1076] and **36** [*m/z* (M+H)+ 425.0835, calcd for $C_{16}H_{26}BrN_2O_4$ 425.1076], having the molecular formula $C_{19}H_{25}BrN_2O_4$ (see Figure 3.6). The amine nitrogen atom of the bromopyridine probe was attached to C-3 on the basis of chemical shift (δ_C 88.0), but no site of attachment for the oxygen atom was available. We therefore proposed that a hydroxylamino group was present at C-3 in **35** and **36**. The parent natural products were then isolated and characterized by NMR. Shared HMBC correlations for **37** from H_3-14 (δ_H 1.95) and H_3-15 (δ_H 1.94) to C-2 (δ_C 164.5), C-3 (δ_C 97.9), C-4 (δ_C 164.5), C-5 (δ_C 105.6), and C6 (δ_C 159.6) defined a 4-hydroxy-substituted α-pyrone. In the same way, HMBC correlations

and chemical shift values for **38** also outlined a 4-hydroxy-substituted α-pyrone. A 5-methylhexyl substituent was attached to C-6 in **37**, whilst a heptane substituent was attached to C-6 in **38**. These natural products, called the saccharomonopyrones A (**37**) and B (**38**) were very recently described by Nam and Fenical.[28] The natural products may react with probe **7** via an addition reaction at the nucleophilic C-3 carbon atom in lieu of an NDA reaction, similar to the reactivity of bufalin intermediate **25** described above (see Figure 3.4C).[11]

Figure 3.6 RGI of conjugated alkene-containing natural products in extracts. LC chromatograms at 254 nm are shown both before (black) and after (red) the labeling reaction. A) Extract from *Streptomyces* strain CNQ-593 gave **32a**/**32b** and regioisomers **33a**/**33b** after reaction, which are derived from piperazimycin A (**34**). B) Extract from *Saccharomonospora* strain CNQ-490 yielded **35** and **36**, which are derived from saccharomonopyrones A (**37**) and B (**38**). **35'** and **36'** are isomers of **35** and **36**, presumably corresponding to the initial cycloadducts formed upon reaction with **7**. ^{1}H-^{1}H COSY and HMBC correlations are shown for both regioisomers of the piperazimycin cycloadduct (**32a**/**33a**) and for the saccharomonopyrone A cycloadduct (**35**) and saccharomonapyrone A (**37**). "Oxide" refers to *N*,*N'*-bis(5-bromopyridin-2-yl)diazene *N*-oxide.

A

Streptomyces sp. CNQ-593

$\delta_{C(18)} = 69.3$
$\delta_{C(19)} = 57.9$

+ regioisomers **33a/33b**
$\delta_{C(18)} = 49.7$
$\delta_{C(19)} = 78.9$

piperazimycin A (**34**)

32a/32b

¹H-¹H COSY

HMBC

32a   **33a**

B

Saccharomonospora sp. CNQ-490

35 (R = CH₃; R' = H)
36 (R = H; R' = CH₃)

saccharomonopyrone A
(**37**, R = CH₃; R' = H)
saccharomonopyrone B
(**38**, R = H; R' = CH₃)

¹H-¹H COSY

HMBC

$\delta_{C(3)} = 88.0$

35   **37**

72
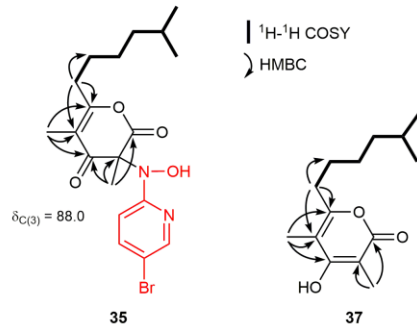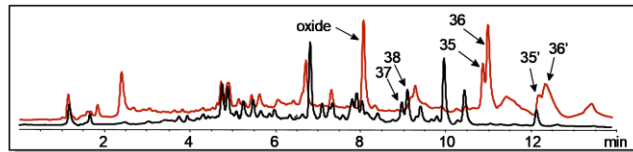
3.3.3 Discovery of nocarditriene from *Nocardiopsis* sp. CNY-503

Treatment of an extract from *Nocardiopsis* sp. strain CNY-503 with probe **7** also showed formation of two brominated products (**39a/39b**) with the molecular formula $C_{22}H_{28}BrN_3O_3$ [*m/z* (M+H)$^+$ 462.1374 and 462.1375, calcd for $C_{22}H_{29}BrN_3O_3$ 462.1392] (Figure 3.7). The natural product (**40**) in the untreated bacterial extract was targeted for purification by HPLC on the basis of its calculated mass $C_{17}H_{25}NO_2$ [*m/z* (M+H)$^+$ 276.1957, calcd for $C_{17}H_{26}NO_2$ 276.1964]. The chiral compound, $[\alpha]_D$ = +30 (*c* 0.2, DMSO), was isolated as a yellow solid. Its ^1H NMR spectrum showed five distinct olefinic protons at δ_H 6.35 (H-4), 6.05 (H-7), 5.95 (H-5), 5.75 (H-3), and 5.58 (H-8). Two COSY spin systems containing these protons, H_3-1 to H-5 and H-7 to H_2-9, were connected via HMBC correlations from a methyl group at H_3-16 (δ_H 1.75) to C-5 (δ_C 130.2), C-6 (δ_C 130.2), and C-7 (δ_C 130.2). This 6-methyl-3,5,7-nonatriene moiety represents the reactive part of the molecule. A 2D NOESY experiment established the all-*E* configuration of the triene unit, showing correlations between H-2 and H-4, H-3 and H-5, H-4 and H-16, H-7 and H-9, and H-8 and H-16. An additional COSY spin system extended from methine protons at H-12 (δ_H 3.70/δ_C 42.6) to H-13 (δ_H 3.64/δ_C 52.9), constituting a *cis* epoxide, and from H-13 to *N*-substituted methylene protons at H_2-15 (δ_H 3.24,3.60/δ_C 42.7). HMBC correlations extending from both ends of this four-carbon spin system to quaternary carbon C-11 (δ_C 171.7) indicated a six-membered imine-containing heterocycle fused to the epoxide. Additional HMBC correlations from the methyl group at H_3-17 to C-9 (δ_C 43.4), C-10 (δ_C 75.0), and C-11 tied the alkyl side chain to the heterocyclic bicycle. The carbon chemical shift at C-10 indicated a tertiary alcohol was present at this position. This new natural product was named nocarditriene.

The reactivity of nocarditriene (**40**) supported our initial structure assignment. When the compound was concentrated from acidified solvents, the chemical shift of C-11 shifted considerably downfield to δ_C 190.7 due to the formation of iminium ion **41**. Furthermore, the imine in **40** was hydrolyzed in the presence of acetic anhydride and triethylamine, via the *N*-acyl iminium species, to form *N*-acetylated epoxyketone **42** [*m/z* (M+Na)$^+$ 358.1999, calcd for $C_{19}H_{29}NO_4Na$ 358.1994], which was also characterized by NMR. The carbon chemical shift of the newly-formed ketone at C11 (δ_C 209.1) was evident.

Nocarditriene (**40**) is a polyketide alkaloid containing a rare epoxy-2,3,4,5-tetrahydropyridine structure. Unless fused to another carbocycle, as in latumcidin (**43**), epoxy-tetrahydropyridines have not been observed in other natural products to date.[29] Reduction of nocarditriene to the corresponding epoxy-piperidine, which has been observed in some cultivations of CNY-503 (unpublished results), revealed the biosynthetic and structural similarities between **40** and cyclizidine (**44**), indolizomycin (**45**), streptazone E (**46**), and several other related metabolites.[30-33] As such, the metabolite is likely biosynthesized by a type I PKS, reductively off-loaded and cyclized to the imine.[34-35]
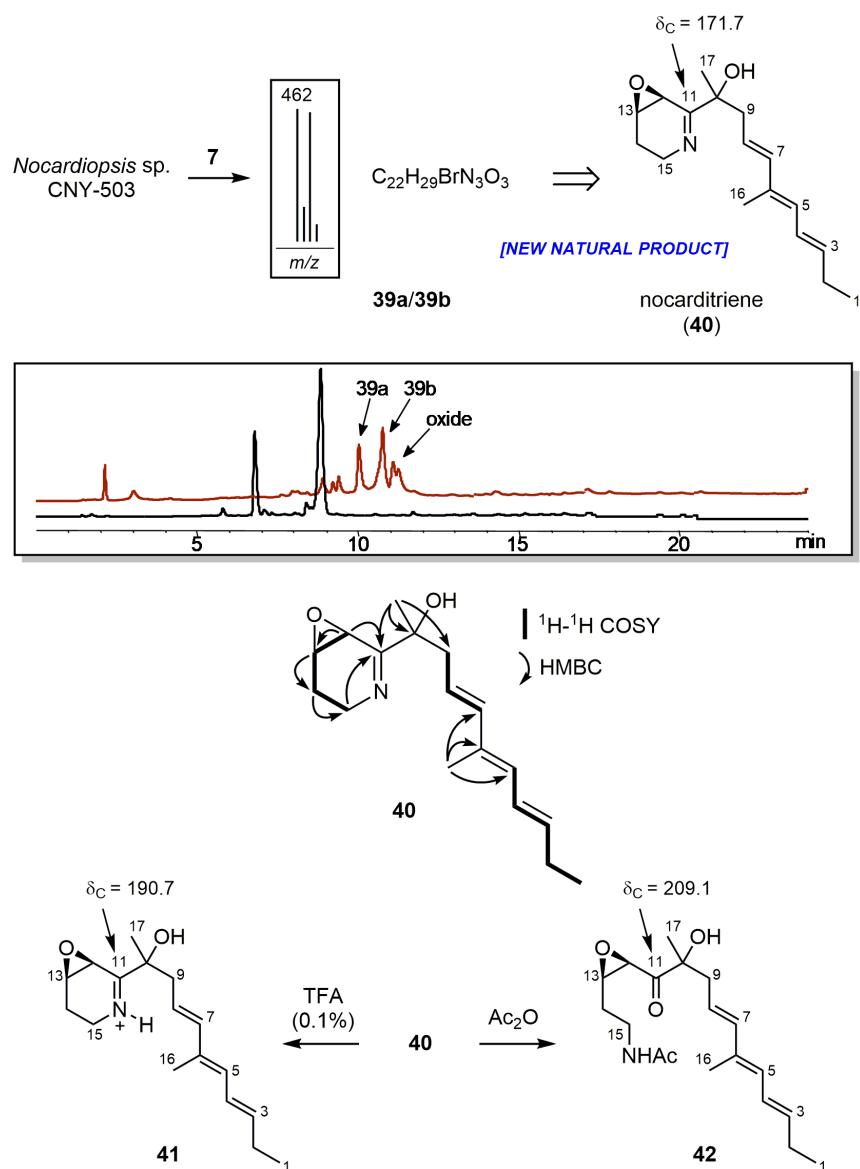
Figure 3.7 RGI of the nocarditriene (**40**). LC chromatograms at 254 nm are shown both before (black) and after (red) the labeling reaction. A) Treatment of extract from *Nocardiopsis* strain CNY-503 with **7** yielded brominated cycloadducts **39a/39b**, as a mixture of isomers, which are derived from nocarditriene (**40**). The relative configuration of the epoxide moiety is shown. Concentration from acidic solutions (0.1% TFA) yielded iminium ion **41**, which is characterized by a C-11 chemical shift of δ_C190.7. Treatment with acetic anhydride and triethylamine gave ketone **42**, which is characterized by a C-11 chemical shift of δ_C 209.1.
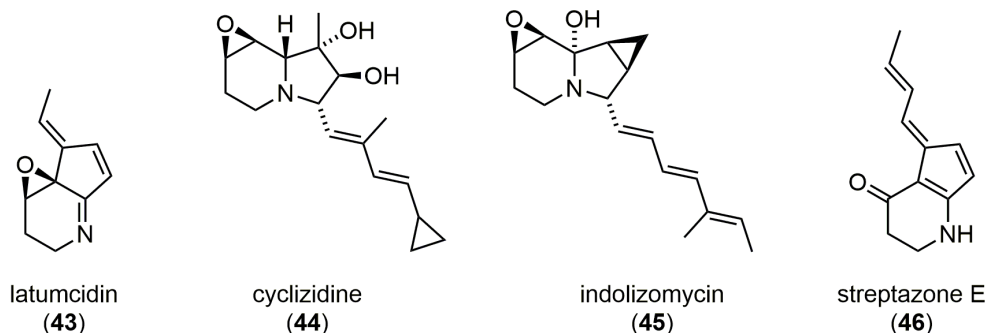
Figure 3.8 Structures of latumcidin (**43**), cyclizidine (**44**), indolizomycin (**45**), and streptazone E (**46**).

3.3.4 Development of Alkene-Seeker, a new genome mining tool for conjugated dienes

In order to increase our chances of finding new natural products with double bonds, we used a genome mining tool to prioritize the study of bacteria with the genetic capacity to produce these types of natural products.

With no particular orphan gene cluster containing alkene-encoding modules in mind, but eager to demonstrate the concept, we first developed a script called AlkeneSeeker. This script identifies successive KS-AT-DH-KR-ACP modules encoding conjugated dienes (n=2), trienes (n=3), tetraenes (n=4), etc., where n represents the number of alkene-encoding modules. This gene signature can be observed in non-iterative type I polyketide synthases (PKS) that produce macrolide natural products. We then used to program to interrogated bacterial reference genome sequences in RefSeq (NCBI Reference Sequence Database). After we queried the sequences for single instances of the alkene-encoding module (n=1), we focused on those with two successive KS-AT-DH-KR-ACP modules. From a list of around 1,450 strains, a total of 99 module pairs (n=2) from 36 diverse actinobacteria were found (Figure 3.9). As

expected, many of the identified strains are known producers of natural products with conjugated alkenes. For instance, spirofungin was isolated from *Streptomyces violaceusniger* Tü 4113,[36] L-681,217 was isolated from *Streptomyces cattleya* NRRL 8057[37], mirilactams were isolated from *Actinosynnema mirum* ATCC 29888[38], and chaxamycins and chaxalactins were isolated from *Streptomyces leeuwenhoekii*[39-41]. We selected five strains to cultivate (*Kutzneria albida* DSM 43870, *Streptomyces pratensis* ATCC 33331, *Saccharopolyspora erythrea* NRRL 2338, *Saccharothrix espanaensis* DMS 44229, and *Micromonospora aurantiaca* ATCC 27029) for the reasons that 1) they could be obtained commercially, 2) no conjugated alkene-containing natural products have been reported from these strains and 3) the biosynthetic gene clusters containing the alkene-encoding modules have a low percentage of genes showing similarity to the closest known gene cluster according to antiSMASH analysis. For example, the gene clusters of interest in the *Kutzneria* and *Streptomyces pratensis* strains are NRPS-type I PKS hybrid clusters with 55% and 70% of genes showing similarity to the vincenistatin gene cluster[42], and for the gene cluster of interest in the *Saccharothrix* strain 28% of genes show similarity to the streptazone gene cluster[33]. In the *Saccharopolyspora* strain there is one gene cluster of interest with 26% of genes showing similarity to that of the ECO-02301 gene cluster,[43] although there is another with 100% of genes showing similarity to the E-837 cluster.[44] Finally, in the gene cluster of interest in the *Micromonospora* strain 35% of the genes show similarity to rifamycin gene cluster.[3]
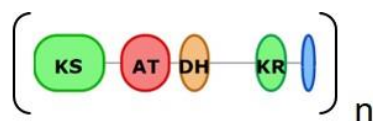
n=1	n=2	Org
28	9	Actinoplanes_sp_N902-109
28	6	Streptomyces_violaceusniger_Tu_4113
12	5	Streptomyces_cattleya_NRRL_8057_=_DSM_46488
21	5	Streptomyces_bingchenggensis_BCW-1
12	5	Actinosynnema_mirum_DSM_43827
13	4	Streptomyces_albus
12	4	Streptomyces_leeuwenhoekii
10	4	Kibdelosporangium_phytohabitans
8	4	**Kutzneria_albida_DSM_43870**
7	4	Salinispora_arenicola_CNS-205
6	4	Salinispora_tropica_CNB-440
14	4	Streptomyces_avermitilis_MA-4680_=_NBRC_14893
7	3	Actinoplanes_sp_SE50/110
5	3	**Streptomyces_pratensis_ATCC_33331**
7	3	Streptomyces_albulus
5	3	Streptomyces_hygroscopicus_subsp_jinggangensis_5008
5	2	**Saccharopolyspora_erythraea_NRRL_2338**
5	2	**Saccharothrix_espanaensis_DSM_44229**
5	2	Verrucosispora_maris_AB-18-032
7	2	**Micromonospora_aurantiaca_ATCC_27029**
7	2	Streptomyces_griseus_subsp_griseus_NBRC_13350
3	2	Pseudonocardia_sp_HH130629-09
6	2	Streptomyces_lydicus_A02
5	2	Frankia_sp_EAN1pec
5	2	Streptomyces_albus_J1074
4	1	Frankia_sp_EuI1c
4	1	Streptomyces_sp_CNQ-509
1	1	Rhodococcus_aetherivorans
3	1	Frankia_alni_ACN14a
2	1	Streptomyces_fulvissimus_DSM_40593
3	1	Streptomyces_ambofaciens
1	1	Methylobacterium_sp_4-46
2	1	Streptomyces_collinus_Tu_365
2	1	Frankia_symbiont_of_Datisca_glomerata
1	1	Rhodococcus_jostii_RHA1
6	1	Amycolatopsis_japonica

Figure 3.9 Output of a newly-created genome-mining tool, AlkeneSeeker, which searches genome sequences for the KS-AT-DH-KR-ACP domain architecture that codes for alkenes. Bacterial strains in bold were selected for cultivation and analysis.

### 3.3.5 Discovery of thrixazol and epostatin B from *Saccharothrix espanaensis* DSM 44229

Although all five strains have the potential to produce polyketide natural products with conjugated alkenes, we want to quickly distinguish producers from non-producers. To do this, we cultured the five bacteria in eight different media and we screened the

extracts using nitrosopyridine probe **7**. The formation of brominated adducts indicated the presence of the molecules. Indeed, an extract of *Saccharothrix espanaensis* with added **7** showed formation of brominated compounds (394.1140 m/z) not present in the original extract. Isolation and structure elucidation of the reactive natural product led to the identification of a new member of the streptazone class of natural products, thrixazol.

Thrixazol-TFA salt was isolated from reversed phase purification and could be neutralized to obtain an optically active ($[α]^{25}_D$ = + 58 (*c* 0.10, MeOH)) thrixazol as a clear film (~7.5 mg/L of culture). The molecular formula of the neutral base was established as $C_{13}H_{21}NO$ by HRESI-Q-TOF-MS [*m/z* (M+H)$^+$ calcd for $C_{13}H_{22}NO$ 208.1696, found 208.1694]. The IR spectrum contained absorption bands indicating presence of hydroxyl (3402 cm^{-1}) and alkene functionalities (=C-H stretch: 3013 cm^{-1}, =C-CH$_3$ stretch: 2928 cm^{-1} and C=C stretch: 1678 cm^{-1}). Analyses of ^{1}H, DQF-COSY, HSQC, HMBC and NOESY NMR data for thrixazol and thrixazol-TFA salt were used to completely establish the planar structure, geometry of double bonds and stereochemistry. In the chosen deuterated solvent (CD$_3$OD), the observed olefinic signals for thrixazol-TFA salt were spread apart, compared to the same protons for the thrixazol base. With no quaternary carbons, a COSY spin system could be traced for the entire carbon skeleton, including a 1, 6-disubstituted triene chain, which represents the nitroso-arene reactive portion of the molecule. Two chemical substitutions on the partial structure were attributed to a methyl (H-13 = 0.96 ppm / C-13 = 15.2 ppm) with a COSY correlation to an sp3-methine (H-9 = 1.80 ppm / C-9 = 39.0ppm), and to a hydroxyl attached to an sp3-methine (H-10 = 3.92 ppm / C-10 = 66.4 ppm). HMBC

correlations between an sp3-methylene (H-12a = 3.17 ppm, H-12b = 3.35 ppm / C-12 = 39.5 ppm) at one of the ends of the spin system with an sp3-methine (H-8 = 3.66 ppm / C-8 = 59.5 ppm) allylic to the triene suggested the presence of a piperidine ring.

Double bond geometry, as well as the conformation and relative stereochemistry about the piperidine ring was established through ^{1}H-NMR and NOESY interpretation. The triene was assigned all-trans based on high *J*-coupling values (>13.8 Hz) for all vinylic protons as well as NOESY correlations between the protons on the upper or lower side of the unsaturated chain. Furthermore, for thrixazol high *J*-coupling values (9-10 Hz) between vicinal protons H-8 and H-9 and between H-12b and H-11, and NOESY correlations between H-8 and H12b and between H-9 and H-11, suggested these were axial substituents on the piperidine arranged in a chair conformation. This meant that on the observed conformation of the piperidine ring, the unsaturated carbon side chain and the methyl were equatorial and the hydroxyl was axial.
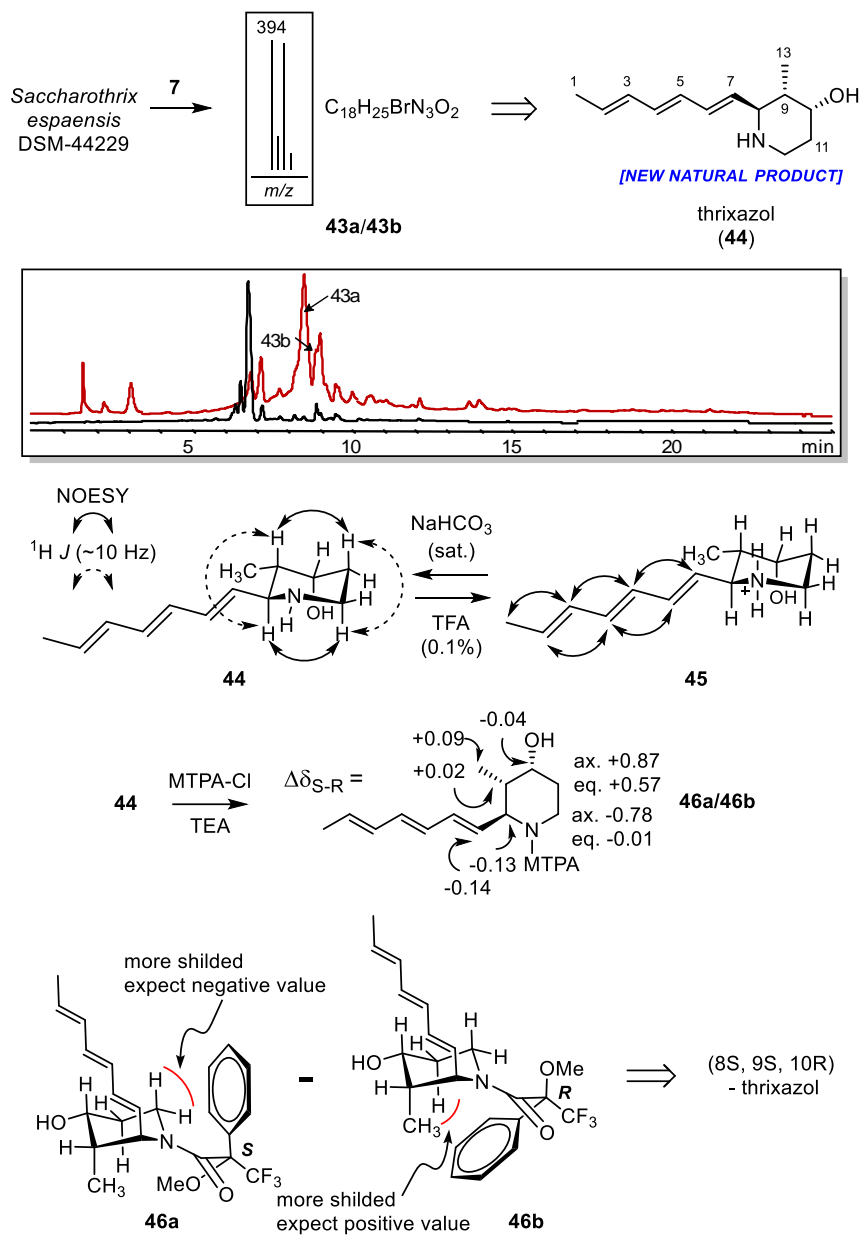
Figure 3.10 RGI of the thrixazol (**44**). LC chromatograms at 254 nm are shown both before (black) and after (red) the labeling reaction. A) Treatment of extract from *Saccharothrix espanaensis* strain DSM-44229 with **7** yielded brominated cycloadducts **43a**/**43b**, as a mixture of isomers, which are derived from thrixazol (**44**). Concentration from acidic solutions (0.1% TFA) yielded ammonium ion **45**. NOESY and 1H *J*-couplings ~10 Hz for **44** and **45** are illustrated. Chemical derivatization with R- and S-Mosher's-Cl (MTPA-Cl) with triethylamine yielded **46a/46b**. Key Δδ$_{S-R}$ for signals around the piperidine ring are shown. Anisotropic effect of phenyl substituent, illustrated in model, explains the observed Δδ$_{S-R}$ for (8S, 9S, 10R)-thrixazol.

In order to elucidate the absolute stereochemistry, we followed Mosher's advanced method for cyclic secondary amines.[45,46] The reaction between equivalent amounts of R- or S-Mosher's-chloride and triethylamine with thrixazol proceeded smoothly in less than an hour. No reaction on the secondary alcohol was observed. HPLC purification of the R- and S-MTPA derivatives, followed by assignment of NMR spectra, revealed a pronounced effect of the MTPA moieties on the conformation of the piperidine ring and the proton chemical shifts. Interpretation of ^{1}H-NMR J-coupling values for the protons on the ring indicated a flipped chair conformation, with respect to underivatized thrixazol (e.g. now the unsaturated side chain was in axial position). Only one rotamer was observed for each of the amides, and since the chemical shift differences ($\Delta\partial_{S-R}$) were most significant for protons on the un-substituted side of the piperidine ring, we assigned the amides to be in *trans* (anti-periplanar) conformation, which is consistent with what has been observed for this system.[45] With this in consideration, the calculated $\partial\Delta_{S-R}$ values for protons in the ring, of which the most significant were +0.87 for H-11$_{ax}$ and of -0.78 for H-12$_{ax}$, only were consistent with (8S, 9S, 10R)-thrixazol.

During the process of isolation of thrixazol, we also isolated compound **47** as a yellow film (~1 mg/L of culture). The molecular formula of the neutral base was established as $C_{23}H_{30}N_2O_4$ by HRESI-Q-TOF-MS [m/z (M+H)$^+$ calcd for $C_{13}H_{22}NO$ 399.2278, found 399.2274]. ^{1}H, DQF-COSY, HSQC, HMBC and NMR data were used to completely establish the planar structure. Apparent from the ^{1}H-NMR were the signals for five olefinic protons. Interestingly, two of these coupled to each other with J-coupling constants of ~7 Hz, which was interpreted as a 1,2-disubstituted alkene in a

five membered ring (*i.e.* cyclopentenyl). The other three olefinic protons had *J*-coupling

constants > 12 Hz and together formed a COSY spin system. HMBC correlations

shared between the five olefinic protons signaled that this was in fact a complex triene

system, with an endocyclic, an exocyclic and an alicyclic double bond. Extending from

the cyclopentenyl, there were four carbons apparently substituted by nitrogen or oxygen

(a methylene, two methines and a quaternary carbon). Careful analysis revealed this to

be a piperidine ring fused to an epoxide on one side and to the cyclopentene on another

adjacent side. A 2-methylpentnyl side chain substituted one of the hydrogens on the

piperidine ring. On the other side of the triene, we could see by HMBC the direct

attachment of a carbonyl (C-1, δ_C = 165.3 ppm), which we predicted to be an amide due

to the presence of a downshifted singlet (2"-NH, δ_H = 10.08 ppm) with HMBC

correlations to the carbonyl. This amide proton also showed HMBC correlations to a

quaternary carbon with δ_C = 114.9 ppm but not much else could be elucidated in this

region by NMR. We suspected the carbonyl was substituted with 2-amino-3-

hydroxycyclopent-2-enone since it made sense in terms of mass and since this moiety

shows a characteristic quaternary carbon ~115 ppm and broadened-to-lack of other

signals in the unit due to keto-enol tautomerization.[25] Indeed, by negative ionization

MS/MS we observed an intense 112 m/z fragment ion previously ascribed to 2-amino-3-

hydroxycyclopent-2-enone.[47]

The relative stereochemistry about the tricycle and the geometry of double bonds

was elucidated from NOESY analysis. Correlations from the amide proton (2"-NH) to the

triene H-2, suggested that these were co-planar. Correlations from H-2 to H-4 and from

H-4 to H-10 suggested the C-2 and C-4 alkenes are *trans*. On the piperidine ring, key

correlations between H-8 and H-12$_a$, H-13 and H-12$_b$ and H-13 and H-10, were key to assign the relative stereochemistry of epostatin B as 8R*, 9R*, 10S*, 11R*. Interestingly, reaction of R- and S-Mosher's chloride with triethylamine and **47** afforded amide derivatives **48a/48b** that had lost all stereocenters, thereby hindering the absolute configuration assignment through this methodology.
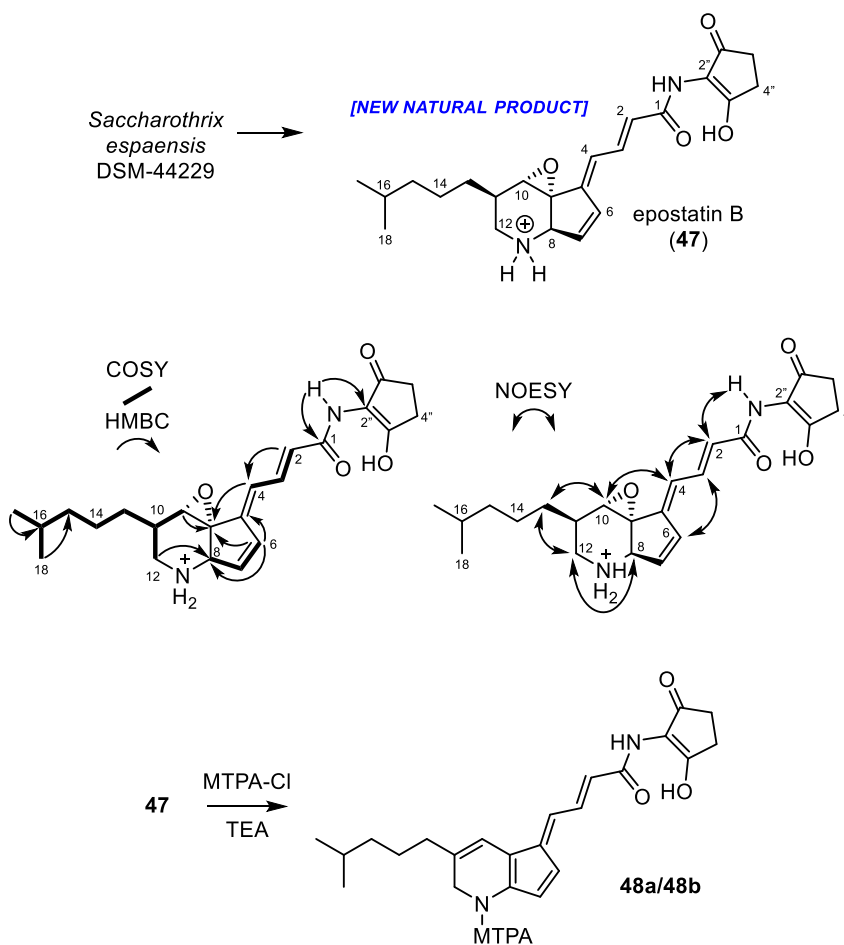
Figure 3.11 Isolation and structural elucidation of epostatin B (**47**). Key COSY, HMBC and NOESY correlation for **47** are illustrated. and for **44** and **45** are displayed. . Chemical derivatization with R- and S-Mosher's-Cl (MTPA-Cl) and triethylamine yielded **48a/48b**.

We hypothesize that the natural product was unreactive to the diene probe since one of the carbons (C-5) that should engage in the Diels-Alder reaction is disubstituted

and sterically impeded. Another possibility is that the dienes cannot adopt an s-*cis*

conformation needed for reactivity.

Similar to the nocarditrienes, these molecules, thrixazol and epostatin B, are part

a growing family of alkaloids isolated from bacteria that are of polyketide origin and

contain a piperidine ring. Epostatin B shows high similarity to epostatin isolated in 1998

from *Streptomyces* sp. MJ995-OF5,[48] to camporidines A-B, which show the same

relative stereochemistry, isolated very recently from *Streptomyces* sp. STA1,[49] and the

argimycins isolated from *Streptomyces argillaceus*.[50,51] The points of differences,

relative to these compounds, seem to be on the aliphatic side chain substitution

extending from the piperidine ring on the substitutions on the carboxy terminus (if

present) and the oxidation state of the piperidine ring.

3.4 CONCLUSION

Reactivity-guided isolation (RGI) is used to select for specific metabolites in an

extract by targeting naturally-occurring structural features. The derivative formed is a

highly detectable, often crystalline entity worthy of characterization because its structure

reveals the structure of the original natural product following simple retrosynthetic

analysis. The subsequent identification of the unlabeled metabolite in the LC-MS

chromatogram of unreacted extract is trivial. Provided the appropriate bioassay is in

place, these natural products could be isolated using traditional bioactivity-guided

isolation (BGI). However, RGI is chemocentric while BGI is completely disconnected

from structure. Here, we show that RGI can also complement genome-mining analyses

since the latter produce predictions of natural product structure that ultimately need to be validated.

When targeting pharmacophores, the labeled metabolite is not expected to retain the biological activity associated with the unlabeled metabolite since the pharmacophore is disrupted in the process.[10] But the targeted functional group need not be a pharmacophore. If the metabolite exhibits bioactivity, the non-pharmacophore nature of the functional group, a conjugated alkene in the present case, means that the labeled metabolites may retain this activity. In many cases, however, alteration of the overall 3D structure of the molecule disrupts binding to its original target. In fact, the association of rapamycin with mTOR was deliberately prevented by reacting the natural product with nitrosobenzene.[17] The effect on biological activity of nitrosobenzene and nitrosopyridine derivatization for the natural products described above, and their isolable derivatives, has not been thoroughly assessed.

RGI allows natural products chemists to uncover metabolites with a specified functional group or structural feature that may otherwise be challenging to find in a complex extract. It does not address other issues in the field that thwart discovery efforts, such as the existence of "silent" biosynthetic gene clusters. Certainly, a somewhat exhaustive chemical analysis of any of the extracts mentioned above would lead to the isolation of the very same metabolites, especially those in high abundance, such as nocarditriene and thrixazol. We contend, however, that with automated LC-MS tools like MeHaloCoA and DeltaMS, RGI can be successfully applied to a large number of extracts and is capable of identifying inconspicuous metabolites that are in very low abundance and hidden in the muck.[20,52]

3.5 METHODS

Preparation, detection, and purification of 1-bromo-4-nitrosobenzene (6).

Nitrosobenzene **6** was prepared according to the literature.[53,54] To a solution of 4-bromoaniline (2.50 g, 14.5 mmol) in DCM (50 mL) was added a solution of oxone (17.9 g, 29.0 mmol) in water (150 mL). The mixture was stirred vigorously overnight, and the layers were then separated. The aqueous layer was extracted with DCM (50 mL). The combined organic layers were washed with 1 M HCl (30 mL), a saturated $NaHCO_3$ solution (30 mL), water (30 mL), brine (20 mL), dried over Na_2SO_4, filtered, and concentrated. The product was dry-loaded onto silica gel and purified by silica gel chromatography [80 g silica gel cartridge, 60 mL min^{-1}, 100% hexanes for 10 min, 0-5% EtOAc in hexanes over 15 min, t_R = 12-25 min] to afford, after trituration with methanol to remove color, 1.18 g (44%) of **6** as a white solid. UV/Vis: λ_{max} = 228, 293, 318 nm; ^{1}H NMR (500 MHz, CDCl$_3$): δ 7.78 (m, 4H); ^{13}C NMR (125 MHz, CDCl$_3$): δ 164.0, 132.8, 131.9, 122.3; the exact mass could not be obtained using ESI-MS.

Preparation, detection, and purification of 5-bromo-2-nitrosopyridine probe (7). Nitrosopyridine **7** was prepared in a similar manner to the literature with crucial modifications as described in Howard, *et al.*[12,16] To a solution of 2-amino-5-bromopyridine (4.78 g, 27.6 mmol) and dimethylsulfide (2.2 mL, 30 mmol) in DCM (25 mL) at 0 °C was added a solution of *N*-chlorosuccinimide (3.69 g, 27.6 mmol) in DCM (100 mL) dropwise via cannula over 1 h. After an additional 1 h at 0 °C, the solution was allowed to warm to rt for 1 h. A solution of sodium ethoxide (15 g, 21 wt%, 46 mmol) was then added, followed 10 min later by the addition of water (25 mL). After 4 h at rt,

additional water (100 mL) was added, and the layers were separated. The aqueous layer was extracted with DCM (50 mL). The combined organic extracts were washed with water, dried over Na_2SO_4, filtered, and concentrated. To a stirring solution of the mCPBA (13.6 g, 70%, 55.2 mmol) in DCM (200 mL) at 0 °C was added a solution of the crude sulfilimine in DCM (50 mL) dropwise via cannula over 15 min. After 30 min at 0 °C, dimethylsulfide (1.0 mL, 13 mmol) was added. A saturated solution of Na_2CO_3 (100 mL) was added, and the layers were separated. The organic layer was washed with water, dried over Na_2SO_4, filtered, and concentrated. The product was dry-loaded onto silica gel and purified by silica gel chromatography [80 g silica gel cartridge, 60 mL min^{-1}, 0-20% EtOAc in hexanes over 25 min, 20% EtOAc in hexanes for 10 min, t_R = 15-33 min] to afford 1.19 g (23%) of **7** as a yellow solid. UV/Vis: λ_{max} = 228, 304, 318 nm; ^{1}H NMR (500 MHz, CDCl$_3$): δ 8.88 (d, J = 2.1 Hz, 1H), 8.20 (dd, J = 8.4, 2.1 Hz, 1H), 7.20 (d, J = 8.4 Hz, 1H), dimer: δ 8.11 (br s, 1H), 8.07 (dd, J = 8.6, 2.1 Hz, 1H), 7.78 (d, J = 8.6 Hz, 1H); ^{13}C NMR (125 MHz, CDCl$_3$): δ 166.9, 154.1, 150.6, 148.1, 142.4, 141.9, 128.0, 122.8, 120.0, 111.5; HRESI-Q-TOF-MS: m/z (M+Na)$^+$ 208.9326 calcd for $C_5H_3{}^{79}BrN_2ONa$, found 208.9326. Nitrosopyridines **8-10** were prepared in a similar manner.

Generation of crude extracts. All strains were obtained from SIO actinomycete culture collection *Streptomyces* sp. CNQ-085, *Salinispora pacifica* CNT-084, *Saccharomonospora* sp. CNQ-490, and *Nocardiopsis* sp. CNY-503 were obtained from and grown in A1 seawater medium (10 g L^{-1} of starch, 4 g L^{-1} of yeast extract and 2 g L^{-1} of peptone in 75% seawater and 25% deionized water) and *Streptomyces sp.* CNQ-593 was grown in a seawater marine medium (chitosan 2 g L^{-1}, krill powder 2 g L^{-1},

menhaden meal 2 g L^{-1}, fish solubles 4 g L^{-1}, starch 5 g L^{-1}). From cryovials, these strains were first grown in starter cultures (50 mL) and after 4-5 days the whole volume was used to inoculate culture media (1 L). If necessary, after 3-4 days, 25 mL aliquots of the pre-cultures were used to inoculate producing cultures (1 L). All cultures were incubated at 27 °C with rotatory shaking at 200 rpm for 2-7 days, after which Amberlite XAD-16N and XAD-7HP (~10 g L^{-1} each) was added and left shaking for 2 h. The resin was filtered through cheesecloth, washed with deionized water, and extracted with acetone. The acetone was removed under reduced pressure, and the resulting aqueous layer was extracted with ethyl acetate. The combined organic extracts were dried over sodium sulfate, and concentrated.

Labeling reactions. To pure natural product or crude extract, probe **6** or **7** was added dry THF and the reaction vessel sealed. In general, reactions with **6** were heated in an oil bath at 60 °C for 12 h, while reactions with **7** were left stirring at room temperature for 3 h. The progress of the reactions was monitored on an analytical Agilent 1100 Series HP system (1.0 mL min^{-1}) with UV (210, 254, and 360 nm) and ELS detection and also on an analytical Agilent 1260 Infinity Series LC system coupled to a 6530 Series Q-TOF mass spectrometer, both using a C18(2) Phenomenex Luna column (5 μm, 100 mm x 4.6 mm) with a 10 or 20 min solvent gradient from 10% to 100% acetonitrile + 0.1% formic acid in water. Probe adducts were purified by isocratic reversed-phase HPLC (acetonitrile and water + 0.1% trifluoroacetic acid (if needed)) using a C8(2), C18(2) or CN Phenomenex Luna columns (5 μm, 250 mm X 10 mm) with UV detection.

3.6 ACKNOWLEDGMENTS

3.7 REFERENCES

(1) Sehgal, S. N., Baker, H., and Vézina, C. (1975) Rapamycin (AY-22,989), a new antifungal antibiotic. II. Fermentation, isolation and characterization. J. Antibiot. (Tokyo). 28, 727–732.

(2) Vezina, C., Kudelski, A., and Sehgal, S. N. (1975) Rapamycin (AY-22,989), a new antifungal antibiotic. I. Taxonomy of the producing streptomycete and isolation of the active principle. J. Antibiot. (Tokyo). 28, 721–726.

(3) Aristoff, P. A., Garcia, G. A., Kirchhoff, P. D., and Hollis Showalter, H. D. (2010) Rifamycins - obstacles and opportunities. Tuberculosis 90, 94–118.

(4) Burg, R. W., Miller, B. M., Baker, E. E., Birnbaum, J., Currie, S. A., Hartman, R., Monaghan, R. L., Putter, I., Tunac, J. B., Wallick, H., and Stapley, E. O. (1979) Avermectins, new family of potent anthelmintic agents: Producing organism and fermentation. Antimicrob. Agents Chemother. 15, 361–367.

(5) Kuhstoss, S., Huber, M., Turner, J. R., Paschal, J. W., and Rao, R. N. (1996) Production of a novel polyketide through the construction of a hybrid polyketide synthase. Gene 183, 231–236.

(6) Schwecke, T., Aparicio, J. F., Molnár, I., König, A., Khaw, L. E., Haydock, S. F., Oliynyk, M., Caffrey, P., Cortés, J., Lester, J. B., Böhm, G. A., Staunton, J., and Leadlay, P. F. (1995) The biosynthetic gene cluster for the polyketide immunosuppressant rapamycin. Proc. Natl. Acad. Sci. U. S. A. 92, 7839–7843.

(7) August, P. R., Tang, L., Yoon, Y. J., Ning, S., Rolf, M., Yu, T., Taylor, M., Hoffmann, D., Kim, C., Zhang, X., Hutchinson, C. R., and Floss, H. G. (1998) Biosynthesis of the ansamycin antibiotic rifamycin: deductions from the molecular analysis of the rif

biosynthetic gene cluster of Amycolatopsis mediterranei S699. Chem. Biol. 4, 69–79.

(8) Ikeda, H., Nonomiya, T., Usami, M., Ohta, T., and Omura, S. (1999) Organization of the biosynthetic gene cluster for the polyketide anthelmintic macrolide avermectin in Streptomyces avermitilis. Proc. Natl. Acad. Sci. U. S. A. 96, 9509–9514.

(9) Leach, A. G., and Houk, K. N. (2001) Transition states and mechanisms of the hetero-Diels-Alder reactions of hyponitrous acid, nitrosoalkanes, nitrosoarenes, and nitrosocarbonyl compounds. J. Org. Chem. 66, 5192–5200.

(10) Yamamoto, H., and Momiyama, N. (2005) Rich chemistry of nitroso compounds. Chem. Commun. 3514.

(11) Zuman, P., and Shah, B. (1994) Addition, reduction, and oxidation reactions of nitrosobenzene. Chem. Rev. 94, 1621–1641.

(12) Li, F., Yang, B., Miller, M. J., Zajicek, J., Noll, B. C., Mollmann, U., Dahse, H. M., and Miller, P. A. (2007) Iminonitroso Diels-Alder reactions for efficient derivatization and functionalization of complex diene-containing natural products. Org. Lett. 9, 2923–2926.

(13) Brulíková, L., Harrison, A., Miller, M. J., and Hlaváč, J. (2016) Stereo- and regioselectivity of the hetero-Diels–Alder reaction of nitroso derivatives with conjugated dienes. Beilstein J. Org. Chem. 12, 1949–1980.

(14) Carosso, S., and Miller, M. J. (2014) Nitroso Diels-Alder (NDA) reaction as an efficient tool for the functionalization of diene-containing natural products. Org. Biomol. Chem. 12, 7445–68.

(15) Priewisch, B., and Rück-Braun, K. (2005) Efficient preparation of nitrosoarenes for the synthesis of azobenzenes. J. Org. Chem. 70, 2350–2352.

(16) Howard, J. A. K., Ilyashenko, G., Sparkes, H. A., Whiting, A., and Wright, A. R. (2008) Mechanistic insights into transition metal-catalysed oxidation of a hydroxamic acid with in situ Diels-Alder trapping of the acyl nitroso derivative. Adv. Synth. Catal. 350, 869–882.

(17) Ruan, B., Pong, K., Jow, F., Bowlby, M., Crozier, R. A., Liu, D., Liang, S., Chen, Y., Mercado, M. L., Feng, X., Bennett, F., von Schack, D., McDonald, L., Zaleska, M. M., Wood, A., Reinhart, P. H., Magolda, R. L., Skotnicki, J., Pangalos, M. N., Koehn, F. E., Carter, G. T., Abou-Gharbia, M., and Graziani, E. I. (2008) Binding of rapamycin analogs to calcium channels and FKBP52 contributes to their neuroprotective activities. Proc. Natl. Acad. Sci. U. S. A. 105, 33–38.

(18) Abou-Gharbia, M. (2009) Discovery of innovative small molecule therapeutics. J. Med. Chem. 52, 2–9.

(19) Becker, Y., Bronstein, S., Eisenstadt, A., and Shvo, Y. (1976) A reaction of α-pyrone and nitrosobenzene. J. Org. Chem. 41, 2496–2498.

(20) Roullier, C., Guitton, Y., Valery, M., Amand, S., Prado, S., Robiou Du Pont, T., Grovel, O., and Pouchus, Y. F. (2016) Automated detection of natural halogenated compounds from LC-MS profiles-Application to the isolation of bioactive chlorinated compounds from narine-derived fungi. Anal. Chem. 88, 9143–9150.

(21) Awakawa, T., Crüsemann, M., Munguia, J., Ziemert, N., Nizet, V., Fenical, W., and Moore, B. S. (2015) Salinipyrone and pacificanone are biosynthetic by-products of the rosamicin polyketide synthase. ChemBioChem 16, 1443–1447.

(22) Omura, S., Kitao, C., and Matsubara, H. (1980) Isolation and characterization of a new 16-membered lactone, protylonolide, from a mutant of tylosin-producing strain, Streptomyces fradiae KA-427. Chem. Pharm. Bull. 28, 1963–1965.

(23) Demars, M. D., Sheng, F., Park, S. R., Lowell, A. N., Podust, L. M., and Sherman, D. H. (2016) Biochemical and structural characterization of MycCI, a versatile P450 biocatalyst from the mycinamicin biosynthetic pathway. ACS Chem. Biol. 11, 2642–2654.

(24) Asolkar, R. N., Jensen, P. R., Kauffman, C. A., and Fenical, W. (2006) Daryamides A-C, weakly cytotoxic polyketides from a marine-derived actinomycete of the genus Streptomyces strain CNQ-085. J. Nat. Prod. 69, 1756–1759.

(25) Sattler, I., and Zeeck, A. (1998) The manumycin-group metabolites. Nat. Prod. Rep. 221–240.

(26) Fu, P., La, S., and MacMillan, J. B. (2017) Daryamide analogues from a marine-derived Streptomyces species. J. Nat. Prod. 80, 1096–1101.

(27) Miller, E. D., Kauffman, C. A., Jensen, P. R., and Fenical, W. (2007) Piperazimycins: Cytotoxic hexadepsipeptides from a marine-derived bacterium of the genus streptomyces. *J. Org. Chem. 72, 323–330*

(28) Yim, C. Y., Le, T. C., Lee, T. G., Yang, I., Choi, H., Lee, J., Kang, K. Y., Lee, J. S., Lim, K. M., Yee, S. T., Kang, H., Nam, S. J., and Fenical, W. (2017) Saccharomonopyrones A–C, new *α*-pyrones from a marine sediment-derived bacterium Saccharomonospora sp. CNQ-490. Mar. Drugs 15, 4–11.

(29) Kono, Y., and Takeuchi, S. et al. (1970) The structure of latumcidin (abikoviromycin) determined by X-ray analysis. J. Antibiot. (Tokyo). 23, 572–573.

(30) Freer, A. A., Gardner, D., Greatbanks, D., Poyser, J. P., and Sim, G. A. (1982) Structure of cyclizidine (antibiotic M146791): X-ray crystal structure of an

indolizidinediol metabolite bearing a unique cyclopropyl side-chain. J. Chem. Soc., Chem. Commun. 1160–1162.

(31) Gomi, S., Ikeda, D., Nakamura, H., Naganawa, H., Yamashita, F., Hotta, K., Kondo, K., Okami, Y., and Umezawa, H. (1984) Isolation and structure of a new antibiotic, indolizomycin, produced by a strain SK2-52 obtained by interspecies fusion treatment. J. Antibiot. (Tokyo).

(32) Huang, W., Kim, S. J., Liu, J., and Zhang, W. (2015) Identification of the polyketide biosynthetic machinery for the indolizidine alkaloid cyclizidine. Org. Lett. 17, 5344–5347.

(33) Ohno, S., Katsuyama, Y., Tajima, Y., Izumikawa, M., Takagi, M., Fujie, M., Satoh, N., Shin-Ya, K., and Ohnishi, Y. (2015) Identification and characterization of the streptazone E biosynthetic gene cluster in Streptomyces sp. MSC090213JE08. ChemBioChem 16, 2385–2391.

(34) Peng, H., Wei, E., Wang, J., Zhang, Y., Cheng, L., Ma, H., Deng, Z., and Qu, X. (2016) Deciphering piperidine formation in polyketide-derived indolizidines reveals a thioester reduction, transamination, and unusual imine reduction process. ACS Chem. Biol. 11, 3278–3283.

(35) Awodi, U. R., Ronan, J. L., Masschelein, J., De Los Santos, E. L. C., and Challis, G. L. (2016) Thioester reduction and aldehyde transamination are universal steps in actinobacterial polyketide alkaloid biosynthesis. Chem. Sci. 8, 411–415.

(36) Höltzel, A., Kempter, C., Metzger, J. W., Jung, G., Groth, I., Fritz, T., Fiedler, H.P. (1998) Spirofungin, a new antifungal antibiotic from Streptomyces violaceusniger Tu 4113. J. Antibiot. (Tokyo) 51, 699–707.

(37) Kempf, A. J., Wilson, K. E., Hensens, O. D., Monaghan, R. L., Zimmerman, S. B., Dulaney, E. L. (1986) L-681,217, a new and novel member of the efrotomycin family of antibiotics. J. Antibiot. (Tokyo) 39, 1361–1367.

(38) Schulze, C. J., Donia, M. S., Siqueira-Neto, J. L., Ray, D., Raskatov, J. A., Green, R. E., McKerrow, J. H., Fishbach, M. A., Linington, R. G. (2015). Genome-directed lead discovery: Biosynthesis, structure elucidation, and biological evaluation of two families of polyene macrolactams against Trypanosoma brucei. ACS Chem. Biol. 10, 2373–2381.

(39) M. E. Rateb, W. E. Houssen, M. Arnold, M. H. Abdelrahman, H. Deng, W. T. A. Harrison, C. K. Okoro, J. A. Asenjo, B. A. Andrews, G. Ferguson, A. T. Bull, M. Goodfellow, R. Ebel, M. Jaspars, J. Nat. Prod. 2011, 74, 1491–1499.

(40) K. Busarakam, A. T. Bull, G. Girard, D. P. Labeda, G. P. van Wezel, M. Goodfellow, Antonie van Leeuwenhoek. 2014, 105, 849–861.

(41) Rateb, M. E., Houssen, W. E., Harrison, W. T. A., Deng, H., Okoro, C. K., Asenjo, J. A., Andrews, B. A., Bull, A. T., Goodfellow, M., Ebel, R., Jaspars, M. (2011) Diverse metabolic profiles of a Streptomyces strain isolated from a hyper-arid environmnent. J. Nat. Prod. 74, 1465–1971.

(42) Shindo, K., Kamishohara, M., Odagawa, A., Matsuoka, M., Kawai, H. (1993) Vicenistatin, a novel 20-membered macrocyclic lactam antitumor antibiotic. J. Antibiot. (Tokyo). 46, 1076–1081.

(43) McAlpline, J. B., Bachmann, B. O., Piraee, M., Tremblay, S., Alarco, A. M., Zazopoulos, E., Farnet, C. M. (2005) Microbial genomics as a guide to drug discovery and structural elucidation: ECO-02301, a novel antifungal agent, as an example. *J. Nat. Prod. 68, 493*–496.

(44) Banskota, A. H., McAlpine, J. B., Sørensen, D, Aouidate, M., Piraee, M., Alarco, A. M., Omura, S., Shiomi, K., Farnet, C. M., Zazopoulos, E. (2006) Isolation and identification of three new 5-alkenyl-3,3(2H)-furanones from two Streptomyces species using a genomic screening approach. J. Antibiot. (Tokyo) 59, 168–176.

(45) Kang, C. Q., Guo, H. Q., Qiu, X. P., Bai, X. L., Yao, H. B., Gao, L. X. (2006) Assignment of absolute configuration of cyclic secondary amines by NMR techniques using Mosher's method: a general procedure exemplified with (–)-isoanabasine. *Magn. Reson. Chem. 44, 20*–24.

(46) Hoye, T. R., Renner, M. K. (1996) MTPA (Mosher) amides of cyclic secondary amines: conformational aspects and a useful method for assignment of amine configuration. *J. Org. Chem.*, *61, 2056*–2064.

(47) Petříčková, K., Pospíšil, S., Kuzma, M., Tylová, T., Jágr, M., Tomek, P., Chroňáková, A., Brabcová, E., Anděra, L., Krištůfek, V., Petříček, M. (2014) Biosynthesis of colabomycin E, a new manumycin-family metabolite, involves an unusual chain-length factor. *ChemBioChem, 15, 1334–1345.*

(48) Akiyama, T., Sawa, R., Naganawa, H., Muraoka, Y., Aoyagi, T., Takeuchi, T. (1998) Epostatin, new inhibitor of dipeptidyl peptidase II, produced by Streptomyces sp. MJ995-OF5: II. Structure elucidation. J. Antibiot. (Tokyo). 51, 372−*374.*

(49) Hong, S. H., Ban, Y. H., Byun, W. S., Kim, D., Jang, Y. J., An, J. S., Shin, B., Lee, S. K., Shin, J., Yoo, Y. J., Oh, D. C. (2019) Camporidines A and B: antimetastatic and anti-inflammatory polyketide alkaloids from a gut bacterium of Camponotus kiusiuensis. *J. Nat. Prod. 82, 903–910.*

(50) Ye, S., Braña, A. F., Zabala, D., Olano, C., Cortés, J., Morís, F., Salas, J. A., Méndez, C. (2017) Identification by genome mining of a type I polyketide gene cluster from Streptomyces argillaceus involved in the biosynthesis of pyridine and

piperidine alkaloids argimycins P. *Front. Microbiol. 9, 194.*

(51) Ye, S., Braña, A. F., González-Sabín, J., Morís, F., Olano, C., Salas, J. A., Méndez, C. (2018) New insights into the biosynthesis pathway of polyketide alkaloid argimycins P in Streptomyces argillaceus. *Front. Microbiol. 9, 252.*

(52) Baumeister, T. U. H., Ueberschaar, N., Schmidt-Heck, W., Mohr, J. F., Deicke, M., Wichard, T., Guthke, R., and Pohnert, G. (2018) DeltaMS: a tool to track isotopologues in GC- and LC-MS data. *Metabolomics 14, 1−10.*

(53) Malpani, Y. R., Oh, S., Lee, S., Jung, Y. S., and Kim, J. M. (2014) Photoinduced phase transition of azobenzene-coupled benzenetricarboxamide. *Bull. Korean Chem. Soc. 35*, 2563–2566.

(54) Nguyen, T. T. T., Türp, D., Wang, D., Nölscher, B., Laquai, F., and Müllen, K. (2011) A fluorescent, shape-persistent dendritic host with photoswitchable guest encapsulation and intramolecular energy transfer. *J. Am. Chem. Soc. 133*, 11194–11204.
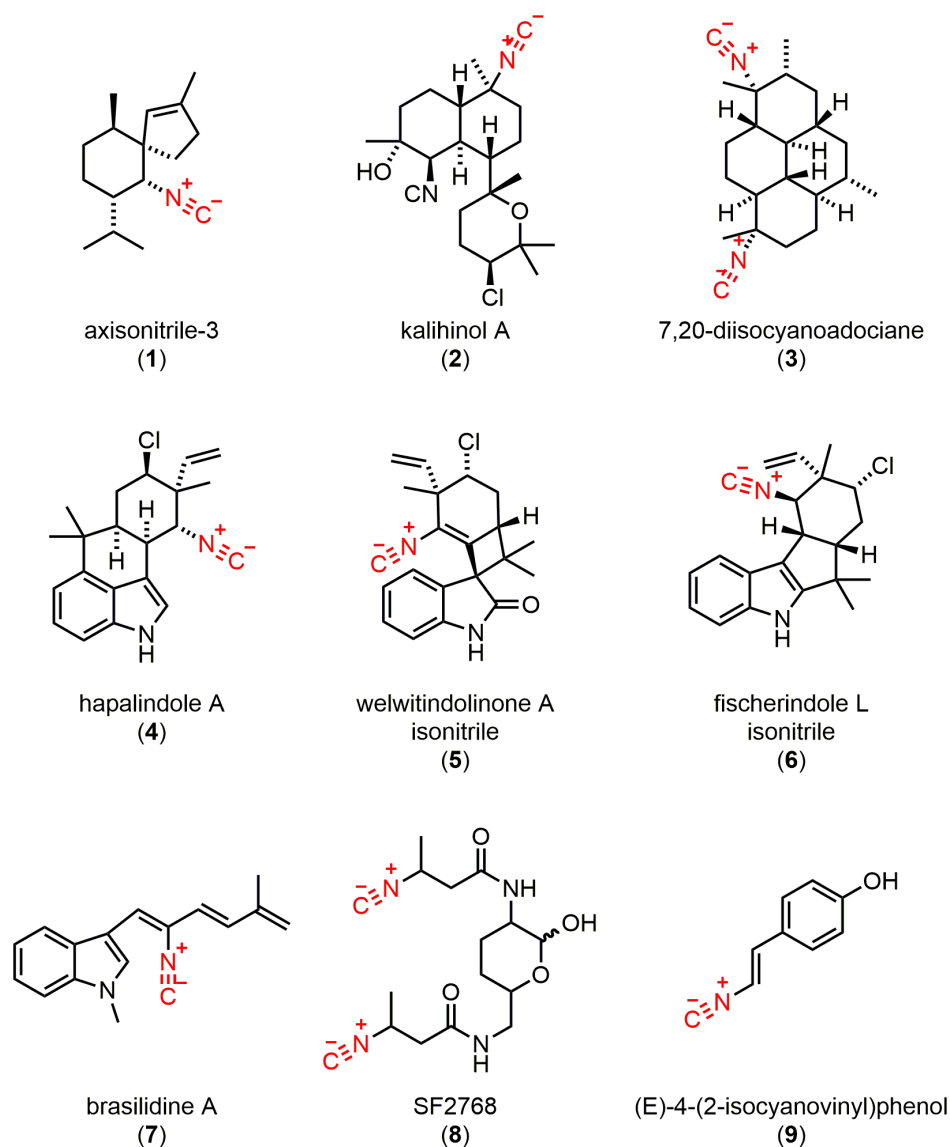
Chapter 4

Tetrazine probes to detect isocyanide-containing natural products in extracts

4.1 INTRODUCTION

Isocyanide-containing natural products have been isolated from nudibranchs, sponges, cyanobacteria, bacteria, and fungi. Marine isocyanides such as axionitrile-3 (**1**), kalihinol A (**2**), and 7,20-diisocyanoadociane (**3**) and cyanobacterial isocyanides like hapalindole A (**4**), welwitindolinone A isonitrile (**5**), and fischerindole L isonitrile (**6**) are complex, polycyclic natural products that are densely substituted with chiral stereocenters (Figure 4.1).[1–3] As such, these compounds have captivated synthetic organic chemists since their initial discovery in the 1970s.[4] Isocyanides from bacteria and fungi, such as brasilidine A (**7**),[5] SF2768 (**8**),[6] and (E)-4-(2-isocyanovinyl)phenol (**9**),[7] are generally simpler in structure. Although their ecological role is likely related to their ability to bind metals,[8,9] many isocyanides have been shown to have pronounced activity against the malaria parasite *Plasmodium falciparum*, in addition to other biological activities related to the treatment of disease.[10]

Most naturally-occurring isocyanides have been isolated using nonspecific chemical screening of extracted organisms with or without a bioassay to help guide the process.[5–7,10–16] Heterologous expression of orphan biosynthetic gene clusters in bacteria has also led to the discovery of isocyanides, and this approach has even revealed genes specific for the production of certain isocyanides.[8,17–19] The tell-tale signatures of the isocyanide functionality are the unique isocyanide IR stretch (2165-2110 cm^{-1}) and characteristic ^{13}C-^{14}N coupling present in ^{13}C NMR spectra. However, these analytical methods are not readily suitable for the directed isolation of isocyanides

from complex mixtures using, for example, liquid chromatography, such that at present putative isocyanide compounds must be purified and analyzed individually. Thus, an isocyanide-specific HPLC-MS method would allow for the rapid detection of isocyanide-containing natural products in complex extracts and, more generally, provide a valuable tool for biochemical and biological investigations involving isocyanide chemistry.

axisonitrile-3
(**1**)

kalihinol A
(**2**)

7,20-diisocyanoadociane
(**3**)

hapalindole A
(**4**)

welwitindolinone A
isonitrile
(**5**)

fischerindole L
isonitrile
(**6**)

brasilidine A
(**7**)

SF2768
(**8**)

(E)-4-(2-isocyanovinyl)phenol
(**9**)

Figure 4.1 Representative isocyanide-containing natural products.

The tetrazine-isocyanide [4+1] cycloaddition was first reported by Seitz and co-workers in 1982.[20] Model tetrazine 3,6-di-2-pyridyl-1,2,4,5-tetrazine (10) reacts with generic isocyanide 11 in a [4+1] cycloaddition reaction to give 12, which is then converted to 4H-pyrazol-4-imine 13 in a retro [4+2] cycloaddition.[21] Tertiary isocyanides give relatively stable pyrazole adducts that hydrolyze slowly in water. When the isocyanide is primary or secondary, however, 13 can aromatize to 14, which is then readily hydrolyzed to give 1H-pyrazol-4-amine 15 and carbonyl compound 16 (Figure 4.2). Certain primary isocyanides like methyl 3-isocyanopropanoate form pyrazoles that are more stable to hydrolysis than expected because 14 further tautomerizes an α,β-unsaturated ester.[21] Recently, the propensity of the pyrazole adducts derived from cycloaddition with primary isocyanide groups to hydrolyze was leveraged as a prodrug strategy where, oxygen, nitrogen, and sulfur heteroatoms in drugs and fluorophores were masked with 3-isocyanopropyl groups and then removed in vivo via a cycloaddition/elimination sequence.[21] Furthermore, the utility of the cycloaddition as a biorthogonal reaction for protein labeling in vitro and glycan labeling in vivo was demonstrated in 2011 and 2013.[22,23]
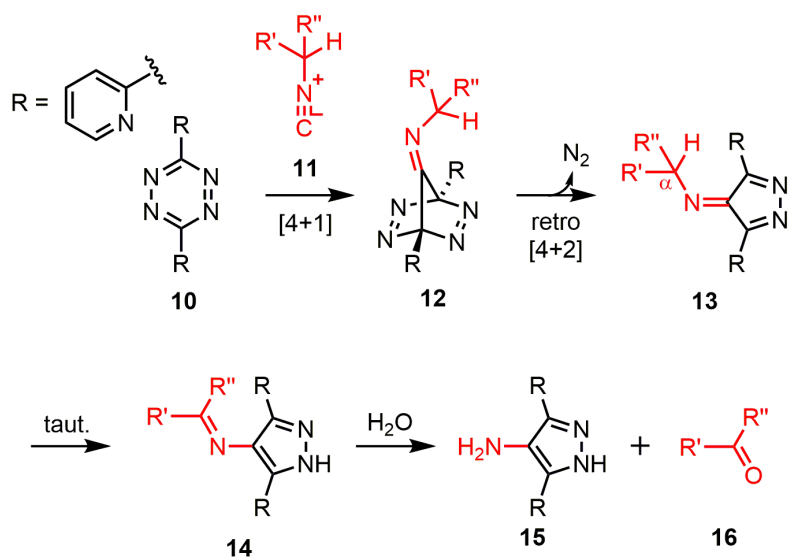
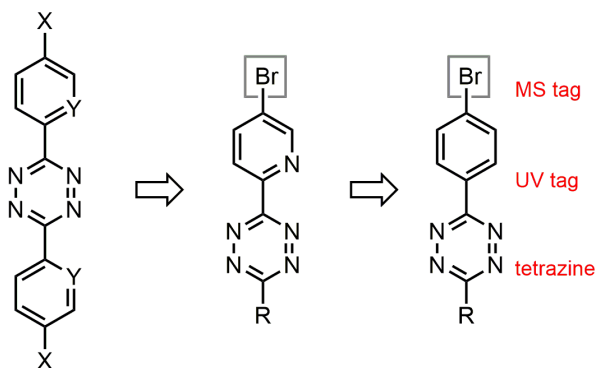**Figure 4.2** The tetrazine-isocyanide [4+1] cycloaddition.

4.2 RESULTS

Provided pyrazole hydrolysis could be minimized, we hypothesized that a general

method for the reactivity-guided isolation of isocyanide-containing natural products

could be developed using a UV-active, brominated, highly crystalline tetrazine reagent

analogous to our previously reported probes.[24–27] In this regard, we were surprised to

find only one example of this reaction with a natural product in the literature, wherein

commercially-available tetrazine **17** was shown to react with known isocyanide **9** in

bacterial culture.[28] Although this reaction is noteworthy, neither tetrazine **17** nor

commercially-available 3,6-diphenyl-1,2,4,5-tetrazine (**10**) are ideal probes because the

resulting pyrazoles do not possess characteristic features for mass detection.

Furthermore, pyrazoles derived from **17** readily hydrolyze in the case of primary and

secondary isocyanides (e.g., **1**, **4**, **6**, and **8**), which is particularly a problem for analysis

using reversed-phase liquid chromatography. Attempts to endow **10** and **17** with a

unique isotope-based signature via chlorination (^{35}Cl:^{37}Cl 3:1) and bromination (^{79}Cl:^{81}Cl

99

1:1) gave tetrazines **18**-**21** exhibiting extremely poor solubility in a wide variety of organic solvents (Figure 4.3).

We then prepared and evaluated 3-(5-bromopyridin-2-yl)-6-methyl tetrazine (**22**) and 3-(5-bromopyridin-2-yl) tetrazine (**23**), These tetrazines, which have greatly improved solubility in organic solvents compared to **17**, were synthesized via reaction of the 5-bromo-2-cyanopyridine, hydrazine, zinc triflate, and either acetonitrile or formamide acetate.[29,30] To evaluate the reactivity of these reagents, we used *t*-butyl isocyanide (**26**), cyclohexyl isocyanide (**27**), *n*-butyl isocyanide (**28**), and 2-naphthyl isocyanide (**29**) as model compounds. Stock solutions of tetrazine in DMF or DMSO were added to solutions of excess isocyanide in acetonitrile at room temperature, and the reaction mixtures were analyzed 24 h later by HPLC-UV-MS using a buffered eluent (NH$_4$OAc, pH 7). The neutral LC conditions were critical, as the presence of formic acid led to rapid hydrolysis and noticeable side-reactivity. Tetrazines **22** and **23** reacted cleanly with **26** to give the corresponding pyrazoles, which possessed a distinct mass signature and long wavelength UV absorption [λ_{max}(**22**) = 340 nm, λ_{max}(**23**) = 348 nm]. However, reaction of these tetrazines with **27** and **28** yielded aminopyrazole **15** as the only observable product, and reaction with **29** gave several unidentified side-products in addition to the desired pyrazole.
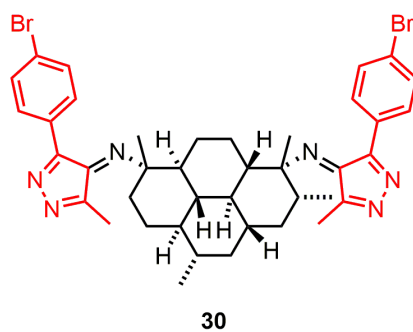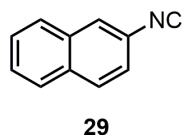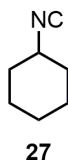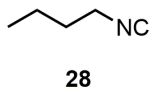
10: X = H, Y = CH   **22**: R = Me   **24**: R = Me
17: X = H, Y = N   **23**: R = H   **25**: R = H
18: X = Br, Y = CH
19: X = Cl, Y = CH
20: X = Br, Y = N
21: X = Cl, Y = N

26   **28**

27   **29**

30
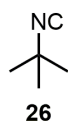
**Figure 4.3** Tetrazines **10**-**25**, isocyanides **26**-**29**, and dipyrazole **30**.

In order to reduce the rate of pyrazole hydrolysis, we prepared and evaluated

more electron-rich tetrazines 3-bromophenyl-6-methyl tetrazine (**24**) and 3-bromophenyl

101

tetrazine (**25**) from 4-bromobenzonitrile using the same conditions described for the synthesis of **22** and **23** (see Figure 4.3). Earlier reactions with **10** demonstrated that more electron-rich tetrazines would yield pyrazoles with improved hydrolytic stability, owing to the decreased acidity of the α-proton in **13** or simply the lack of basic pyridines in the reaction (see Figure 4.2). Indeed, tetrazines **24** and **25** reacted cleanly with **26-29** to give the corresponding pyrazoles, which again had a distinct mass signature and long wavelength UV absorption (λ_{max}(**24**) = 371 nm; λ_{max}(**25**) = 370 nm], although the pyrazole derived from the primary isocyanide underwent significant hydrolysis to **15**. Given that it could be obtained in higher yield than **25** and that any rate enhancement from the less sterically-hindered tetrazines was unwarranted, we decided that **24** was our most suitable tetrazine probe at this point. Its reaction in acetonitrile with 7,20-diisocyanoadociane (**3**) at room temperature to give **30** in 65% isolated yield is notable (see Figure 4.3). Also notable is the transformation of a marine diterpene lacking any UV activity into a highly UV-active chemical entity.

We then set out to further optimize the MS characteristics of the pyrazoles derived from tetrazine **24** by placing substituents on the phenyl ring that would improve ionization efficiency and MS/MS fragmentation. In this way, the precursor ion of the pyrazoles would be more pronounced, lowering the detection limit, and chromatograms could be rapidly screened by searching for the characteristic product ions. To this end, we coupled various substituted amines to 4-(6-methyl-1,2,4,5-tetrazin-3-yl)benzoic acid (**31**) with the expectation that fragmentation would readily occur across the amide bond (Figure 4.4). First, 2-picolylamine, 2-(2-pyridyl)ethylamine, and 3-morpholinopropylamine were coupled to **31** to give tetrazines **32-34**. The morpholino

amine in **34** was then quaternized with methyl iodide to give a probe (**35**) with a permanent positive charge. Adding basic tertiary amines and charged quaternary ammonium salts is an established method in untargeted metabolomics using HPLC-ESI-MS.[31,32] Tetrazines **36**-**38** were also synthesized via coupling of **31** to the appropriate amine. Although **36** and **37** do not possess a basic or quaternary nitrogen atom, they have a bromine atom as a distinguishing mass feature and were expected to readily fragment via a tropylium ion. Tetrazine **37** has a fluorine atom that could be utilized in ^{19}F NMR experiments. Finally, tetrazine **38** contains both a basic pyridine ring and bromine atom.

In order to directly compare the physicochemical properties, ionization efficiencies, and MS/MS fragmentation of the pyrazole products, stock solutions of tetrazines **24** and **33**-**37** in DMF or DMSO were added to a single vessel containing either *t*-butyl isocyanide (**26**) or cyclohexyl isocyanide (**27**) in acetonitrile. Since pyrazoles derived from tetrazines **32** and **33** co-eluted, **32** was not included in the pooled reaction. Tetrazine **38** was also not included because of its poor solubility and hydrolytic instability. LC-UV chromatograms at 360 nm showed clean conversion of all tetrazines to the corresponding pyrazole adducts for both **26** and **27** (Figure 4.4B-C). It was possible to see with the LC-MS chromatograms from 100-1700 *m/z* that the pyrazole adducts from probes **33**-**35** had increased ionization than those obtained with the benzylamine probes **36** and **37,** possibly due the presence of the morpholino and pyridine rings. The ratio of ionization intensity as measured using the area under the peak for **34+26** and **36+26** is almost 4:1, while for **34+27** and **36+27** is almost 10:1.
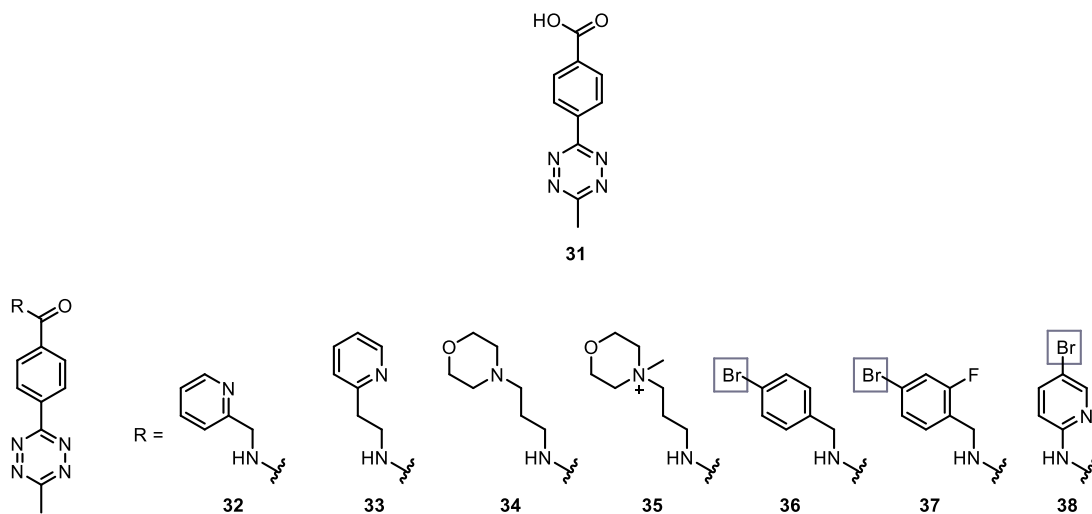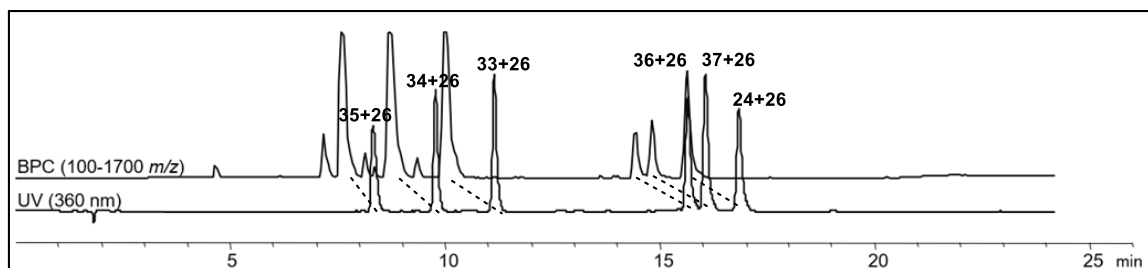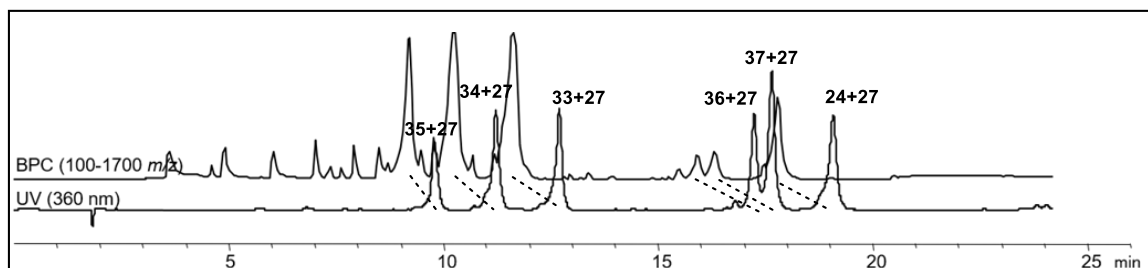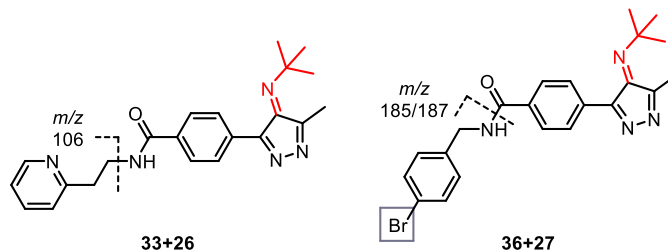
Figure 4.4 A) Core tetrazine **31** and tetrazines **32**-**38**. B) LC-UV (360nm) and LC-MS (BPC) chromatograms after reaction of pooled tetrazines **24** and **33-37** with *t*-butyl isocyanide (**26**). C) LC-UV (360nm) and LC-MS (BPC) chromatograms after reaction of pooled tetrazines **24** and **33-37** with cyclohexyl isocyanide (**27**). D) Selected pyrazoles **40** and **43**, with characteristic MS/MS fragments indicated.

Gratifyingly, pyrazole adducts from probes **33-35** show intense "reagent-specific fragments" when the mass spectrometer collision induced dissociation (CID) is set to 30 eV (Figure 4.5). Interestingly, both fragments coming from the pyrazole adducts of **34** and **35** have the same mass (187 *m/z*) and as of yet remains of unknown structure. Nonetheless, the fragment of adducts of **33** (106 *m/z*) as well as the fragments of adducts of **36** and **37** most likely involve cleavage of the CH_2-NHCO bond (*i.e.* the z-fragment of the peptide bond, Figure 4.5A)
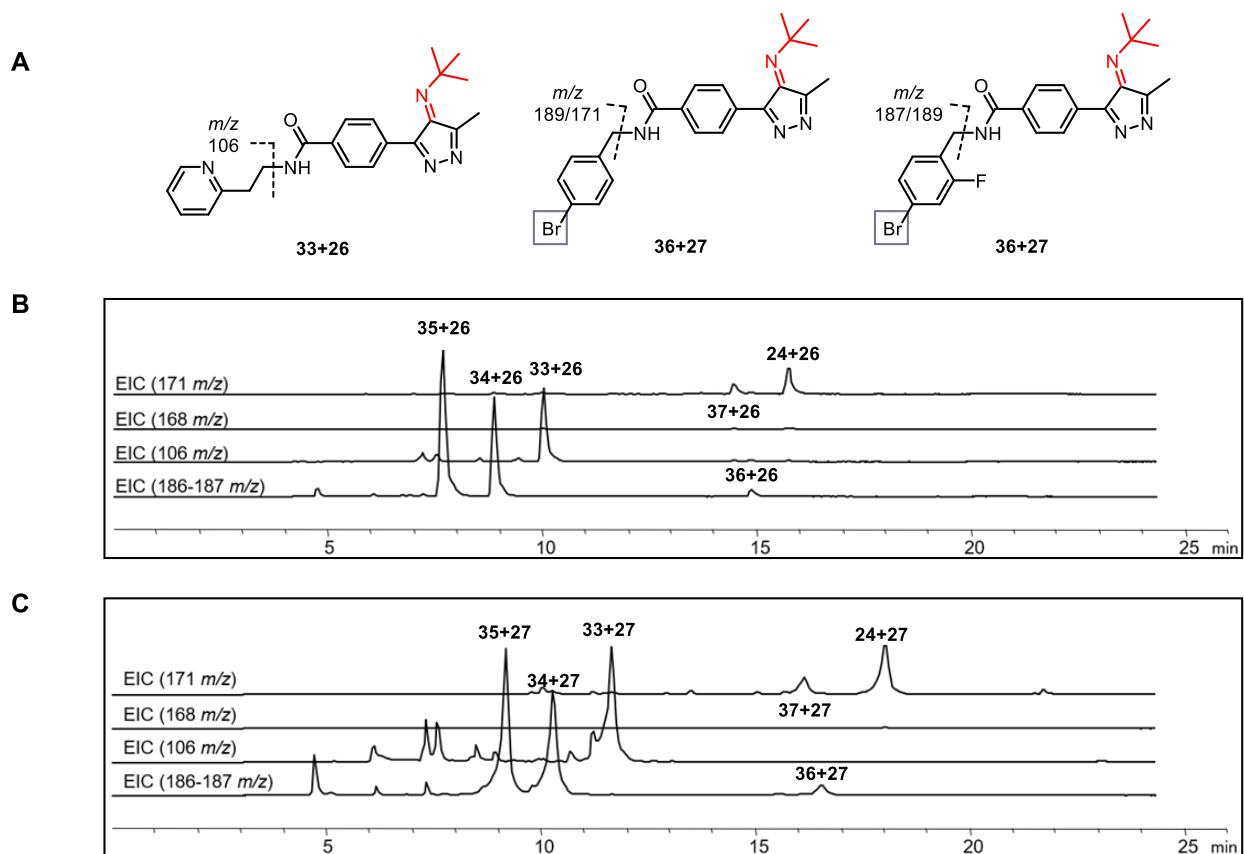
Figure 4.5 A) Pyrrazole adducts of **33**, **36** and **37** with **26** showing likely cleaved bond of "reagent-specific fragment". B) LC-MS extracted ion chromatograms (EIC) for the observed "reagent-specific fragments" after reaction of pooled tetrazines **24** and **33-37** with *t*-butyl isocyanide (**26**). ". B) LC-MS extracted ion chromatograms (EIC) for the observed "reagent-specific fragments" after reaction of pooled tetrazines **24** and **33-37** with *t*-butyl isocyanide (**27**).

4.3 CONCLUSION

Given their conspicuous UV/vis absorption profiles with two maxima (λ_{max}) at 230-240 and another at 370 nm, pyrazoles **25-27** and **29** can be easily detected in an HPLC chromatogram (Figure 4.3). Using an HPLC-MS format, the additional bromine isotopic pattern (^{79}Br:^{81}Br 1:1) associated with these compounds makes them unmistakable. As the majority of marine isocyanide-containing terpenoids, including **14**, lack any discernible UV/vis absorption and contain no bromine atoms, these features are highly distinguishing. Amino-pyrazole **28**, the product of pyrazole hydrolysis, also has a distinct UV/vis profile with one absorption maximum (λ_{max}) at 256 nm. Although a pyrazole adduct from reaction of tetrazine **23** and primarily isocyanides does not persist, the presence and abundance of primary isocyanides in a mixture can be monitored via formation of **28**. Coincidentally, to the best of our knowledge, there is only one report of a natural product containing a primary isocyanide group.[33]

The purpose of the tetrazine probes, and of the probes we develop in general, is not only to aid in the detection and isolation of natural products with the targeted functionality but also to aid in structure elucidation. The probe's bromo(hetero)arene endows the labeled natural product with a degree of crystallinity that facilitates X-ray crystallographic and cryoEM analyses. Through anomalous dispersion, the bromine atom further provides an avenue for determinations of absolute stereochemistry.

Mass fragmentation from tandem MS/MS data often show a loss of 27 amu, corresponding to *m/z* (M$^+$−HCN), but this feature depends largely on the bonding environment of the isocyanide group. Here, we designed highly tetrazines that form

highly ionizable pyrazole adducts that produce "reagent-specific fragments" that could be very helpful in the process of identifying unknown isocyanide-containing natural products in a crude extract.

4.4 METHODS

Preparation of tetrazine 22. The synthesis of tetrazine **22** has been previously reported.[34] To a solution of 4-bromobenzonitrile (2.0 g, 11 mmol, 1.0 eq) and Zn(OTf)$_2$ (2.0 g, 5.5 mmol, 0.5 eq) in acetonitrile (10 mL) was added hydrazine monohydrate (13.3 mL, 273 mmol, 25 eq) via syringe. The mixture was heated at 70 °C under nitrogen atmosphere for 12 h and then allowed to cool to room temperature, after which volatile components were removed under reduced pressure. The residue was redissolved in AcOH (100 mL) at room temperature and sodium nitrite (1.14 g, 16.5 mmol) was added. The solution was stirred for 2 h and then diluted with EtOAc (200 mL) and water (200 mL). The layers were separated. The water layer was extracted with EtOAc (100 mL). The combined organic extracts were washed with a saturated sodium bicarbonate solution (3 x 100 mL), brine (50 mL), dried, filtered, and concentrated. The product was dry-loaded onto Celite and purified by column chromatography (40 g silica, 40 mL min^{-1}, 0-60% DCM in hexanes over 15 min, t_R = 6-14 min) to give 865 mg (31%) of **22** as a red solid. All spectroscopic and analytical data for **22** are in agreement with the previous report.

Preparation of tetrazine 23. The synthesis of tetrazine **23** has been previously reported using an alternative procedure.[35] To a solution of 5-bromo-2-cyanopyridine (2.0 g, 11 mmol, 1.0 eq) and Zn(OTf)$_2$ (2.0 g, 5.5 mmol, 0.5 eq) in acetonitrile (10 mL) at

room temperature was added hydrazine monohydrate (13.3 mL, 273 mmol, 25 eq) via

syringe. The mixture was then heated at 70 °C under nitrogen atmosphere for 24 h and

then allowed to cool to room temperature, after which volatile components were

removed under reduced pressure. The residue was redissolved in AcOH (100 mL) at

room temperature and sodium nitrite (1.14 g, 16.5 mmol) was added. After 2 h

additional sodium nitrite (700 mg) was added, and, after another 30 min, the mixture

was diluted with EtOAc (200 mL) and water (200 mL). The layers were separated. The

water layer was extracted with EtOAc (100 mL). The combined organic extracts were

washed with a saturated sodium bicarbonate solution (3 x 50 mL), brine (30 mL), dried,

filtered, and concentrated. The product was dry-loaded onto Celite and purified by

column chromatography (40 g silica, 40 mL min^{-1}, 0-60% EtOAc in hexanes over 15

min, t_R = 13-18 min; then 12 g silica, 30 mL min^{-1}, 0-20% EtOAc in DCM over 12 min, t_R

= 6-9 min) to give 205 mg (7%) of **23** as a red solid. All spectroscopic and analytical

data for **23** are in agreement with the previous report.

Test reactions with tetrazines 22-38 and isonitriles 26-29. To individual

solutions (5 mM, 20 μL) of tetrazines **22**-**38** in DMF in an HPLC vial with insert were

added solutions of n-butyl isocyanide (**26**), cyclohexenyl isocyanide (**27**), t-butyl

isocyanide (**28**) or 2-naphthyl isocyanide (**29**) in MeCN (20 mM, 20 μL). The solutions

were left standing for 24 h, after which the reaction mixtures were analyzed by

reversed-phase HPLC [254 nm, 10-100% MeCN in water (10 mM ammonium acetate,

pH 7) over 10 min, C18(2) Phenomenex Luna, 100 x 4.6 mm, 5 μ, 1.0 mL min^{-1}].

Diisocyanoadociane reaction with 24. To a solution of 7,20-

diisocyanoadociane (5.0 mg, 0.015 mmol) in MeCN (1.0 mL) was added tetrazine **24**

(8.5 mg, 0.034 mmol).). The solution were left stirring for 24 h, after which the reaction mixture was analyzed by reversed-phase HPLC [254 nm, 10-100% MeCN in water (10 mM ammonium acetate, pH 7) over 10 min, C18(2) Phenomenex Luna, 100 x 4.6 mm, 5 μ, 1.0 mL min^{-1}] and indicated complete conversion to a single product. This was subsequently purified by normal phase HPLC [65% ethyl acetate in hexanes, tR = 10 min, silica(2) Phenomenex Luna, 250 x 10 mm, 5 μ, 3 mL min–1] to afford 8.0 mg (67%) of **30** as an orange solid.

Synthesis of compound 23: To a stirring solution of 5-bromo-2-cyanopyridine (200 mg, 1.1 mmol, 1.0 equiv.) in 50% EtOH(aq.) (2.2 mL) was added sulfur flowers (70 mg, 2.2 mmol, 2.0 equiv.), DCM (70 μL, 1.1 mmol, 1.0 equiv.), and hydrazine (276 μL, 8.8 mmol, 8.0 equiv.). The reaction flask was sealed and stirred at 50°C for 24 hours. The reaction was allowed to cool to 22°C, and then diluted with 100 mL H2O and 10 mL EtOAc. NaNO2 (760 mg, 11 mmol, 10 equiv.) was added with stirring, and conc. HCl was added slowly to the stirring mixture until gas evolution ceased. The mixture was extracted with EtOAc, and the organic phase was washed with sat. NaHCO3, water, and brine. The organic layer was dried over Na_2SO_4, filtered, and evaporated onto Celite. The product was purified by flash chromatography (0 to 100% DCM in hexanes, 12 g column, then, 0 to 60% EtOAc in hexanes, 12 g column). 3-(5-bromopyridin2-yl)-1,2,4,5-tetrazine (**23**) was recovered as a pink solid (20 mg, 7.7% yield). UV/Vis: λmax = 308 nm, 538 nm. ^{1}H NMR (CDCl3) δ 10.38 (s, 1H), 9.02 (s, 1H), 8.59 (d, J = 8.4 Hz, 2H), 8.15 (d, J = 8.8 Hz). ^{13}C NMR (CDCl3) δ 165.6, 158.5, 152.5, 148.4, 140.5, 125.4, 125.3. HR-ESI-TOFMS: m/z (M+H)+ calcd for $C_7H_5{}^{79}BrN_5$ 237.9723, found 237.9723.

Synthesis of compound 25: To a stirring solution of 4-bromobenzonitrile (200 mg, 1.1 mmol, 1.0 equiv.) in 50% EtOH (aq.) (2.2 mL) was added sulfur flowers (70 mg, 2.2 mmol, 2.0 equiv.), DCM (70 µL, 1.1 mmol, 1.0 equiv.), and hydrazine (276 µL, 8.8 mmol, 8.0 equiv.). The reaction flask was sealed and stirred at 50°C for 16 hours. The reaction was allowed to cool to 22°C, and then diluted with 100 mL H2O. NaNO2 (760 mg, 11 mmol, 10 equiv.) was added with stirring, and conc. HCl was added slowly to the stirring mixture until gas evolution ceased. The mixture was extracted with EtOAc, and the organic phase was washed with water, sat. NaHCO3, water, and brine. The organic layer was dried over Na2SO4, filtered, and evaporated onto Celite. The product was purified by flash chromatography (0 to 100% DCM in hexanes, 12 g column). 3-(4-bromophenyl)-1,2,4,5-tetrazine (**25**) was recovered as a pink solid (44 mg, 17% yield). ^{1}H NMR (CDCl3) δ 10.24 (s, 1H), 8.51 (d, J = 8.6 Hz, 2H), 7.76 (d, J = 8.6 Hz, 2H). ^{13}C NMR (CDCl3) δ 166.1, 158.0, 132.9, 130.6, 129.8, 128.6.

Synthesis of compound 31: A mixture of pyridin-2-ylmethanamine (34 µL, 333 µmol, 1.4 equiv.) and 4-(6-methyl-1,2,4,5-tetrazin-3-yl)benzoic acid (50 mg, 231 µmol, 1.0 equiv.) was stirred in DMF (2.3 mL). HBTU (105 mg, 278 µmol, 1.2 equiv.) was added, followed by iPr2NEt (70 µL, 400 µmol, 1.6 equiv.). The reaction was stirred at 22°C for 12 hours, then diluted in EtOAc. The organic phase was washed successively with sat. aq. Na2CO3, H2O, and brine, then dried over Na2SO4. The solvent was evaporated to afford the pure product as a pink solid (51 mg, 72% yield). UV/Vis: λmax = 270 nm, 525 nm. ^{1}H NMR (CDCl3): δ 8.69 (d, J = 8.4 Hz, 2H), 8.59 (d, J = 4.7 Hz, 1H), 8.09 (d, J = 8.4 Hz, 2H), 7.79 (s, br, 1H), 7.71 (t, J = 7.7 Hz, 1H), 7.35 (d, J = 7.8 Hz, 1H), 7.25 (m, overlap, 1H), 4.81 (d, J = 4.4 Hz, 2H), 3.13 (s, 3H). ^{13}C NMR (CDCl3): δ

167.7, 166.6, 163.8, 155.8, 149.2, 138.1, 137.1, 134.6, 128.3, 128.1, 122.8, 122.4, 44.9, 21.4. HR-ESI-TOFMS: m/z (M+H)+ calcd for $C_{16}H_{15}N_6O$ 307.1302, found 307.1300.

Synthesis of compound 32: A mixture of 2-(pyridin-2-yl)ethan-1-amine (40 µL, 333 µmol, 1.4 equiv.) and 4-(6-methyl-1,2,4,5-tetrazin-3-yl)benzoic acid (50 mg, 231 µmol, 1.0 equiv.) was stirred in DMF (2.3 mL). HBTU (105 mg, 278 µmol, 1.2 equiv.) was added, followed by iPr$_2$NEt (70 µL, 400 µmol, 1.6 equiv.). The reaction was stirred at 22°C for 12 hours, then diluted in EtOAc. The organic phase was washed successively with sat. aq. Na_2CO_3, H_2O, and brine, then dried over Na_2SO_4. The solvent was evaporated to afford the pure product as a pink solid (69 mg, 93% yield). UV/Vis: λmax = 265nm, 525 nm. ^{1}H NMR (CDCl$_3$): δ 8.65 (d, J = 8.2 Hz, 2H), 8.59 (d, J = 4.4 Hz, 1H), 7.99 (d, J = 8.2 Hz, 2H), 7.89 (s, br, 1H), 7.64 (t, J = 7.6 Hz, 1H), 7.19-7.24 (m, overlap, 2H), 3.90 (m, J = 5.7 Hz, 2H), 3.13 (m, overlap, 5H). ^{13}C NMR (CDCl$_3$): δ 167.7, 166.4, 163.8, 160.0, 149.3, 138.5, 137.1, 134.4, 128.2, 128.0, 123.8, 122.0, 39.4, 36.4, 21.4. HR-ESI-TOFMS: m/z (M+H)+ calcd for $C_{17}H_{17}N_6O$ 321.1458, found 321.1458.

Synthesis of compound 33: 4-(6-methyl-1,2,4,5-tetrazin-3-yl)benzoic acid (100 mg, 463 µmol, 1.0 equiv.) and HBTU (219 mg, 579 µmol, 1.25 equiv.) were added to a flask with a stir bar. DMF (4.6 mL) was added and the mixture was stirred to dissolve. To the flask was added 3-morpholinopropan-1-amine (68 µL, 463 µmol, 1.0 equiv.), followed by iPr$_2$NEt (121 µL, 694 µmol, 1.5 equiv.). The reaction was stirred at 22°C for 3 hr., at which point HPLC monitoring indicated reaction completion. The reaction was diluted with EtOAc, washed with sat. $NaHCO_3$, then with brine. The organic phase was dried over Na_2SO_4, filtered, and evaporated onto Celite. Flash chromatography (12 g

column, 0 to 20% MeOH in DCM) afforded pure **33** (89 mg, 56% yield). UV/vis. λmax = 270 nm. ^{1}H NMR (CD$_3$OD) δ 8.64 (d, J = 8.3 Hz, 2H), 8.05 (d, J = 8.3 Hz, 2H), 3.71 (br. s, 4H), 3.49 (t, J = 7.0 Hz, 2H), 3.06 (s, 3H), 2.53 (m, 6H), 1.88 (m, J = 7.0 Hz, 2H). ^{1}H NMR (CDCl$_3$) δ 8.67 (d, J = 8.4 Hz, 2H), 8.28 (br. s, 1H), 8.02 (d, J = 8.4 Hz, 2H), 3.72 (t, J = 4.3 Hz, 4H), 3.62 (q, J = 5.6 Hz, 2H), 3.12 (s, 3H), 2.60 (t, J = 5.9 Hz, 2H), 2.50 (br. s, 3H), 1.83 (m, J = 6.0 Hz, 2H), 1.77 (br. s, 2H). ^{13}C NMR (CDCl$_3$, 500 MHz) δ 167.7, 166.6, 163.7, 138.6, 134.5, 128.2, 128.0, 67.1, 59.0, 54.0, 41.0, 24.0, 21.4. HR-ESI-TOFMS: m/z (M+H)+ calcd for $C_{17}H_{23}N_6O_2$ + 343.1877, found 343.1874.

Synthesis of compound 34: To 4-(6-methyl-1,2,4,5-tetrazin-3-yl)-N-(3-(piperidin-1- yl)propyl)benzamide (89 mg, 260 µmol, 1.0 equiv.) stirred in 5.2 mL 1:1 MeCN:THF was added MeI (32 µL, 520 µmol, 2.0 equiv.) at 22°C. The reaction was stirred for 12 hours, and monitoring by an adapted analytical HPLC method (0.1% formic acid replaced by 10 mM ammonium acetate) indicated completion of the reaction. The mixture was evaporated to dryness under a stream of N$_2$, and re-dissolved in 95% MeOH(aq). The product was purified by preparative HPLC (20% MeCN in H2O, 0.1% formic acid, 13 mL/min, r.t. 6 to 8 min.) to afford 1-methyl-1-(3-(4-(6-methyl-1,2,4,5-tetrazin-3- yl)benzamido)propyl)piperidin-1-ium iodide as a pink solid (57 mg, 45% yield). UV/vis: λmax = nm, nm. ^{1}H NMR (CD$_3$OD): δ 8.65 (d, J = Hz, 2H), 8.47 (br. s, 1H), 8.08 (d, J = Hz, 2H), 4.02 (br., overlapping, 4H), 3.4-3.6 (br., overlapping, 8H), 3.24 (s, 3H), 3.07 (s, 3H), 2.18 (br. s, 2H). ^{13}C NMR (CD$_3$OD): δ 169.6, 169.1, 164.8, 138.7, 136.6, 129.2, 128.9, 64.6, 61.6, 61.2, 47.3, 38.0, 23.2, 21.2. HR-ESITOFMS: m/z (M+H)+ calcd for $C_{18}H_{26}N_6O_2$ + 357.2034, found 357.2030.

Synthesis of compound 35: A mixture for 4-bromobenzylamine-HCl (29 mg, 129 µmol, 1.4 equiv.) and 4-(6-methyl-1,2,4,5-tetrazin-3-yl)benzoic acid (20 mg, 93 µmol, 1.0 equiv.) was stirred in DMF (1.0 mL). HBTU (42 mg, 111 µmol, 1.2 equiv.) was added, followed by iPr$_2$NEt (42 µL, 242 µmol, 2.6 equiv.). The reaction was stirred at 22°C for 12 hr, at which time a pink precipitate had formed. The precipitate was recovered by filtration (filter paper of sintered glass vacuum funnel) and rinsed with MeOH to afford the pure product as a pink solid (35 mg, quant.). UV/Vis: λmax = 270 nm, 535 nm. ^{1}H NMR (DMSO-d$_6$): δ 9.31 (s, br, 1H), 8.56 (d, J = 8.2 Hz, 2H), 8.14 (d, J = 8.2 Hz, 2H), 7.53 (d, J = 8.2 Hz, 2H), 7.31 (d, J = 8.1 Hz, 2H), 4.48 (d, J = 5.5 Hz, 2H), 3.02 (s, 3H). ^{13}C NMR (DMSO-d$_6$): δ 167.4, 165.6, 162.9, 139.0, 137.4, 134.4, 131.2, 129.6, 128.3, 127.4, 119.9, 42.2, 20.9. HR-ESITOFMS: m/z (M+H)+ calcd for C$_{17}$H15^{79}BrN$_5$O 384.0454, found 384.0457.

Synthesis of compound 36: A mixture of 4-bromo-2-fluorobenzylamine-HCl (167 mg, 694 µmol, 1.5 equiv.) and 4-(6-methyl-1,2,4,5-tetrazin-3-yl)benzoic acid (100 mg, 463 µmol, 1.0 equiv.) was stirred in DMF (5 mL). HBTU (219 mg, 578 µmol, 1.25 equiv.) was added, followed by iPr$_2$NEt (161 µL, 926 µmol, 2.0 equiv.). The reaction was stirred at 22°C for 4 hr., then diluted with EtOAc. The organic phase was washed with successively with 10% aq. citric acid, H$_2$O, sat. aq. NaHCO$_3$, H$_2$O, and brine. The organic phase was dried over Na$_2$SO$_4$, filtered, and evaporated onto Celite. Column chromatography (4 g column, 0 to 100% EtOAc in hexanes) yielded the product as a pink solid (100 mg, 53.8% yield). UV/Vis: λmax = 270 nm, 540 nm. ^{1}H NMR (DMSO-d$_6$): δ 9.29 (s, br, 1H), 8.56 (d, J = 8.2 Hz, 2H), 8.14 (d, J = 8.2 Hz, 2H), 7.55 (d, J = 9.4 Hz, 1H), 7.37-7.43 (m, 2H), 4.51 (d, J = 3.6 Hz, 2H), 3.02 (s, 3H). ^{13}C NMR (DMSO-d$_6$): δ

167.3, 165.7, 162.9, 160.0 (d, J = 250 Hz), 137.2, 134.5, 131.3 (d, J = 4.9 Hz), 128.3, 127.5 (d, J = 3.0 Hz), 127.4, 125.6 (d, J = 14.7 Hz), 120.2 (d, J = 9.8 Hz), 118.5 (d, J = 24.8 Hz), 36.4, 20.9. HR-ESITOFMS: m/z (M+H)+ calcd for $C_{17}H_{14}BrFN_5O$ 402.0360, found 402.0363.

Reaction between pooled tetrazines 33-37 and isonitriles 26-27. Solutions (5 mM, 20 µL) of tetrazines **22-38** in DMF were pooled into an HPLC vial with insert and were added solutions of *n*-butyl isocyanide (**26**) or cyclohexanyl isocyanide (**27**) in MeCN (1.0 M, 20 µL). The solutions were left standing for 4 h, after which the reaction mixtures were analyzed by reversed-phase HPLC [254 nm, 10-100% MeCN in water (10 mM ammonium acetate, pH 7) over 20 min, C18(2) Phenomenex Luna, 100 x 4.6 mm, 5 µ, 1.0 mL min^{-1}].

4.5 ACKNOWLEDGMENTS

4.6 REFERENCES

(1) Garson, M. J., and Simpson, J. S. (2004) Marine isocyanides and related natural products–structure, biosynthesis and ecology. Nat. Prod. Rep. 21, 164–179.

(2) Emsermann, J., Kauhl, U., and Opatz, T. (2016) Marine isonitriles and their related compounds. Mar. Drugs 14, 1–83.

(3) Bhat, V., Dave, A., MacKay, J. A., and Rawal, V. H. (2014) The Chemistry of Hapalindoles, Fischerindoles, Ambiguines, and Welwitindolinones. Alkaloids Chem. Biol. 1st ed. Elsevier Inc.

(4) Schnermann, M. J., and Shenvi, R. A. (2015) Syntheses and biological studies of marine terpenoids derived from inorganic cyanide. Nat. Prod. Rep. 32, 543–577.

(5) Kobayashi, J., Tsuda, M., Nemoto, A., Tanaka, Y., Yazawa, K., and Mikami, Y. (1997) Brasilidine A, a new cytotoxic isonitrile-containing indole alkaloid from the actinomycete Nocardia brasiliensis. J. Nat. Prod. 60, 719–720.

(6) Tabata, Y., Hatsu, M., Amano, S., Shimizu, A., and Imai, S. (1995) SF2768, a new isonitrile antibiotic obtained from Streptomyces. Sci. Rep. Meiji Seika Kaisha 34, 1–9.

(7) Evans, J. R., Napier, E. J., and Yates, P. (1976) Isolation of a new antibiotic from a species of pseudomonas. J. Antibiot. (Tokyo). 29, 850–852.

(8) Wang, L., Zhu, M., Zhang, Q., Zhang, X., Yang, P., Liu, Z., Deng, Y., Zhu, Y., Huang, X., Han, L., Li, S., and He, J. (2017) Diisonitrile natural product SF2768 functions as a chalkophore that mediates copper acquisition in Streptomyces thioluteus. ACS Chem. Biol. 12, 3067–3075.

(9) Sandoval, I. T., Manos, E. J., Van Wagoner, R. M., Delacruz, R. G. C., Edes, K., Winge, D. R., Ireland, C. M., and Jones, D. A. (2013) Juxtaposition of chemical and mutation-induced developmental defects in zebrafish reveal a copper-chelating activity for kalihinol F. Chem. Biol. 20, 753–763.

(10) König, G. M., Wright, A. D., and Angerhofer, C. K. (1996) Novel potent antimalarial diterpene isocyanates, isothiocyanates, and isonitriles from the tropical marine sponge Cymbastela hooperi. J. Org. Chem. 61, 3259–3267.

(11) Amano, S. I., Sakurai, T., Endo, K., Takano, H., Beppu, T., Furihata, K., Sakuda, S., and Ueda, K. (2011) A cryptic antibiotic triggered by monensin. J. Antibiot. (Tokyo). 64, 703.

(12) Moore, R. E., Cheuk, C., and Patterson, G. M. L. (1984) Hapalindoles: New alkaloids from the blue-green alga Hapalosiphon fontinalis. J. Am. Chem. Soc. 106, 6456–6457.

(13) Chang, C. W. J., Patra, A., Roll, D. M., Matsumoto, G. K., and Clardy, J. (1984) Kalihinol-A, a highly functionalized diisocyano diterpenoid antibiotic from a sponge. J. Am. Chem. Soc. 106, 4644–4646.

(14) Baker, J. T., Wells, R. J., Oberhaensli, W. E., and Hawes, G. B. (1976) A new diisocyanide of novel ring structure from a sponge. J. Am. Chem. Soc. 98, 4010–4012.

(15) Di Blasio, B., Fattorusso, E., Magno, S., Mayoi, L., Pedone, C., Santacroce, C., and Sica, D. (1976) Axisonitrile-3, axisothiocyanides-3 and axamide-3. Sesquiterpenes

with a novel spiro[4,5]decane skeleton from the sponge Axinella cannabina. Tetrahedron 32, 473–478.

(16) Stratmann, K., Moore, R. E., Bonjouklian, R., Deeter, J. B., Patterson, G. M. L., Shaffer, S., Smith, C. D., and Smitka, T. A. (1994) Welwitinolides, unusual alkaloids from the blue-green alga Hapalisophon welwitschii and Westiella intricata. Relationship to fisherindoles and hapalindoles. J. Am. Chem. Soc. 116, 9935–9942.

(17) Brady, S. F., and Clardy, J. (2005) Cloning and heterologous expression of isocyanide biosynthetic genes from environmental DNA. Angew. Chem. Int. Ed. Engl. 44, 7063–7065.

(18) Brady, S. F., Bauer, J. D., Clarke-Pearson, M. F., and Daniels, R. (2007) Natural products from isnA-containing biosynthetic gene clusters recovered from the genomes of cultured and uncultured bacteria. J. Am. Chem. Soc. 129, 12102–12103.

(19) Harris, N. C., Sato, M., Herman, N. A., Twigg, F., Cai, W., Liu, J., and Zhu, X. (2017) Biosynthesis of isonitrile lipopeptides by conserved nonribosomal peptide synthetase gene clusters in Actinobacteria. Proc. Natl. Acad. Sci. 114, 7025–7030.

(20) Imming, B. P., Mohr, R., Miiller, E., Overheu, W., and Seitz, G. (1982) [4+1] cycloaddition of isocyanides to 1,2,4,5-tetrazines: A novel synthesis of pyrazole. Angew. Chem. Int. Ed. 21, 20133.

(21) Tu, J., Xu, M., Parvez, S., Peterson, R. T., and Franzini, R. M. (2018) Bioorthogonal removal of 3-isocyanopropyl groups enables the controlled release of fluorophores and drugs in vivo. J. Am. Chem. Soc. 140, 8410–8414.

(22) Henning, S., Neves, A. A., Stairs, S., Brindle, K. M., and Leeper, F. J. (2011) Exploring isonitrile-based click chemistry for ligation with biomolecules. Org. Biomol. Chem. 9, 7303–7305.

(23) Stairs, S., Neves, A. A., Stçckmann, H., and Wainman, Y. A. (2013) Metabolic glycan imaging by isonitrile–tetrazine click chemistry. ChemBioChem 14, 1063–1067.

(24) Castro-Falcon, G., Hahn, D., Reimer, D., and Hughes, C. C. (2016) Thiol probes to detect electrophilic natural products based on their mechanism of action. ACS Chem. Biol. 11, 2328–2336.

(25) Reimer, D., and Hughes, C. C. (2017) Thiol-based probe for electrophilic natural products reveals that most of the ammosamides are artifacts. J. Nat. Prod. 80, 126–133.
(26) Castro-Falcón, G., Seiler, G., Demir, O., Rathinaswamy, M., Hamelin, D., Hoffmann, R. M., Makowski, S., Letzel, A.-C., Field, S., Burke, J., Amaro, R. E., and

Hughes, C. C. (2018) Neolymphostin A is a Covalent Phosphoinositide 3-Kinase (PI3K)/Mammalian Target of Rapamycin (mTOR) Dual Inhibitor that Employs an Unusual Electrophilic Vinylogous Ester. J. Med. Chem. 61, 10463–10472.

(27) Castro-Falcón, G., Millán-Aguiñaga, N., Roullier, C., Jensen, P. R., and Hughes, C. C. (2018) Nitrosopyridine probe to detect polyketide natural products with conjugated alkenes: Discovery of novodaryamide and nocarditriene. ACS Chem. Biol. 13, 3097–3106.

(28) Tørring, T., Shames, S. R., Cho, W., Roy, C. R., and Crawford, J. M. (2017) Acyl histidines: New N-acyl amides from Legionella pneumophila. ChemBioChem 18, 638–646.

(29) Kozma, E., Estrada Girona, G., Paci, G., Lemke, E. A., and Kele, P. (2017) Bioorthogonal double-fluorogenic siliconrhodamine probes for intracellular super-resolution microscopy. Chem. Commun. 53, 6696–6699.

(30) Cserép, G. B., Demeter, O., Bätzner, E., Kállay, M., Wagenknecht, H. A., and Kele, P. (2015) Synthesis and Evaluation of Nicotinic Acid Derived Tetrazines for Bioorthogonal Labeling. Synth. 47, 2738–2744.

(31) Santa, T. (2013) Derivatization in LC-MS bioanalysis, in Handbook of LC-MS bioanalysis: Best practices, experimental protocols, and regulations (Li, W., Zhang, J., and Tse, F. L. S., Eds.), pp 239–248. John Wiley & Sons, Inc.

(32) Qi, B. L., Liu, P., Wang, Q. Y., Cai, W. J., Yuan, B. F., and Feng, Y. Q. (2014) Derivatization for liquid chromatography-mass spectrometry. Trends Anal. Chem. 59, 121–132.

(33) Mayol, L., Piccialli, V., and Sica, D. (1987) Nitrogenous sesquiterpenes from the marine sponge Acanthella acuta: Three new isocyanide-isothiocyanate pairs. Tetrahedron 43, 5381–5388.

(34) Suh, S. E., Barros, S. A., and Chenoweth, D. M. (2015) Triple aryne-tetrazine reaction enabling rapid access to a new class of polyaromatic heterocycles. Chem. Sci. 6, 5128–5132.

(35) Qu, Y., Sauvage, F. X., Clavier, G., Miomandre, F., and Audebert, P. (2018) Metal-Free Synthetic Approach to 3-Monosubstituted Unsymmetrical 1,2,4,5-Tetrazines Useful for Bioorthogonal Reactions. Angew. Chemie - Int. Ed. 57, 12057–12061.